

19. SITE 687¹

Shipboard Scientific Party²

HOLE 687A

Date occupied: 0700 L, 3 December 1986

Date departed: 1830 L, 3 December 1986

Time on hole: 11 hr 30 min

Position: 12°51.78'W, 76°59.43'W

Water depth (sea level; corrected m, echo-sounding): 306.8

Water depth (rig floor; corrected m, echo-sounding): 317.3

Bottom felt (m, drill pipe): 316.3

Penetration (m): 207.0

Number of cores: 22

Total length of cored section (m): 207.0

Total core recovered (m): 108.29

Core recovery (%): 52.3

Oldest sediment cored

Depth (mbsf): 207.0

Nature: diatomaceous mud

Age: Quaternary/Pliocene

HOLE 687B

Date occupied: 1830 L, 3 December 1986

Date departed: 0600 L, 4 December 1986

Time on hole: 11 hr 30 min

Position: 12°51.78'W, 76°59.43'W

Water depth (sea level; corrected m, echo-sounding): 306.8

Water depth (rig floor; corrected m, echo-sounding): 317.3

Bottom felt (m, drill pipe): 315.6

Penetration (m): 195.3

Number of cores: 22

Total length of cored section (m): 195.3

Total core recovered (m): 87.43

Core recovery (%): 44.8%

Oldest sediment cored

Depth (mbsf): 195.3

Nature: diatomaceous mud

Age: Quaternary/Pliocene

Principal results: Site 687 is located on the seaward flank of the tectonically stable Lima Platform, which forms the eastern and southern boundaries of the Lima Basin in this area. This shallow-water site was selected (1) to obtain a high-resolution record of Quaternary/late Neogene upwelling and climatic histories, (2) to evaluate the role of the oxygen-minimum zone on organic matter burial, and (3) to document in detail early diagenetic reactions and products specific to the coastal-upwelling environment.

The sediment at Site 687 consists of diatomaceous mud with large variations in composition and texture. The compositional variation reflects different proportions of authigenic dolomite and calcite as well as biogenic calcium carbonate, mainly foraminifers and mollusks. The texture varies according to its sand and silt contents, which are higher at Site 687 than anywhere else along this paleoceanographic transect off Peru. Lithologic units are subdivided by the frequency of sand and silt interlayers. These units display a trend from laminated intervals with little textural variation and rare bioturbation to laminated and bioturbated intervals containing more frequent sand beds. Accordingly, the depositional environment at Site 687 is thought to have changed over the past 2.5 m.y. from one equivalent to today's slope environment to an outer-shelf environment and then back to upper-slope environment. These changes are consistent with assemblages of benthic foraminifers, which also indicate low oxygen contents for the deep habitats. In all sections, diatom floras were found to be characteristic of different intensities of coastal upwelling and fertility. At least five prolonged phases of intense coastal upwelling and high productivity occurred during shallow- and deep-water periods at Site 687.

Diagenetic products are common throughout the cores of Site 687. Of these, friable phosphates occur only in diatomaceous mud units, but dense phosphate peloids are present in all lithologic units, especially as conglomerates at the base of erosional contacts. Both authigenic calcite and dolomite are abundant in the sediments as dis-

¹ Suess, E., von Huene, R., et al., 1988. *Proc. ODP, Init. Repts.*, 112: College Station, TX (Ocean Drilling Program).

² Erwin Suess (Co-Chief Scientist), Oregon State University, College of Oceanography, Corvallis, OR 97331; Roland von Huene (Co-Chief Scientist), U.S. Geological Survey, Branch of Pacific Marine Geology, 345 Middlefield Rd. M/S 999, Menlo Park, CA 94025; Kay-Christian Emeis (ODP Staff Scientist), Ocean Drilling Program, Texas A&M University, College Station, TX 77843; Jacques Bourgois, Département de Géotectonique, Université Pierre et Marie Curie, 4 Place Jussieu, 75230 Paris Cedex 05, France; José del C. Cruzado Castañeda, Petroleos del Peru S. A., Paseo de la Republica 3361, San Isidro, Lima, Peru; Patrick De Wever, CNRS, Laboratoire de Stratigraphie, Université Pierre et Marie Curie, 4 Place Jussieu, 75230 Paris Cedex 05, France; Geoffrey Eglinton, University of Bristol, School of Chemistry, Cantock's Close, Bristol BS8 1TS, England; Robert Garrison, University of California, Earth Sciences, Applied Sciences Building, Santa Cruz, CA 95064; Matt Greenberg, Lamont-Doherty Geological Observatory, Columbia University, Palisades, NY 10964; Elard Herrera Paz, Petroleos del Peru, S. A., Paseo de la Republica 3361, San Isidro, Lima, Peru; Phillip Hill, Atlantic Geoscience Centre, Bedford Institute of Oceanography, Box 1006, Dartmouth, Nova Scotia B2Y 4A2, Canada; Masako Ibaraki, Geoscience Institute, Faculty of Science, Shizuoka University, Shizuoka 422, Japan; Miriam Kastner, Scripps Institution of Oceanography, SVH, A-102, La Jolla, CA 92093; Alan E. S. Kemp, Department of Oceanography, The University, Southampton SO9 5NH, England; Keith Kvenvolden, U.S. Geological Survey, Branch of Pacific Marine Geology, 345 Middlefield Rd., M/S 999, Menlo Park, CA 94025; Robert Langridge, Department of Geological Sciences, Queen's University at Kingston, Ontario K7L 3A2, Canada; Nancy Lindsley-Griffin, University of Nebraska, Department of Geology, 214 Bessey Hall, Lincoln, NE 68588-0340; Janice Marsters, Department of Oceanography, Dalhousie University, Halifax, Nova Scotia B3H 4J1, Canada; Erlend Martini, Geologisch-Paläontologisches Institut der Universität Frankfurt, Senckenberg-Anlage 32-34, D-6000, Frankfurt/Main, Federal Republic of Germany; Robert McCabe, Department of Geophysics, Texas A&M University, College Station, TX 77843; Leonidas Ocola, Laboratorio Central, Instituto Geofísico del Peru, Lima, Peru; Johanna Resig, Department of Geology and Geophysics, University of Hawaii, Honolulu, HI 96822; Agapito Wilfredo Sanchez Fernandez, Instituto Geológico Minero y Metalúrgico, Pablo Bermudez 211, Lima, Peru; Hans-Joachim Schrader, College of Oceanography, Oregon State University, Corvallis, OR 97331 (currently at Department of Geology, University of Bergen, N-5000 Bergen, Norway); Todd Thornburg, College of Oceanography, Oregon State University, Corvallis, OR 97331; Gerold Wefer, Universität Bremen, Fachbereich Geowissenschaften, Postfach 330 440, D-2800 Bremen 33, Federal Republic of Germany; Makoto Yamano, Earthquake Research Institute, University of Tokyo, Bunkyo-ku, Tokyo 113, Japan.

seminated crystals in unlithified sands, silts, or muds and as fully lithified nodules and beds. The first dolomite bed occurs below the zone of sulfate depletion and coincides with an increase in methane. In this zone, biogenic methane is accompanied by persistent and anomalously high ethane contents, the source of which is unclear. A subsurface saline brine is evident in a strong chloride anomaly. There are subtle differences in the Ca^{2+} , Mg^{2+} , alkalinity, NH_4^+ , and PO_4^{3-} profiles affected by the brine between Sites 686 and 687. These are thought to be related to the rates of sedimentation, authigenic mineral formation, and metabolism. We believe that the loading of metabolites occurs during the brine's subsurface passage through organic-rich sediments that undergo decomposition by sulfate reduction.

BACKGROUND AND SCIENTIFIC OBJECTIVES

Sites 686 and 687 are important stations on the main paleoceanographic transects across upper-slope water masses and along the latitudinal range of sedimentary basins underlying the Peru coastal upwelling regime. These transects were designed to study the history of the upwelling environment in a three-dimensional framework. The sites constituting the depth transect are Site 681 at a water depth of 146 m, Site 680 at 252 m, Site 687 at 307 m, and Site 686 at 443 m. The sites of the latitudinal transect are Site 684 at 9°S, Site 679 at 11°S, and Site 686 at 13°S (see "Background and Scientific Objectives" section, Site 679 chapter, Fig. 1); all these latter sites are within the same water depth of 450 ± 20 m. Some general considerations apply equally to Sites 686 and 687, while others apply specifically to each site. Therefore, the first part of the respective "Background and Scientific Objectives" sections of the Site 686 and 687 chapters (this volume) are identical, whereas the second parts contain separate discussions for each site.

General Objectives

Site 687 at the southernmost end of the Lima Basin (Fig. 1) and Site 686 in the West Pisco Basin were selected to provide a continuous high-resolution record of the upwelling and climatic histories, mass accumulation rates of biogenic constituents from an upwelling regime, and detailed documentation of early diagenetic reaction pathways and products of Quaternary and possibly Neogene sediments. Upwelling objectives address the development of (1) the oxygen-minimum zone and its role in organic-matter sedimentation and preservation through time, (2) latitudinal shifts of upwelling centers during climate cycles, and (3) records of water-column parameters, especially temperature.

The History of Oxygen-Minimum Zones and Upwelling

The oxygen-minimum zone in the Peruvian upwelling regime today is strongly developed and intensifies from north to south because of cumulative oxygen consumption within the poleward-flowing undercurrent (Packard et al., 1983; Codispoti, 1983). Consequently, it shoals along its path by about 300 m through the sites on the latitudinal transect. Sea-level fluctuations and tectonism superimpose additional long-term trends on the distribution depth of sediments that were deposited within the oxygen-minimum zone. We expected sampling at the latitudinal and water/depth transects to allow us to evaluate these trends separately.

Upwelling plumes generated along today's eastern-boundary current system off Peru show a distinct zonation along their paths. The temperature increases offshore from the center, then nearshore toward the margin. The nutrient pattern changes from silica-dominated to nitrogen-dominated compositions, and the resulting biological succession likewise displays a zonal nearshore/offshore pattern that changes from phytoplankton to zooplankton dominance (Jones et al., 1983; Dugdale, 1983). Site 686 is located at the northern fringe of a prominent upwelling center around Capo Nazca (14.5°S), with Site 687 at its extreme edge. Comparing both sites to each other and to Site 681, which

is in the middle of the upwelling center at 11°S, may document the zonal structure and probable spatial shifts during climatic cycles. Bulk-sediment accumulation rates and accumulation rates of individual components (i.e., organic matter, calcium carbonate, phosphate, nitrogen, and silica) can be determined from the samples drilled at these sites.

Early Diagenesis

Rapid sedimentation rates of organic-rich sediments promote rapid sulfate reduction, methanogenesis, and associated early diagenetic carbonate reactions. Calcite and dolomite are the most widespread authigenic minerals formed during these carbon-fueled biogeochemical processes. Sites 686 and 687, with their continuous and rapid sedimentation of biogenic silica, phosphorus, and carbon, were expected to provide ample data about dissolved and gaseous compounds of pore waters, isotope characteristics, and *in-situ* temperatures of dolomite formation. With these data, the diagenesis reactions can be modeled in detail with a temporal extent rarely possible before.

Effects of Hypersaline Fluids

A new objective that affects our understanding of early diagenetic dolomitization processes emerged after Leg 112 drilling began. We consistently found indications of saline brines at sites on the shelf and upper slope. These fluids were discovered in the subsurface at Sites 680, 681, and 684. Their areal extent over the Peru margin appears enormous, but their origin remains speculative. This phenomenon is of great significance because hypersaline pore fluids strongly affect reaction pathways. Preliminary interstitial-water and gas analyses suggest that this brine continuously replenishes dissolved sulfate as the oxygen donor used by sulfate-reducing bacteria. Consequently, the competing microbial methanogenesis pathway is suppressed. Such a process could strongly alter the carbon-isotope signal of the metabolic carbon dioxide, which is incorporated in dolomites or any other authigenic carbonate minerals. The brine also is an inexhaustible source of calcium and magnesium for dolomitization. Therefore, sampling of interstitial water from Sites 686 and 687 was intensified. Special attention was directed toward detecting elevated salinity, sulfate, magnesium, and calcium contents, and any indication of methanogenesis. New data from Sites 686 and 687 about the distribution and chemistry of the this brine were expected to aid in understanding the full implications of this phenomenon.

Specific Objectives

Site 687 lies on the landward margin of the southernmost end of the Lima Basin (Fig. 1; Thornburg and Kulm, 1981). The distance from shore is only 50 km. We expected high sedimentation rates and terrigenous influx. Seismic data across the site indicated a shallow mud lens about 60 m thick that prograded seaward over older strata. This mud lens indicated strong multiple internal reflectors and retained a constant thickness upslope. The seismic section was generally thinner at Site 687 than at Site 686, which is consistent with its position higher up on the basin margin. The recent subsidence history of the Lima Basin shows slower vertical motion than that of the West Pisco Basin, which would account for the different sedimentation rates expected at both sites. Thus, at Site 687, we expected to penetrate older strata within the upper 200 m than we obtained at Site 686. We believe that, because of slower subsidence, this site recorded the oscillations of sea level during climatic cycles better than Site 686. Drilling to 200 mbsf at Sites 686 and 687 provided a 100-m overlap for depths penetrated. This was sufficient for a good correlation between sites and enabled us to compare the response of upwelling to sea-level-changes on both stable and subsiding slopes. We drilled two holes at Site 687, using the APC-XCB

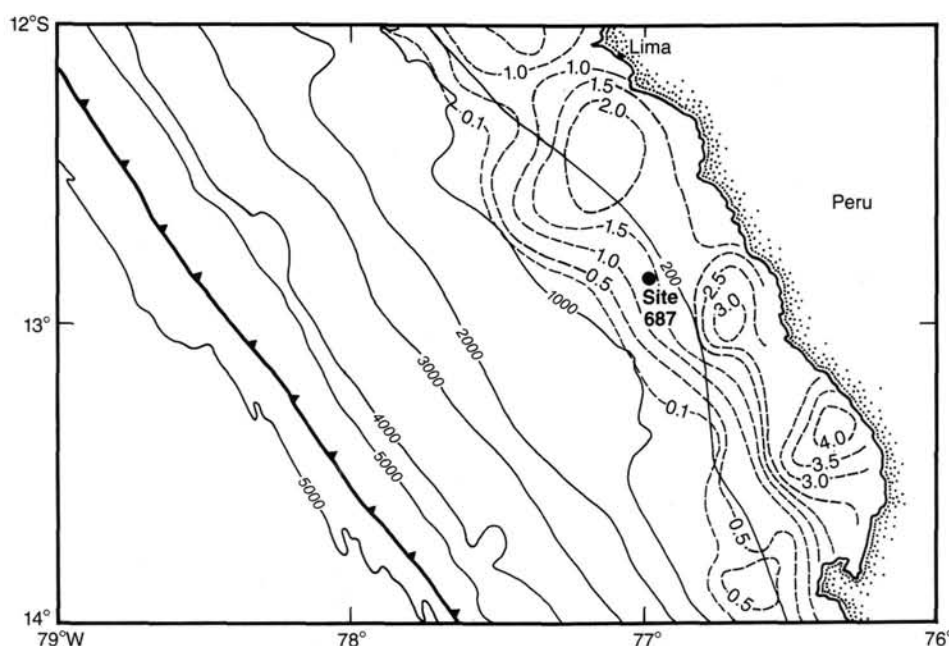


Figure 1. Bathymetry and sediment isopachs along Peru Continental Margin near Site 686. Depth contours are in 1000-m increments, beginning at a water depth of 200 m; sediment isopachs in increments of 0.5 km, beginning with 0.1 km. For an overview of all sites, see Figure 1, Site Chapter 679.

coring combination. The penetration depth provided enough sample coverage for high-resolution studies of the uppermost sediment sequence.

OPERATIONS

The ship approached Site 687 on 3 December 1986 at 1000 UTC (0500 Local) after a short transit from the previous site. The course followed SCS line YALOC 13-03-74 (Fig. 2) to locate the new site. Site 687 is situated on the broad, heavily sedimented and gently seaward-dipping flank of the West Pisco Basin in 306.8 m of water. We deployed our geophysical gear, reduced speed to 6 kt, and began our seismic survey at 1025 UTC. The survey was conducted to make sure that no acoustically turbulent features, "wipe-out" zones, or "pull-down" structures were present in the subsurface to signal free methane gas. We observed no indications of such features. During this run, the shallow seismic and depth information allowed us to readily correlate existing YALOC seismic records, as we did on the approach to the previous site. Thus, we easily identified the new site and deployed a marker buoy at 1052 hr. We retrieved our seismic gear after surveying for a short distance past this marker. The ship reversed course and was stationed over a positioning beacon, which was lowered on a taut wire.

The first APC core came on deck at 1310 hr, 3 December (0810 L). Hole 687A was drilled to a total depth of 207.0 mbsf, using the APC tool to 55.0 mbsf and the XCB tool for the remainder of the hole. Recovery of all APC cores was 100% (Table 1). Excessive overpull to retrieve Core 112-687A-6H forced us to change to XCB coring, which yielded poor recovery in a sandy interval about 50 m thick. XCB core recovery improved markedly when the sediment changed to diatomaceous silt. Modified jets on the drill bit and the soft formation encountered probably contributed to the improved recovery. Bottom-hole temperatures were measured at the following intervals: 36.0 and 55.0 mbsf using the heat-flow shoe on Cores 112-687A-4H and 112-687A-6H, and 169.0 mbsf using the *in-situ* probe after Core 112-687A-18X. Our instruments performed well during all deployments.

Hole 687B was cored in 306.8 m of water, after moving about 8 m south. The previously used APC-XCB coring combination yielded only moderately good recovery. APC core recovery was 72% down to Core 112-687B-10H at 81.3 mbsf; the next core failed to penetrate. After changing to the XCB mode of drilling, we successfully penetrated the thick sand zone but failed to recover more than 20% of the intervals cored. This variable performance continued and was probably controlled by alternating sandy and muddy layers to total depth at 195.3 mbsf (Core 112-687B-22X). Recovery was hindered by coring thick dolomite rocks twice in Cores 112-687B-17X and 112-687B-18X. We had not seen these lithologies previously during Leg 112, nor had we observed so much coarse sand as occurred at Hole 687B. During these coring operations at shallow-water depths, we used the same procedure for fast retrieval of the barrel as previously modified. The last core was brought on deck at 0355 hr. The ship was under way to the next site by 0600 L (1100 UTC) 4 December; we had spent less than one day drilling at Site 687.

LITHOSTRATIGRAPHY

Lithologic Units

The sediments recovered at Site 687 (Fig. 3 and Table 2) are divided into three lithologic units, based on visual core descriptions, smear-slide analysis, and carbonate determinations (Fig. 4 and Table 3). Units I and III are further subdivided into subunits, described in detail next.

Unit I

Cores 112-687AA-1H to 112-687A-7X, CC (15 cm); depth, 0-57.2 mbsf; age, Quaternary (<0.9 Ma).

Cores 112-687B-1H to 112-687B-7H-2, 12 cm; depth, 0-54.3 mbsf; age, Quaternary (<0.9 Ma).

Unit I is divided into two subunits (Fig. 3 and Table 2). Subunit IA consists of partly laminated, olive gray, dark olive gray, and black diatomaceous mud and extends from the surface to 20 mbsf in Hole 687A (Sample 112-687A-3H-3, 105 cm) and to

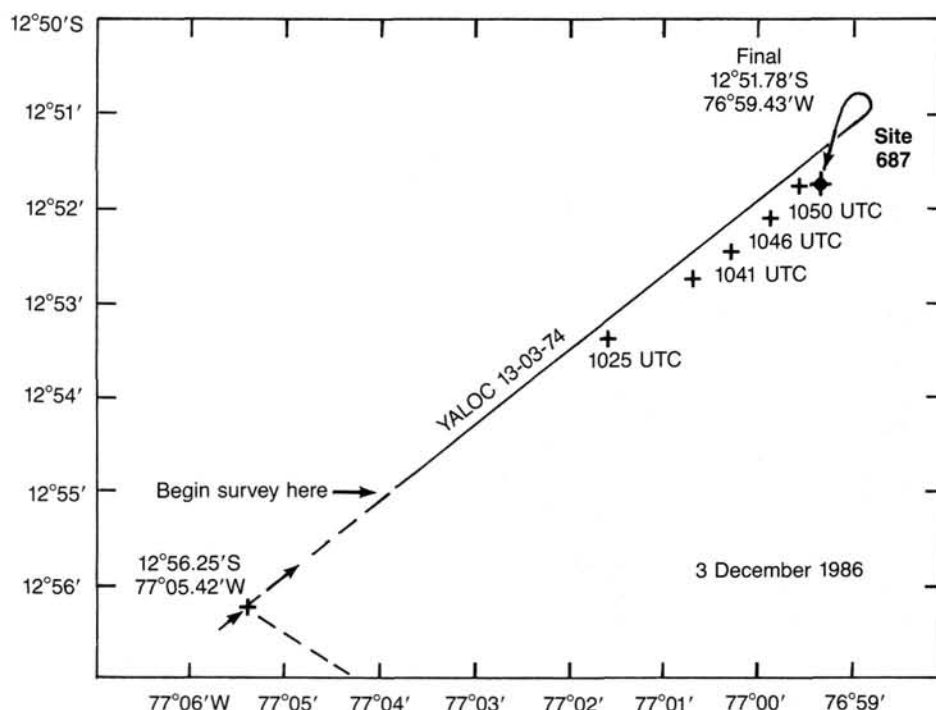


Figure 2. Track chart showing approach to Site 687 location.

26.6 mbsf in Hole 687B (Sample 112-687B-4H-2, 90 cm). Subunit IB consists of bioturbated, olive gray and gray, calcareous diatomaceous silty mud, silt, and sand.

Subunit IA is characterized by olive gray, dark olive, and black, coarsely banded and partly bioturbated diatomaceous mud and silty mud. Diatom content ranges from 3% to 100% and averages 25%. Foraminifers and nannofossils are rare or absent. Terrigenous components are quartz, feldspar, and rock fragments (in decreasing frequency). Pyrite, mica, and hornblende are common as minor constituents. Carbonate content is low (0.5% to 3%) in Subunit IA. The lamination of the diatomaceous mud consists of alternating colored bands ranging from olive to dark olive gray and black (Fig. 5). The individual bands are generally about 1 cm thick. Olive-colored bands and small specks are rich in or consist entirely of diatoms. The laminated sediments are often slightly bioturbated. Bioturbation is indicated by large (several centimeters long) burrows, olive-colored small specks, or mottling. The shallowest fluid-escape structure occurs at 8 mbsf.

Graded, 1- to 10-cm-thick sand beds containing up to 90% quartz, feldspar, and rock fragments are common in the diatomaceous muds and silts, especially in Cores 112-687A-2H and 112-687A-3H of Hole 687A. A series of six graded, olive gray, sand layers is present over a 1-m interval in Section 112-687A-2H-4. We found a 60-cm-thick layer of fine- to medium-grained, very dark gray sand in Section 12-687A-3H-1. The coarse interbeds at about 10 mbsf may be the reason for our failure to recover sediment in Core 112-687B-2H of Hole 687B.

In Hole 687B between 14.7 and 19.6 mbsf (Section 112-687B-3H-1 to Sample 112-687B-3H-4, 40 cm), we observed an interval having numerous indications of soft-sediment deformation. Folds of finely laminated material and microfaults are common. Generally, dewatering veins are associated with microfault structures when the lamination is well developed. Microfaults in gray sand are shown in Figure 6. The top of this slightly deformed interval contains a conglomerate layer of sandstone pebbles cemented by dolomite and phosphate nodules.

In comparison to the overlying section, Subunit IB is characterized by coarser and more bioturbated sediments. This unit consists of dark olive gray and gray sand and muddy silt. We observed a 6-m-thick gray and greenish-gray quartzo-feldspathic sand bed at the top of Subunit IB. The gray, well-sorted sand contains 50% to 65% quartz, feldspar, and rock fragments, 10% to 20% calcite (bioclasts and micrite), 10% to 20% pyrite, and about 10% hornblende. Foraminifers make up a percentage of the total sand, and diatoms were found in trace amounts. The transition between the sand and the overlying diatomaceous mud is indicated by an erosional contact and a 30-cm-thick layer of phosphatic sand and phosphate nodules (Fig. 7). The contact at the base of the sand bed is also indicated by an erosional contact (Fig. 8). Burrows filled with phosphatic sand from the overlying transition zone penetrate the top of the diatomaceous mud. The uppermost 5 cm of this diatomaceous mud is dolomitic, possibly indicating a longer period without deposition and lithification by carbonate precipitation.

Olive and olive gray diatomaceous mud and silt underlie the 6-m-thick sand bed and are interbedded with gray quartzo-feldspathic-lithic sand and silt. The muddy sediments contain 20% diatoms, and foraminifer and nannofossil contents range from 0% to 10%. The silts are rich in dolomite rhombs and anhedral carbonate crystals (probably calcite). Black phosphate nodules are common at the base of most sandy layers. Carbonate content ranges between 0.3% and 36% (Fig. 4 and Table 3). One-half the measured carbonate can be attributed to foraminifer tests. In smear slides, carbonate is estimated as traces to 10%. Higher estimates of foraminifer carbonate correlate well with carbonate-content measurements and were observed near the base of Subunit IB. The rest of the carbonate was probably contributed by authigenic calcite and dolomite. Coarser intervals of Subunit IB consist of calcareous silts that contain up to 35% small anhedral crystals, probably calcite. Carbonate content is 36.6% in one sample from Subunit IB (112-687A-5H-4, 82–83 cm) (Fig. 3 and Table 3). Smear-slide observations indicate that calcite is the main carbonate constituent.

Table 1. Coring summary for Site 687.

Core-section	Date (Dec. 1986)	Time (L)	Depth (mbsf)	Length cored (m)	Length recovered (m)	Recovery (%)
112-687A-1H	3	0810	0-7.5	7.5	7.55	100.0
2H	3	0820	7.5-17.0	9.5	9.74	102.0
3H	3	0830	17.0-26.5	9.5	9.72	102.0
4H	3	0905	26.5-36.0	9.5	9.85	103.0
5H	3	0920	36.0-45.5	9.5	9.55	100.0
6H	3	0945	45.5-55.0	9.5	9.65	101.0
7X	3	1015	55.0-64.5	9.5	2.30	24.2
8X	3	1040	64.5-74.0	9.5	0.25	2.6
9X	3	1055	74.0-83.5	9.5	0.05	0.5
10X	3	1115	83.5-93.0	9.5	0.30	3.2
11X	3	1140	93.0-102.5	9.5	0.28	3.0
12X	3	1200	102.5-112.0	9.5	1.82	19.1
13X	3	1220	112.0-121.5	9.5	9.32	98.1
14X	3	1245	121.5-131.0	9.5	0.70	70.5
15X	3	1305	131.0-140.5	9.5	2.68	28.2
16X	3	1325	140.5-150.0	9.5	0.05	0.5
17X	3	1340	150.0-159.5	9.5	8.63	90.8
18X	3	1410	159.5-169.0	9.5	2.32	24.4
19X	3	1610	169.0-178.5	9.5	6.12	64.4
20X	3	1630	178.5-188.0	9.5	0.95	10.0
21X	3	1655	188.0-197.5	9.5	5.68	59.8
22X	3	1720	197.5-207.0	9.5	4.78	50.3
112-687B-1H	3	1930	0-5.2	5.2	5.20	100.0
2H	3	1947	5.2-14.7	9.5	0.05	0.5
3H	3	2000	14.7-24.2	9.5	8.74	92.0
4H	3	2018	24.2-33.7	9.5	9.43	99.2
5H	3	2047	33.7-43.2	9.5	3.69	38.8
6H	3	2143	43.2-52.7	9.5	9.69	102.0
7H	3	2206	52.7-62.2	9.5	8.48	89.2
8H	3	2235	62.2-71.7	9.5	3.05	32.1
9H	3	2310	71.7-81.2	9.5	9.48	99.8
10H	3	2340	81.2-90.7	9.5	9.94	104.0
11H	4	0005	90.7-100.2	9.5	0.04	0.4
12X	4	0104	90.8-100.3	9.5	7.67	80.7
13X	4	0120	100.3-109.8	9.5	0.30	3.2
14X	4	0133	109.8-119.3	9.5	0.65	6.8
15X	4	0147	119.3-128.8	9.5	3.33	35.0
16X	4	0202	128.8-138.3	9.5	1.51	15.9
17X	4	0220	138.3-147.8	9.5	0.10	1.1
18X	4	0232	147.8-157.3	9.5	0.04	0.4
19X	4	0252	157.3-166.8	9.5	4.32	45.5
20X	4	0317	166.8-176.3	9.5	1.42	14.9
21X	4	1336	176.3-185.8	9.5	0.00	0.0
22X	4	0355	185.8-195.3	9.5	0.30	3.2

H = hydraulic piston; X = extended-core barrel; L = local time.

Graded sand beds are abundant in Subunit IB. In Hole 687A, a total of 123 graded beds were counted in the 37-m-thick Subunit IB, while this sequence contained 57 graded beds in Hole 687B. The graded beds show sharp basal contacts (Fig. 9); the top of each bed is burrowed. Cross-lamination and convoluted intervals occur in the graded beds.

Ash layers are present in three intervals. Section 112-687A-6H-4 (at 50.4 mbsf) contains a 9-cm-thick vitric tuff layer consisting of two beds. A 2-cm-thick white layer is overlain by a 7-cm-thick light gray ash layer (Fig. 10). Potassium/argon dating yields an age of 1.36 ± 0.05 m.y. for the white ash layer (Sample 112-687A-6H-4, 16-18 cm). Parts of the two ash layers can be traced 3.3 m downhole as lumps included in diatomaceous mud. We interpreted these lumps as having been transported downward by drilling, but not representing a slumping event. Similar vitric ash lumps were observed in Section 112-687B-6H-7 of Hole 687B. Another white vitric tuff layer was observed at 65 cm in Section 112-687B-6H-1 (Fig. 11). The two distinct ash layers found at 50.5 mbsf were observed previously at Site 686 (Sample 686A-17X-3, 45-57 cm; 154.6 mbsf). Thus, these layers can be used to correlate the two sites.

Unit II

Cores 112-687A-7X, CC (15 cm) to 112-687A-11X, CC; depth, 57.2-102.5 mbsf; age, Quaternary.

Cores 112-687B-7H-2, 12 cm, to 112-687B-12X-5, 150 cm; depth, 54.3-98.3 mbsf; age, Quaternary.

Unit II consists of poorly sorted, dark gray, fine sand containing 50% to 65% quartz, feldspar, and rock fragments, 5% to 15% calcite, and a percentage of pyrite, hornblende, glauconite, and mica, respectively. Diatoms are present in traces reaching up to 10%. Foraminifers are absent or rare. Shell fragments are present throughout the unit but are not common. Carbonate content is relatively high and averages 8.5% (Fig. 4 and Table 3). Because of fluidizing of the sand during drilling, no primary structure was preserved. A 3-m-thick band of gray silty mud or silty sand is interbedded in the fine sand of Hole 687B. The silty mud contains 2- to 10-cm-thick bioturbated, and possibly graded, silt and silty sand beds.

Unit III

Cores 112-687A-12X-1 to 112-687A-22X, CC; depth, 102.5-205.7 mbsf; age, Pliocene.

Cores 112-687B-12X, CC to 112-687B-22X, CC; depth, 98.3-195.3 mbsf; age, Pliocene.

Unit III is divided into two subunits (Fig. 3 and Table 2). Subunit IIIA consists of olive gray, silty, calcareous, diatomaceous mud rich in shell fragments. This unit extends from 102.5 to 155.7 mbsf in Hole 687A (Sample 112-687A-17X-4, 120 cm) and from 98.3 to 157.3 mbsf in 687B (Section 112-687B-18X, CC). Subunit IIIB consists of olive gray, calcareous, diatomaceous mud. The boundary between Subunits IIIA and IIIB was observed in Hole 687A. Shell fragments are common in Subunit IIIB and disappear below Section 112-687A-17X-4. The first dolomite bed below the disappearance of shell beds was interpreted as the transition between Subunits IIIA and IIIB.

Subunit IIIA is characterized by olive gray and greenish-gray, shell-rich silty mud that is generally bioturbated, calcareous, and diatomaceous. Diatom content ranges from 5% to 25%, and foraminifers and nannofossils range from 3% to 40% (average 5% to 20%). The terrigenous fraction consists of quartz, feldspar, and rock fragments (in decreasing frequency). Pyrite framboids are common (5% to 15%). The sediment is faintly bedded and mottled. Dolomite beds are common in both holes. Carbonate content averages 4%, but can reach values as high as 55% in shell-rich layers (Fig. 4 and Table 3). A wood fragment is present at 103 cm in Section 112-687A-17X-1. A vitric tuff layer containing 90% volcanic glass was found in Section 112-687B-16X, CC. We did not observe this distinct layer in Hole 687A, probably because of poor recovery of core.

Shell layers 1 to 15 cm thick are conspicuous in Subunit IIIA (Fig. 12). These layers consist of shell hash in a muddy matrix. The shells are mainly fragmented, although many of them may have been broken during splitting of the cores. Shells were also found in a growth position. This observation indicates that at least some of the shells are autochthonous, but the more concentrated layers may have resulted from current sorting or winnowing. Shelly intervals are common in the top section and near the base of Subunit IIIA. Between 130 and 150 mbsf, recovery of core was poor, possibly indicating the presence of sandy sediments in this interval.

Subunit IIIB consists of olive gray, calcareous, silty, diatomaceous mud and gray, dolomitic and calcitic, diatomaceous mud. Diatom content ranges from 10% to 30%. Foraminifers and nannofossils are 5% to 20% of the total sediment. The ol-

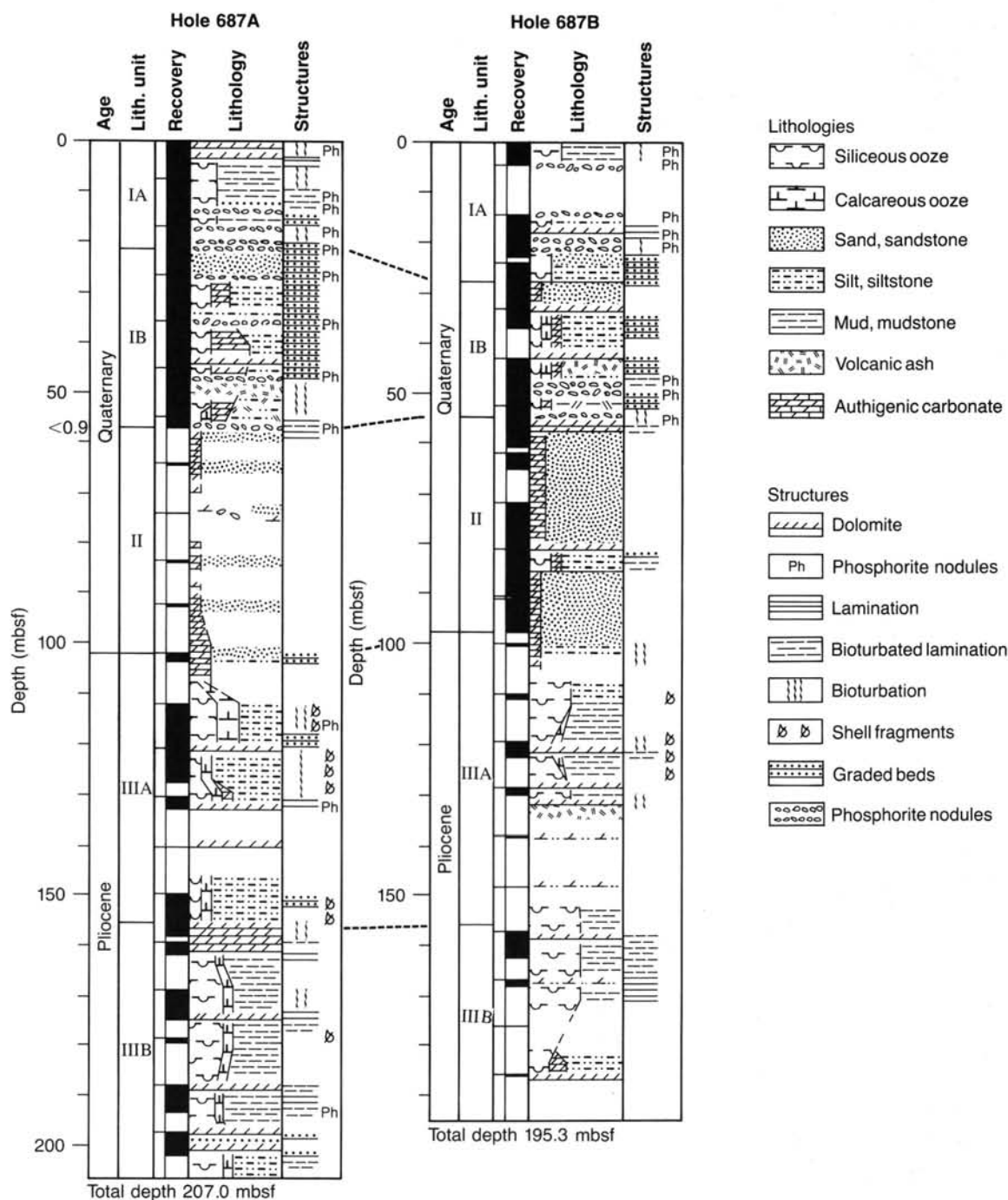


Figure 3. Generalized stratigraphic column of Site 687. Holes 687A and 687B were correlated using ash beds, dolomite layers, sand beds, and other distinct breaks in lithology. Width of the lithological columns is proportional to amounts estimated from smear-slide analysis.

ive gray diatom-foraminifer mud is laminated, and the gray dolomitic-calcitic mud is massive. Dolomite layers are common throughout the subunit, especially at the top. Carbonate content is similar to average values of Subunit IIIA (about 4%).

Diagenesis

Phosphates

Friable phosphates ("F-phosphates"; for definitions see "Lithostratigraphy" section of Site 680 chapter, this volume) are rare at Site 687. They occur as small yellow brown nodules,

mainly in the diatomaceous mud of Subunit IA. The shallowest occurrence was at 1.9 mbsf (Sample 112-687A-1H-2, 40 cm).

Dense phosphates ("D-phosphates") are abundant in Unit I, although these are present throughout the three units of Site 687. The shallowest occurrence is a single, hard, phosphate nodule at 0.65 mbsf (Sample 112-687B-1H-1, 65 cm). These phosphates are dispersed as either single nodules in the sediment or are included in the graded beds as a major component. Phosphate conglomerates are also common at erosional contacts (Figs. 8 and 13), and phosphate-cemented shells (Fig. 7) or bones are present in several cores.

Table 2. Lithologic units at Site 687.

Lith. unit	Lithology	Core-section interval (cm)	Depth (mbsf)
I	Core catcher placed below -7X-2 but not on top of -7X-8	112-687A-1H-1 to -7X, CC (15) 112-687B-1H-1 to -7H-2, 12	0-57.2 0-54.3
IA	Diatomaceous mud, laminated	112-687A-1H-1 to -3H-3, 105 112-687B-1H-1 to -4H-2, 90	0-20.0 0-26.6
IB	Calcareous diatomaceous silty mud and silt, bioturbated	112-687A-3H-3, 105 to -7X, CC (15) 112-687B-4H-2, 90 to -7H-2, 12	20.0-57.2 26.6-54.3
II	Fine sand	112-687A-7X-CC, 15 to -11X, CC 112-687B-7H-2, 12 to -12X-5, 150	57.2-102.5 54.3-98.3
III		112-687A-12X-1 to -22X, CC 112-687B-12X, CC to -22X, CC	102.5-205.7 98.3-195.3
IIIA	Calcareous diatomaceous mud, shell rich, bioturbated	112-687A-12X-1 to -17X-4, 120 112-687B-12X, CC to -18X, CC	102.5-155.7 98.3-157.3
IIIB	Calcareous diatomaceous silty mud, dolomitic	112-687A-17X-4, 120 to -22X, CC 112-687B-19X-1 to -22X, CC	155.7-205.7 157.3-195.3

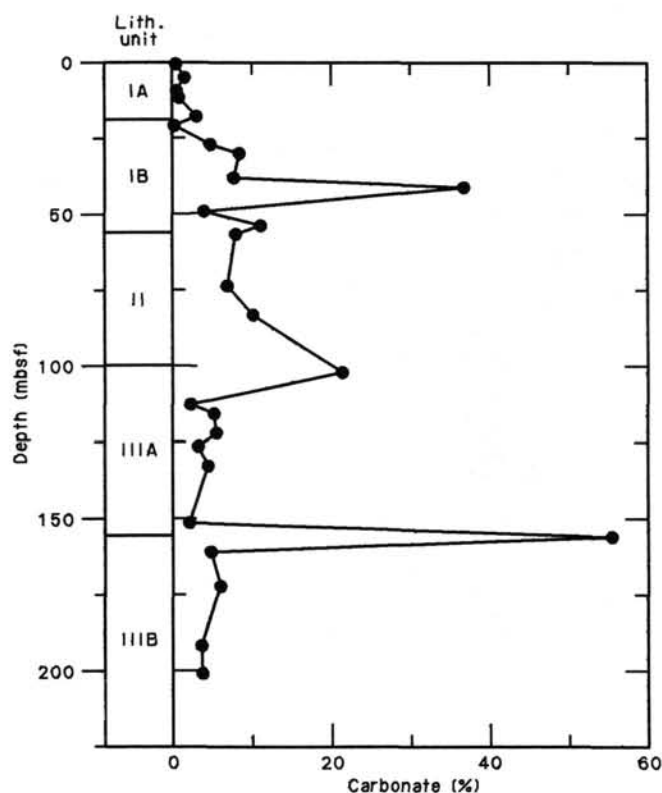


Figure 4. Carbonate contents in Hole 687A. See Table 3 for a listing of data.

Authigenic Carbonates

Both authigenic calcite and dolomite are present in the sediments at Site 687 as disseminated crystals in unlithified sediments and as fully lithified nodules and beds. Dolomitic nodules or dolomitized sands, silts, or muds are most abundant in Units I and III. The first lithified carbonate observed was a small porous dolomitic nodule in black diatomaceous mud at a sub-bottom depth of 71-74 cm in Section 112-687A-1H-1. Hard beds are commonly dolomitized sands, silts, or shell beds. Differences in grain-size distribution and the bedding of the original sediment are still preserved (Fig. 14), and burrows filled with different sediments are still visible in the dolomitic rock (Fig. 15).

A cemented shell bed was found in both holes at about the same depth below seafloor (Samples 112-687A-14X-1, 10-15 cm,

Table 3. Carbonate contents in Hole 687A.

Core-section interval (cm)	Depth (mbsf)	CaCO ₃ (%)
112-687A-1H-1, 61-62	0.61	0.50
1H-4, 61-62	5.11	1.58
2H-2, 55-56	9.55	0.67
2H-3, 142-143	11.92	0.92
3H-1, 86-87	17.86	3.09
3H-3, 86-87	20.86	0.33
4H-1, 58-59	27.08	4.84
4H-3, 58-59	30.08	8.42
5H-2, 82-83	38.32	7.84
5H-4, 82-83	41.32	36.61
6H-3, 96-97	49.46	4.00
6H-6, 102-103	54.02	11.18
7X-2, 34-35	56.84	8.01
8X, CC, 11-12	73.91	7.01
10X, CC, 11-12	83.41	10.17
11X, CC, 13-14	102.43	21.27
13X-1, 75-76	112.75	2.34
13X-3, 75-76	115.75	5.25
14X-1, 47-48	121.97	5.50
14X-4, 47-48	126.47	3.25
15X-2, 44-45	132.94	4.50
17X-2, 30-31	151.80	2.09
17X-5, 30-31	156.30	55.13
18X-2, 35-36	161.35	4.84
19X-3, 46-47	172.46	6.00
21X-3, 103-104	192.03	3.67
22X-3, 61-62	201.11	3.75

and 112-687B-15X-2, 63-67 cm). The incorporated shells are single as well as paired (Fig. 16). The shell material was partially dissolved, leaving open moldic porosity. If the shells originally contained both calcitic and aragonitic layers, then the aragonitic part might have been dissolved. In Section 112-687B-15X-2, the calcitic or dolomitic bed was apparently formed in association with a shell-hash zone. In this case, the shells seem to be concentrated at the base of the carbonate layer. The coincidence in the depth below seafloor of the shell-bearing carbonates between the two holes suggests that individually cemented beds are laterally continuous. This hypothesis is further supported by frequent occurrence of dolomitic hard beds in distinct intervals, e.g., at about 160 mbsf (Fig. 3).

Dolomite and calcite are common in all units as disseminated crystals. These are most abundant in Subunits IB and IIIB, Unit II, and the shell-barren sections of Subunit IIIA. The highest authigenic carbonate values (estimated from smear slides) occur in the sandy and silty sediments of Subunit IB. Dolomite is more common than calcite. Calcite is usually more abundant

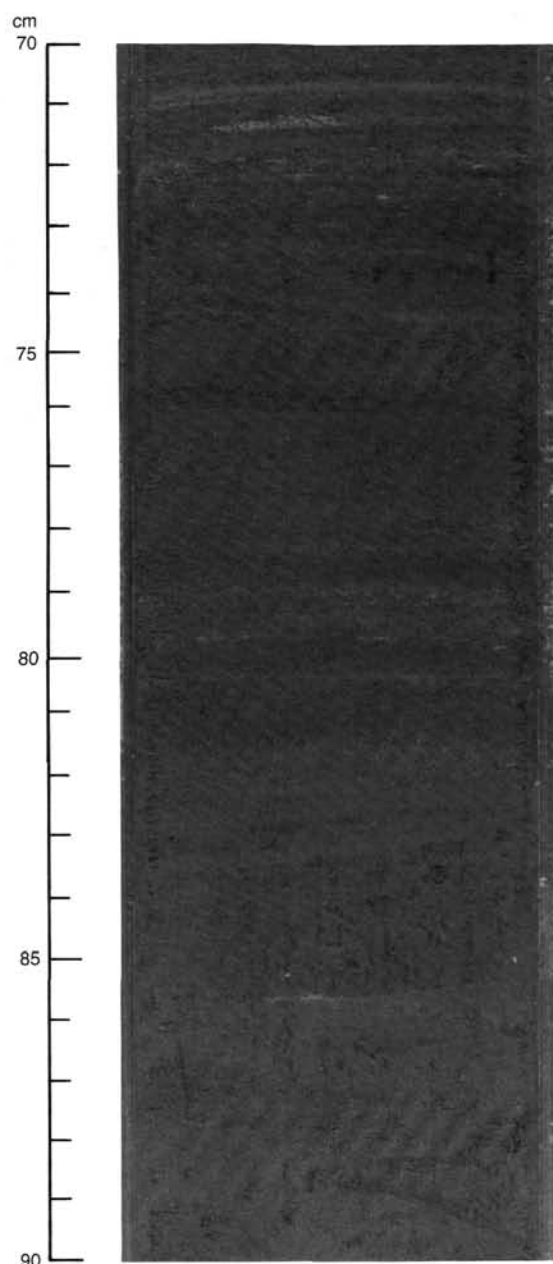


Figure 5. Olive gray and dark olive gray, laminated, diatomaceous mud, slightly bioturbated (Sample 112-687A-1H-4, 70–90 cm).

in the muds, and dolomite is more common in the silts and sands.

Environments of Deposition

The three lithologic units recognized at Site 687 consist of a fine-grained sediment of Pliocene age (Unit III), a coarser unit of early and/or middle Quaternary age mostly of sand (Unit II), and a section of fine-grained material interrupted by mostly graded sand (Unit I) of less than 0.9 m.y.

We believe that this sequence is related to changes in sea level. In the Pliocene, during deposition of the lower unit of Site 687, water depth was probably similar to or deeper than today. Water depth decreased toward the Pliocene/Pleistocene transition. From biostratigraphic data (see "Biostratigraphy" section, this chapter), the sandy interval (Unit II) should have been deposited between about 1.8 and 0.9 Ma. The sand may have been

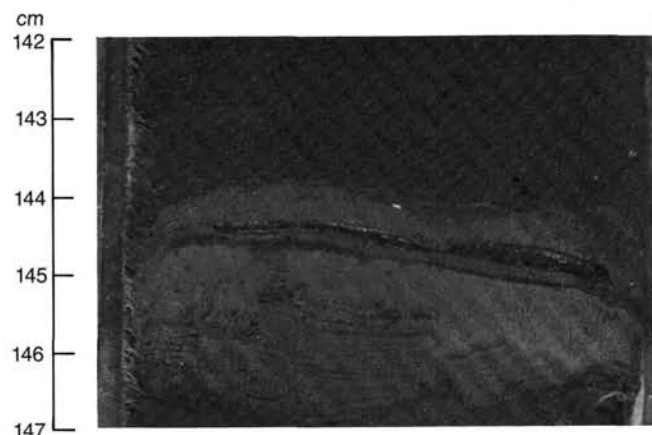


Figure 6. Normal microfaults developed by differential compaction across a sandy bed in diatomaceous muds; see sketch in Figure 18C (Sample 112-687B-3H-3, 142–147 cm).

deposited in a relatively short period of time, and Unit II may contain major hiatuses. Major hiatuses, indicated by numerous phosphate nodule conglomerates associated with sharp breaks in lithology and deep burrows at the base of the conglomerate, are present. Water depth was probably lower during this interval. Starting at about 0.9 Ma, water depth increased, resulting in the deposition of fine-grained material.

The deposition of Subunit IB, rich in graded sand beds, possibly started at the time when larger amplitudes in the $\delta^{18}\text{O}$ -curves were observed (e.g., 0.8 Ma; Shackleton and Opdyke, 1973) as a result of major glaciations and more substantial lowering of sea levels during glacial periods. Thus, Unit I was deposited in a slope environment, where the water depth fluctuated markedly with time.

The shell-rich layers in Subunit IIIA, probably deposited during the late Pliocene, represent a different depositional environment. At least some of the shells are still in a growth position. Therefore, we believe that bivalves lived in this environment, perhaps at intermediate water depths between the upper slope (deposition of Subunit IIIB) and shelf (deposition of Unit II). An outer-shelf environment with sufficient oxygen (provided by the surface waters) and a high food supply (from nearby upwelling) may have provided the optimum conditions for the bivalve fauna of Subunit IIIA.

Deposition of Graded Beds

Graded silt and sand beds occurred throughout the cores of Site 687 and were abundant in Subunit IB. Table 4 gives an example of size- and component-distribution in a graded bed of Subunit IB. In general, the graded beds have a sharp base and a bioturbated top section. The sediments just above the base contain 95% sand-sized particles. The sand content decreases upward to 10% in the top interval of the bed. Several depositional processes may explain the presence of these beds: turbidity currents, contour currents, or spillover from the shelf break.

The relatively immature composition of these sediments, which includes up to 8% hornblende (Table 4) in the sand fraction, implies rapid transportation from a terrigenous source to the upper slope. We believe it unlikely that such immature sands could have spent much time in a high-energy shelf or coastal environment.

The graded bedding of the sediments indicates deposition from a poorly sorted suspension, such as a turbidity current. However, in the relatively shallow water depths suggested for Subunit IB, processes other than turbidity currents should be considered. Graded beds may result from resuspension on the

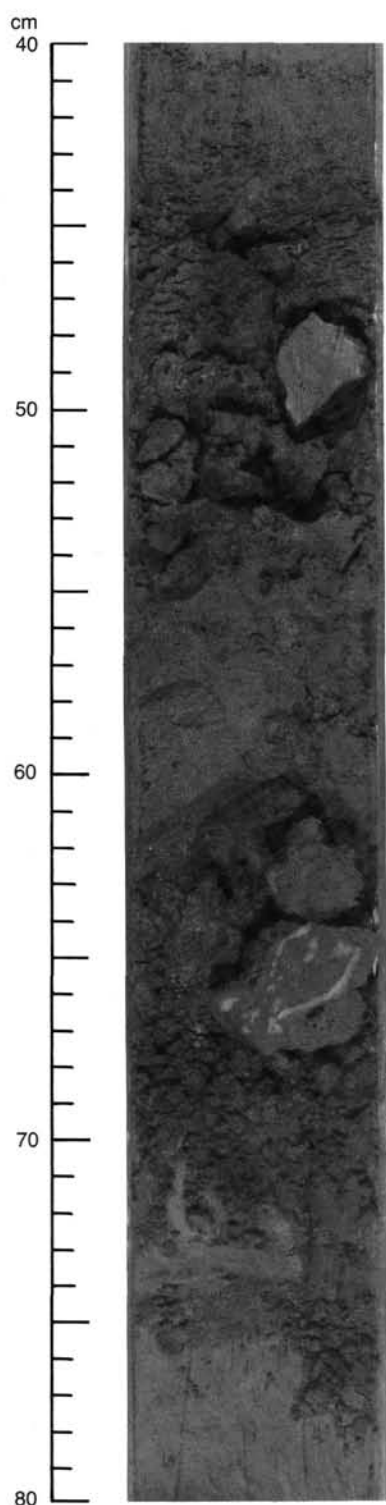


Figure 7. Phosphatic sand and nodules interbedded in dark olive gray diatomaceous mud. One nodule contains bivalve shell fragments (Sample 112-687A-3H-3, 40–80 cm).

shelf in response to wave- or wind-forced currents, followed by a waning of the high-energy conditions (Walker, 1984). Thornton (1984) described upper-slope sand sheets transported by shelf currents in the Santa Barbara Basin. Such reworking of shelf deposits tends both to sort the source sediment on the shelf and to mature the sediments compositionally. Obviously, the graded

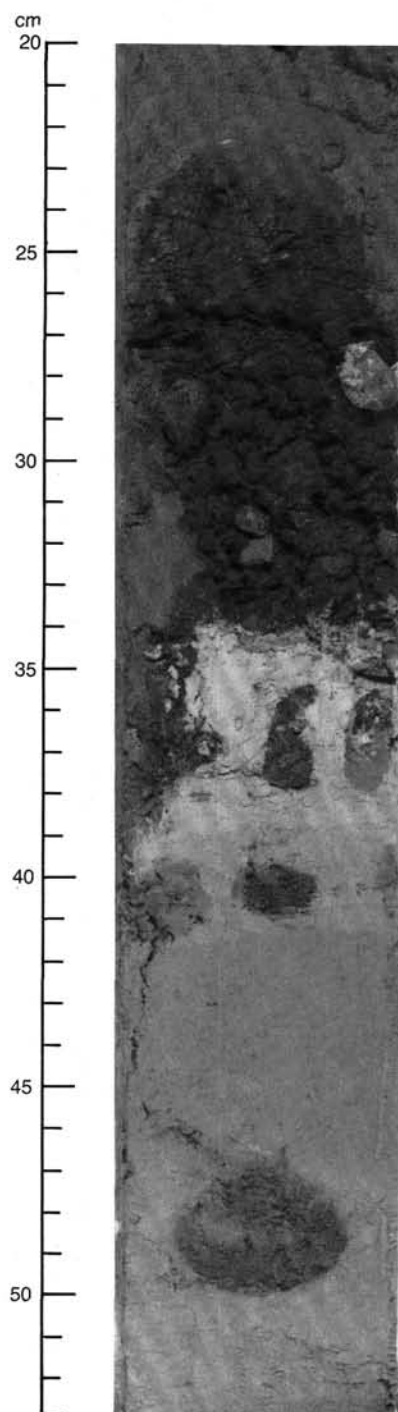


Figure 8. Erosional contact between gray green and olive green mud (bottom of figure) and very dark gray sand (top of figure). The transition zone consists of dark brown diatomaceous mud having black phosphate nodules. The light-colored interval between 34 and 39 cm consists of dolomicrite, probably indicating a break in deposition and the formation of a hardground (Sample 112-687A-5H-1, 20–53 cm).

beds have a composition distinct from the background hemipelagic deposits and contain small amounts of biogenic material, even in the finer fraction. Therefore, these beds probably do not derive from shelf resuspensions.

We interpreted the graded beds of Subunit IB as turbidites. We did not have enough detailed shelf bathymetry to recognize transportation routes (such as gullies or canyons), although it

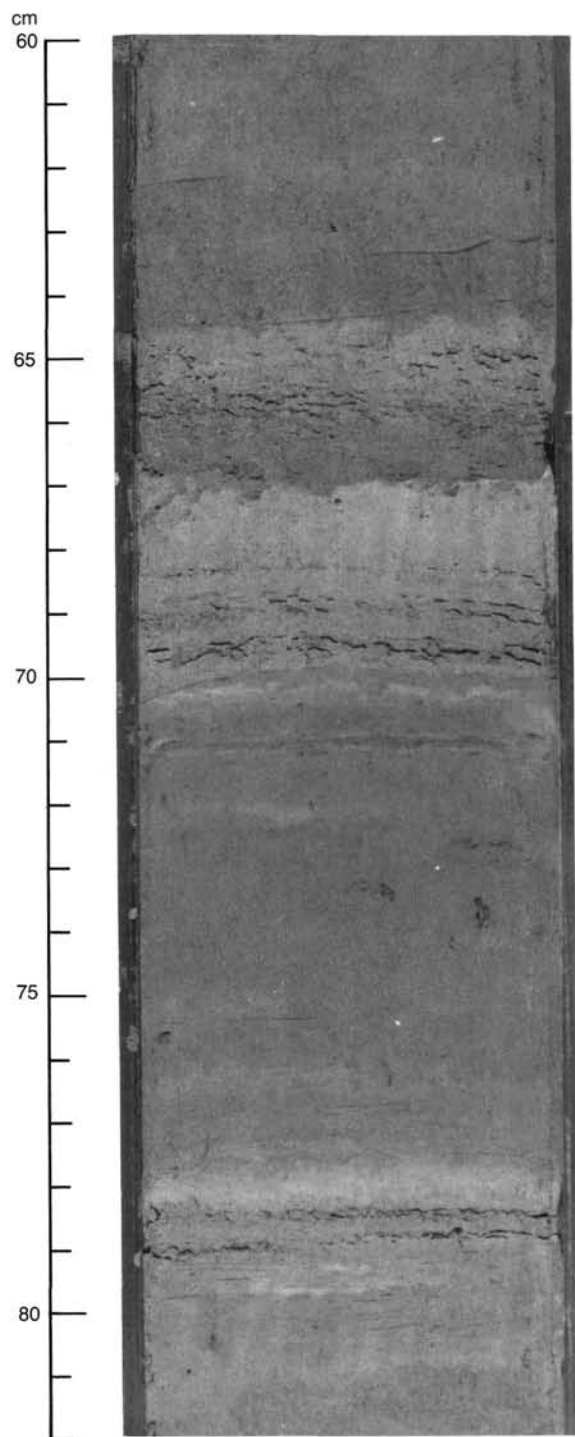


Figure 9. Graded sand beds showing sharp contacts at the base (e.g., at 67 and 70 cm) and burrows at the top of the graded interval (Sample 112-687A-4H-2, 60–82 cm).

seems likely that the turbidity currents originated in shallow water, where a terrigenous sediment supply was available. Floods related to El Niño-type events are common in the Andes foothills (Quinn et al., 1978), and it is possible that a direct river outflow may have generated the turbidity currents. However, a more detailed seismic and coring program will be required to substantiate such a hypothesis.

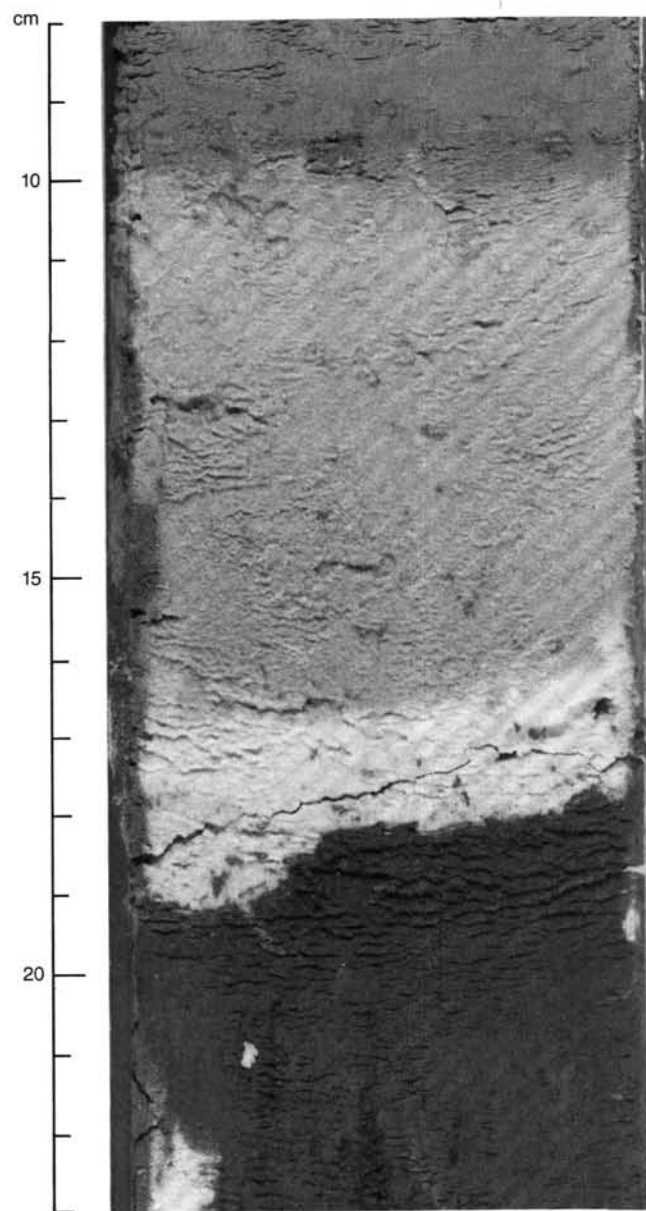


Figure 10. A 9-cm-thick, white and light gray, vitric tuff layer consisting of two graded beds (Sample 112-687A-6H-4, 8–23 cm).

Structure

Structures observed at Site 687 include slump folds and convolute bedding, dewatering veins, and both normal and reversed microfaults.

Slump Folds and Related Features

Fold noses, inclined bedding, and convolute bedding that result from slumping and intraformational sliding were observed in only a few cores at Site 687. Such features probably cannot be recognized in bioturbated or massive intervals, or where drilling disturbance and poor recovery preclude recognition, as is true for much of the material recovered at this site. Slump folds and related features occur at Samples 112-687A-2H-2, 65–75 cm, 112-687A-2H-3, 85–115 cm, 112-687A-5H-3, 45–52 cm, and throughout 112-687B-3H, especially at 112-687A-1H, 85–150 cm, 112-687A-1H-2, 10–100 cm, and 112-687A-1H-4, 40–43 cm.

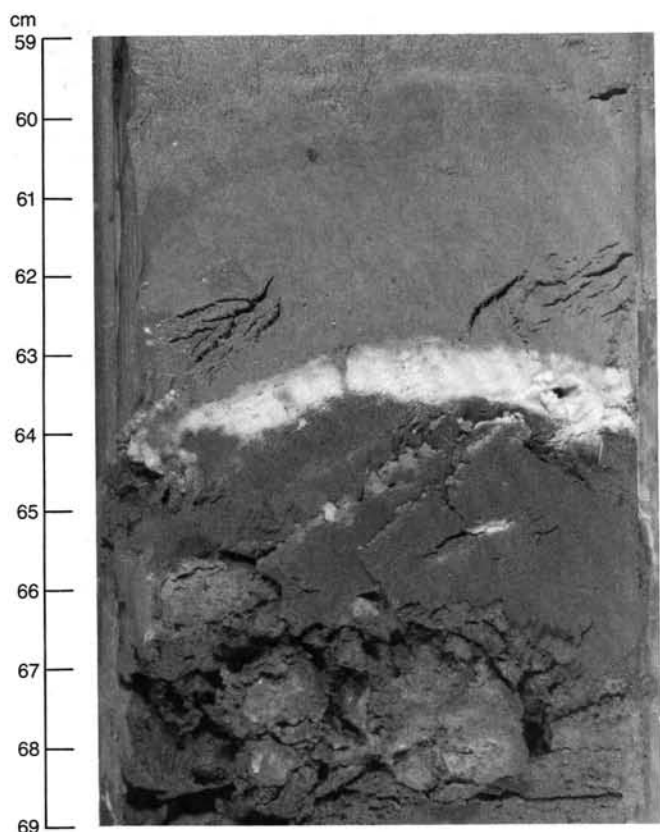


Figure 11. White vitric tuff layer overlying olive gray mud with dolomitized zone (Sample 112-687B-6H-1, 59–69 cm).

Dewatering Veins

Mud-filled veins that are oriented perpendicular to bedding are present throughout at least the upper parts of Holes 687A and 687B (e.g., Core 112-687A-2H, all sections; Sections 112-687A-3H-2 and 112-687A-3H-3; Sections 112-687A-6H-1 to 112-687A-6H-3; Core 112-687B-3H, Sections -2, -3, -5; and Core 112-687B-6H, Sections -4 to -6). These veins typically originate within a coarser-grained silty or sandy interbed and may be sigmoidal in shape (Fig. 17), which suggests a shearing component. In some cases, the veins are located along extensional microfaults (e.g., Sample 112-687B-3H-2, 70–150 cm), which suggests that dewatering and extension occurred contemporaneously.

Microfaults

Only one example of a reverse microfault, in which a slump fold nose is cut by a reverse fault (Sample 112-687B-3H-4, 40–43 cm; See Fig. 18) was observed at Site 687. In most cases, normal microfaults (Samples 112-687A-21X-4, 29–34 cm; 112-687B-3H-1, 25–30 cm; 112-687B-3H-2, 70–150 cm; 112-687B-3H-3, 142–147 cm) are associated with dewatering veins (Fig. 18) or with compaction (Figs. 18 and 6). The microfaults in Figure 18 rise to, but do not penetrate, a zone of decollement above which the beds are folded by slumping or by intraformational sliding. Presumably, the zone of decollement itself served as a dewatering conduit so that the veins did not develop above it. Movement of fluid along such a surface could have facilitated development of the folds. The microfaults shown in Figures 18 and 6 developed in a bed of gray sand having offset laminae but do not penetrate beds above and below the sand. This suggests that the microfaults in this case developed as a result of differential compaction of the sand bed.

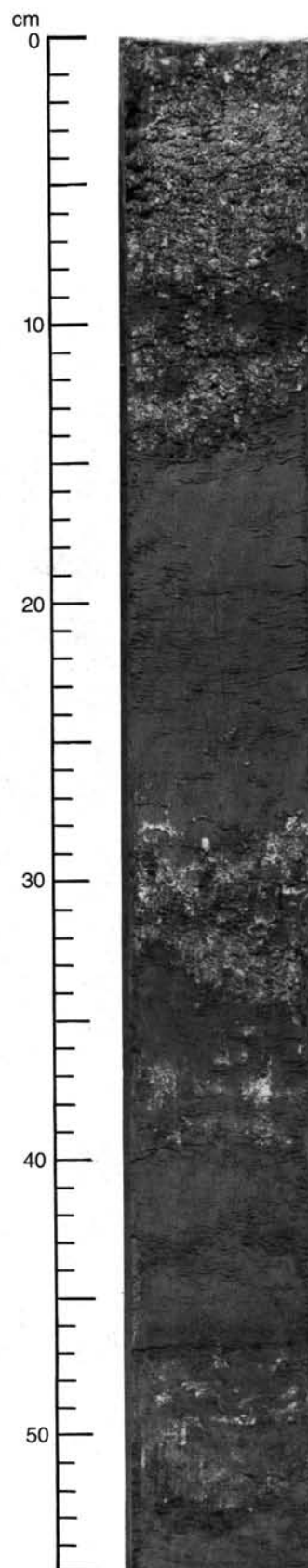


Figure 12. Shell concentrations containing broken bivalve shells. Some shells are in a growth position (47–50 cm) (Sample 112-687A-13X-2, 0–55 cm).



Figure 13. Erosional contact between silty muds (top and bottom). The transition zone consists of dark olive gray to black phosphatic sand and phosphatic nodules. The top of the underlying section shows burrows filled with phosphatic sand (Sample 112-687B-3H-5, 27–57 cm).

BIOSTRATIGRAPHY

Two holes were drilled at Site 687 to recover upwelling sediments of late Neogene and Quaternary age. Hole 687A penetrated 207.0 m, and Hole 687B penetrated 195.3 m of Quaternary and Pliocene sediments. The base of the Quaternary was reached at 127.92 m in Hole 687A and at 110.22 in Hole 687B.

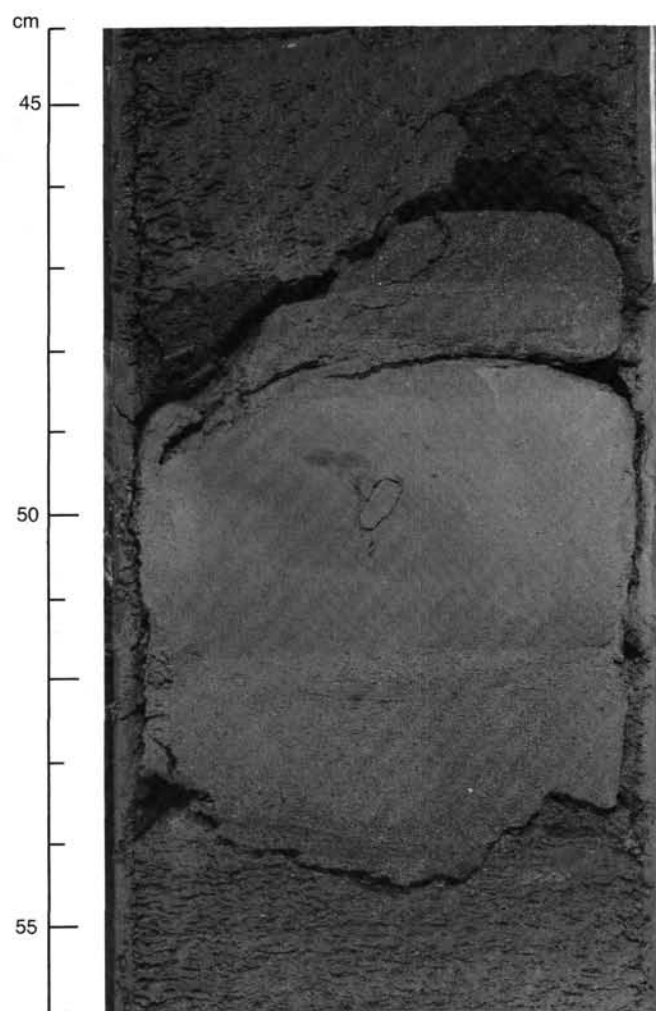


Figure 14. Dolomicrite or dolomitized diatomaceous sandy silt with about 50% authigenic carbonate, interbedded with olive dolomitic diatomaceous silt. About one-half of the minerals are dolomitic rhombs and the other one-half consist of anhedral crystals, probably calcite (Sample 112-687A-5H-6, 44–56 cm).

As usual in upwelling areas, diatoms form the major part of fossil assemblages and show frequent blooms as well as indications of cold- and warm-water masses at various times. These indicate different periods with strong persistent coastal upwelling and periods with more oceanic influence and less persistent upwelling. Calcareous nannoplankton, planktonic foraminifers, radiolarians, and silicoflagellates were found occasionally but were poorly distributed in both Holes 687A and 687B. Benthic foraminifers are common throughout. These document eustatic sea-level fluctuations as well as subsidence of the seafloor from a middle-shelf depth of about 50 m in the middle part of the section to a depth of 307 m.

We noticed reworked Miocene and Eocene microfossils (calcareous nannoplankton, diatoms, and radiolarians) in several samples from both holes. The sedimentation rate in the Quaternary is about 55 to 60 m/m.y.

Diatoms

Preservation of diatoms was very good to excellent; abundant diatoms were observed in the hemipelagic muds recovered at Site 687 and drilled in a water depth of 306.8 m. These fossils are rare and have moderate to poor preservation in sandy intervals. Floras are indicative of strong coastal upwelling, which can

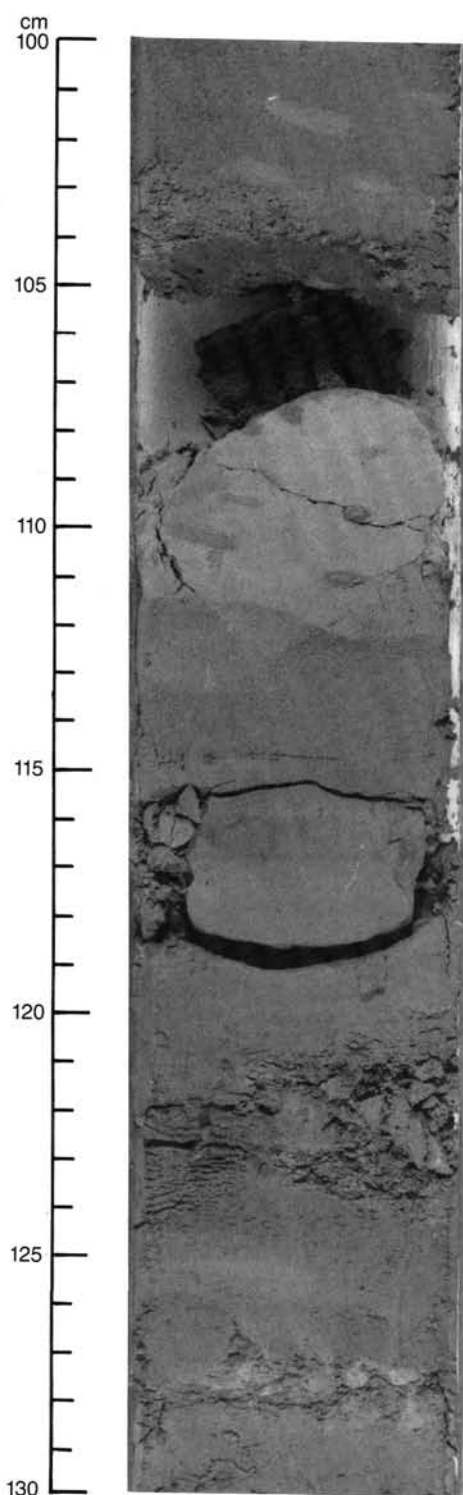


Figure 15. Dolomitic siltstone (containing 55% dolomite) interbedded in diatomaceous mud (Sample 112-687A-5H-3, 100–130 cm).

be grouped into four stages (see Fig. 19 and Table 5). Based on core-catcher samples, Holes 687A and 687B penetrated identical sedimentological units at about the same depth down to 100 mbsf. Below that depth, the correlation was obscured by extremely poor recovery.

A major floral change occurs in Cores 112-687A-14X (121.50–127.92 mbsf) and 112-687B-14X (109.80–110.22 mbsf). New

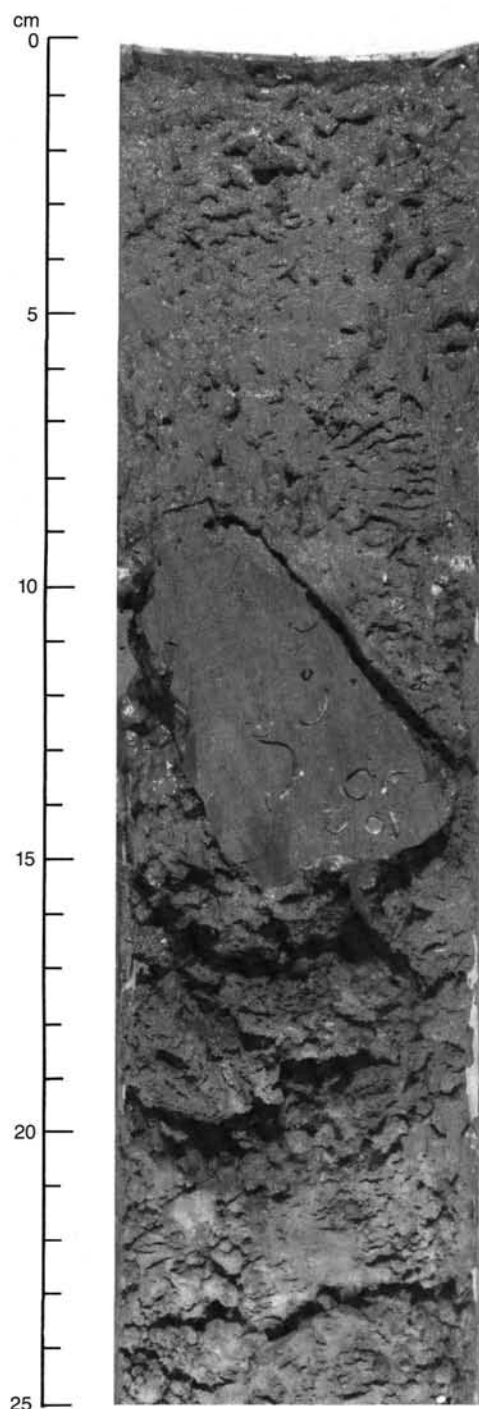


Figure 16. Cemented limestone containing paired and single bivalve shells. The carbonate of the shells is partially dissolved, leaving open moldic porosity (Sample 112-687A-14X-1, 0–25 cm).

members of the *Nitzschia* and *Thalassiosira* genera occur; these are not present above these levels.

In the hemipelagic mud sequences (which are interrupted by sand layers), thin, grayish-brown diatomaceous layers do occur. These frequently contain monospecific assemblages of diatoms (*Cyclotella striata/stylorum*, *Thalassiosira eccentrica/nordenskiöldii*, *Chaetoceros* spore/setae), and silicoflagellates (*Dictyocha messanensis*). Whether these monospecific layers are produced by huge monospecific surface blooms or by size-sorting bottom currents remains unresolved.

Table 4. Distribution of grain sizes and components in a graded bed (Section 687B-4H-1).

Interval (cm)	S	S (%)	C	QFR (%)	H (%)	Clay (%)	Calc/Dol (%)	Foram. (%)	Diatoms (%)	Other (%)
104	10	60	30	40	5	20	20	2	5	8
104.5	15	75	10	70	8	2	3	1	1	15
105	20	70	10	72	5	5	3	3	5	7
106	95	5	—	73	—	—	10	—	—	17

SSC = sand, silt, and clay; QFR = quartz, feldspar, and rock fragments; H = hornblende; Foram. = foraminifers; Calc/Dol = calcitic/dolomitic.

Rhizosolenia matuyama was last seen in Core 112-687A-6H (55.07 mbsf) and in Core 112-687B-7H (61.13 mbsf); the first occurrence was detected in Section 112-687A-13X, CC (121.15 mbsf). Poor recovery in Hole 687B did not reveal this first appearance datum (FAD). *Pseudoeunotia doliolus* was present in samples above Sections 112-687A-14X, CC (127.92 mbsf) and 112-687B-14X, CC (110.22 mbsf). *Nitzschia fossilis* was present in all diatom-bearing samples below these two zones and occurred sporadically above them. Ecological exclusion of either *Pseudoeunotia doliolus* or *Nitzschia fossilis* is not a factor in their distribution; thus, we placed the Pliocene/Pleistocene boundary at 127.92 mbsf in Hole 687A and at 110.22 mbsf in Hole 687B. *Nitzschia kolaczekii* occurred in Section 112-687A-16X, CC and below, and in Section 112-687B-15X, CC. This species was reported by Akiba (1985) in Nankai Trough and Japan Trench DSDP sites from the *Neodenticula seminae* Zone, which is of latest Quaternary age. As Akiba (1985) counted only 100 diatom valves per sample, ranges of rare diatom species are unreliable. As no *Thalassiosira convexa* and only a sin-

gle specimen of *Actinocyclus oculatus* were encountered, the lowermost samples of both holes are slightly older than the FAD of *A. oculatus* (around 2.1 Ma) and younger than the last appearance datum (LAD) of *T. convexa* (around 2.3 Ma). The truly oceanic *Rhizosolenia praebergonii* is excluded from this highly variable (in terms of temperature and salinity) environment.

Sedimentation rates, based on the LAD of *Rhizosolenia matuyama* and on the LAD of *Pseudoeunotia doliolus*, are about 65 m/m.y.; this rate seems to be slightly higher in Hole 687A (see Fig. 20).

Correlation between the two holes is based on the occurrence of nonrepetitive floral assemblages, which seem to be confined to short periods of time. Several zones stand out, such as the major floral change, the mass occurrence of a delicate *Thalassiosira*, and the occurrence of triangular *Actinopterychus* aff. *undulatus* (see Fig. 19).

Phytoplankton assemblages were grouped into four coastal upwelling phases that can be clearly separated from oceanic high productivity (see Table 5). In general, the spacing of core-catcher samples does not permit continuous resolution of the temporal variability of the "southern" Peruvian upwelling center. However, even at this stage of investigation, we foresee major trends (compare left side of Fig. 20), such as periods having strong, persistent coastal upwelling between 0–0.45, 0.65–1.4, 1.75–1.85, 2.0–2.5 and 2.6–? Ma, and periods with more oceanic influence and less persistent coastal upwelling during the intervening periods. Once the stratigraphic sequence and dating of the major sequence is complete, a more refined subdivision will be possible.

Reworked Miocene (*Denticula hustedtii*) and Eocene (*Pyxilla reticulata* and *Hemiaulus* sp.) diatoms were observed only rarely in some samples (Sections 112-687A-13X, CC; 112-687A-16X, CC; 112-687A-20X, CC and 112-687A-22X, CC; 112-687B-14X, CC; 112-687B-15, CC; 112-687B-16X, CC, and 112-687B-22X, CC). No displaced freshwater diatoms were found in the core-catcher samples. Displaced marine benthic diatoms were exceptionally rare, compared with those observed in the northern sites from comparable water depth.

The coarse fraction of the diatomaceous core-catcher samples contained large quantities of fish scales, some fish teeth, benthic and planktonic foraminifers (see section on "Biogenic Groups, Coarse Fraction Analysis" below for detailed occurrence plots), radiolarians in abundances of more than 10 individuals per slide, amorphous organic matter clumps, and infrequent terrestrial organic matter in traces of cuticular plates and tracheoidal wood fragments. The terrestrial component did not seem to be enriched in the more sandy core-catcher samples.

Silicoflagellates

We studied only core-catcher samples from Hole 687A for silicoflagellates. The Quaternary silicoflagellate assemblage is dominated by members of the *Dictyocha messanensis* group. *Mesocena quadrangula* was found in Sections 112-687A-4H, CC (36.0 mbsf) and 112-687A-13, CC (121.1 mbsf). *Distephanus*

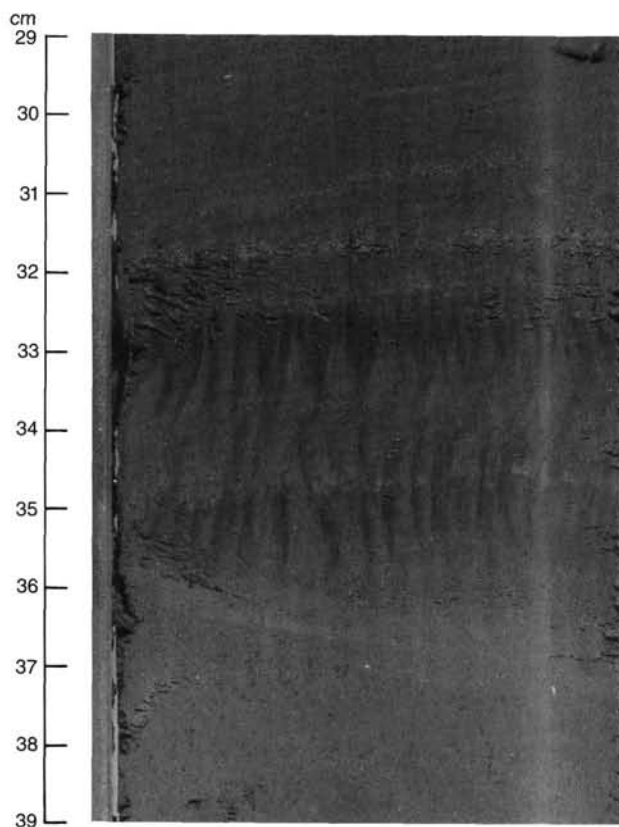


Figure 17. Sigmoidal dewatering veins filled with dark mud (Sample 112-687A-6H-1X, 29–39 cm).

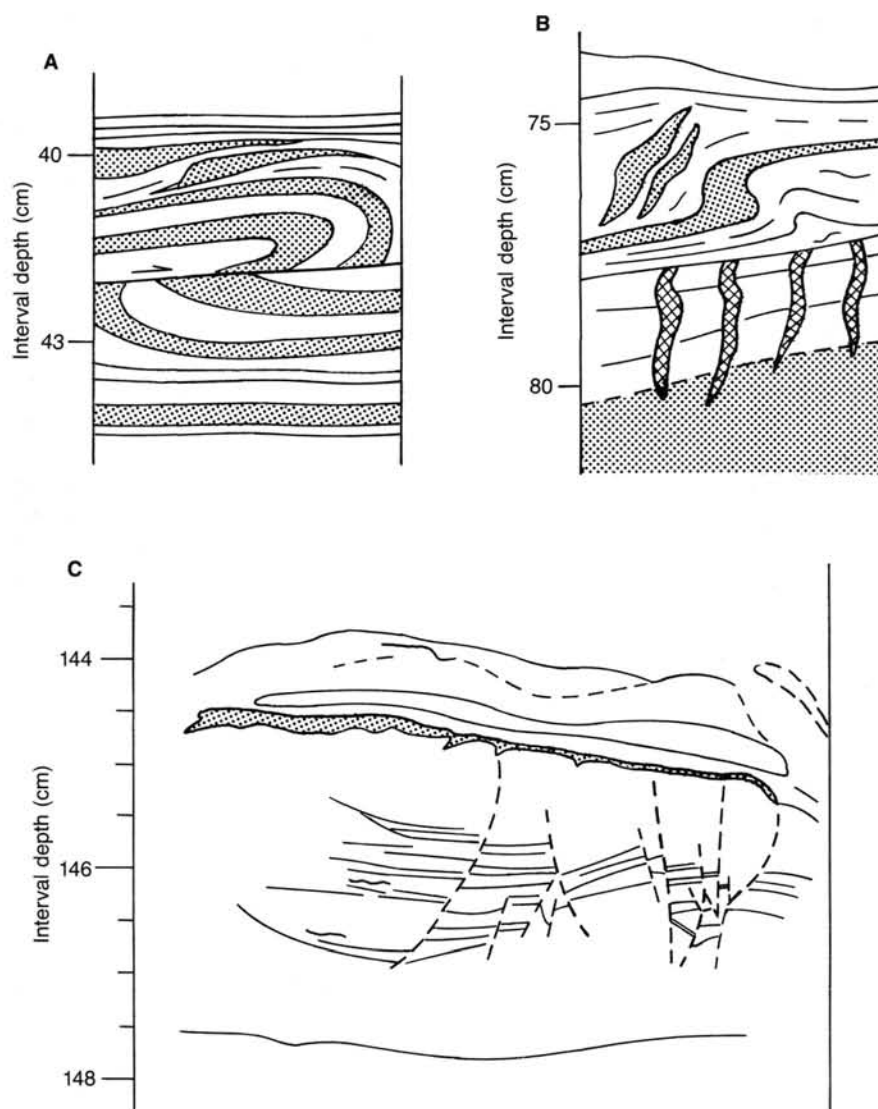


Figure 18. Sketches of structural features at Site 687. A) Slump fold nose offset by reverse microfault (Sample 112-687B-3H-4, 40–43 cm). B) Dewatering veins and normal microfaults overlain by décollement and folded beds; see text for discussion (Sample 112-687B-3H-2, 75–80 cm). C) Interpretive sketch of normal microfaults shown in Figure 6 (Sample 112-687B-3H-3, 144–148 cm).

bioconarius bioconarius occurs between Sections 112-687A-1H, CC (7.4 mbsf) and 112-687A-17X, CC (158.3 mbsf).

Calcareous Nannoplankton

All core-catcher samples from both holes together with additional samples from sections within Hole 687A were studied for calcareous nannoplankton.

Sample 112-687A-1H, CC (7.41 mbsf) contains a well-preserved but poorly diversified late Quaternary nannoplankton assemblage. Most of the remaining samples are barren of calcareous nannoplankton. Occasionally, impoverished and poorly preserved assemblages having *Gephyrocapsa* species, *Coccolithus pelagicus*, and rare *Helicosphaera carteri* were encountered. *Helicosphaera sellii* was found in Samples 112-687A-14X, CC (127.92 mbsf), 112-687B-9X, CC (81.06 mbsf), 112-687B-16X, CC (130.01 mbsf), and 112-687B-22X, CC (185.80 mbsf). This occurrence, along with the highest occurrence of *Cyclcoccolithus macintyreii* in Section 112-687B-9X, CC (81.0 mbsf), seems to indicate the presence of the early Quaternary nannoplankton Zone NN19a (lower part of the *Pseudoemiliania lacunosa* Zone) at this level.

In some cases, the meager nannoplankton assemblages were associated with reworked early to middle Miocene and middle to late Eocene nannoplankton species. The displaced species found in Sections 112-687A-19X, CC (175.00 mbsf), 112-687A-22X, CC (202.0 mbsf), 112-687B-20X, CC (167.90 mbsf), and 112-687B-22X, CC (185.80 mbsf) include *Discoaster deflandrei*, *Cyclcoccolithus floridanus*, *Reticulofenestra pseudoumbilica*, *Dictyococcites dictyodus*, *Discoaster tani*, and *Reticulofenestra umbilica*.

Section 112-687B-9X, CC (81.0 mbsf), which contains *Cyclcoccolithus macintyreii*, has an age of at least 1.45 Ma, which was indicated for the last occurrence of *C. macintyreii* by Backman and Shackleton (1983). Thus, the sedimentation rate in the Quaternary at Site 687 is at least 56 m/m.y.

Radiolarians

All core-catcher samples from Hole 687A were studied for radiolarians. These are well to moderately preserved in all samples but are generally rare.

A radiolarian assemblage containing *Didymocyrtis tetrathalamus* and *Lamprocyrtis nigrinae* was found in Sections 112-

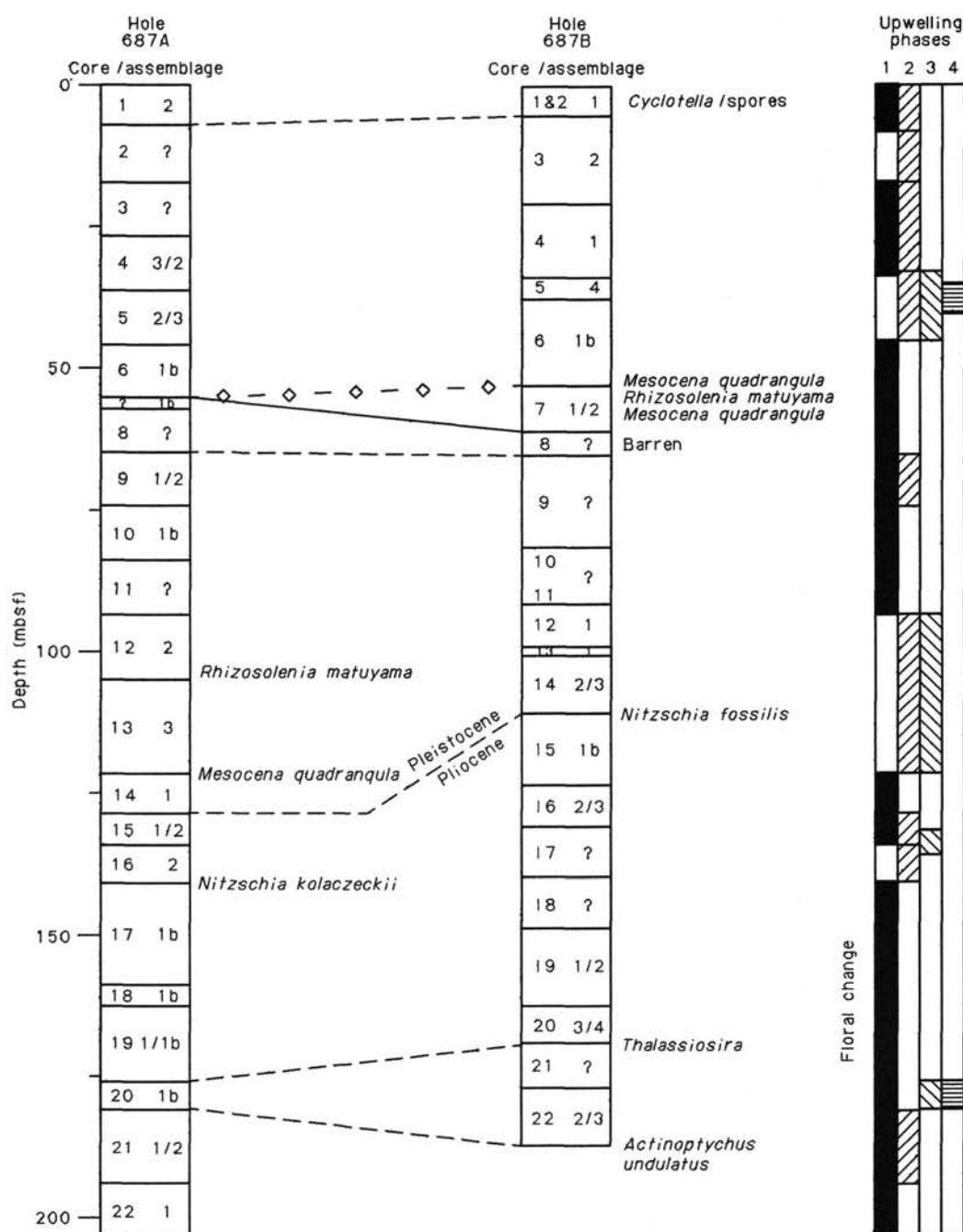


Figure 19. Correlation between Holes 687A and 687B, based on distinct occurrences of sediments and diatom assemblages. Note dramatic floral change in Sections 112-687A-14X, CC and 112-687B-14X, CC. Upwelling phases are based on core-catcher samples; see Table 5 for definitions.

687A-1H, CC (7.41 mbsf) and 112-687A-14X, CC (127.92 mbsf), indicating a Quaternary age. Because no collosphaerids were found, we could not subdivide the Quaternary sequence.

Sections 112-687A-6H, CC to 112-687A-7X, CC, 112-687A-10X, CC to 112-687A-15X, CC, and 112-687A-17X, CC to 112-687A-19X, CC did not yield enough radiolarians to assign an age. Section 112-687A-10X, CC (83.5 mbsf) yielded *Didymocystis tubaria*, which indicates an early Miocene age and thus was probably reworked.

Sections 112-687A-2H, CC to 112-687A-5H, CC, 112-687A-8X, CC, 112-687A-20X, CC, and 112-687A-22X, CC were barren. Sections 112-687A-11X, CC to 112-687A-13X, CC, and 112-687A-16X, CC were not available for investigating radiolarians.

Planktonic Foraminifers

All core-catcher samples from Site 687 were examined. Planktonic foraminifers were rare but well preserved.

Hole 687A

Planktonic foraminifers occurred in the entire upper part of this hole, from Sections 112-687A-1H, CC through 112-687A-13X, CC (7.41 to 121.15 mbsf), except in Sections 112-687A-2H, CC, 112-687A-3H, CC, 112-687A-7X, CC, and 112-687A-8X, CC. Below Section 112-687A-14X, CC (127.92 mbsf), planktonic foraminifers were absent in most samples. *Globigerina bulloides*, *G. quinqueloba*, and *Globigerinita glutinata* were found

Table 5. Characterization of coastal upwelling by phytoplankton.

Phase 1a: strong upwelling, very high primary productivity
Preservation: excellent

- | | |
|-------------------------------|------------------------------------|
| 1. <i>Delphineis</i> | 2. <i>Chaetoceros</i> spores/setae |
| 3. <i>Thalassiosira</i> | 4. <i>Skeletonema</i> |
| 5. <i>Distephanus pulchra</i> | 6. <i>Dictyocha epidon</i> |
| 7. <i>Cyclotella</i> | |

Phase 1b: intermittent strong upwelling, high primary productivity
Preservation: excellent to very good

- | | |
|------------------------------------|---------------------------|
| 1. <i>Chaetoceros</i> spores/setae | 2. <i>Delphineis</i> |
| 3. <i>Thalassiosira</i> | 4. <i>Actinopterychus</i> |
| 5. <i>Distephanus pulchra</i> | 6. <i>Stephanopyxis</i> |
| 7. <i>Cyclotella</i> | |

or

- | | |
|---------------------------|------------------------------------|
| 1. <i>Thalassiosira</i> | 2. <i>Chaetoceros</i> spores/setae |
| 3. <i>Actinopterychus</i> | 4. <i>Delphineis</i> |
| 5. <i>Nitzschia</i> | 6. <i>Distephanus pulchra</i> |

Phase 2: sporadic upwelling, oceanic-temperate influence
Preservation: good

- | | |
|---------------------------------|------------------------------------|
| 1. <i>Thalassionema</i> | 2. <i>Thalassiothrix</i> |
| 3. <i>Thalassiosira</i> | 4. <i>Chaetoceros</i> spores/setae |
| 5. <i>Dictyocha messanensis</i> | 6. <i>Actinopterychus</i> |
| 7. <i>Cyclotella</i> | |

Phase 3: prolonged times with no upwelling, normal eutrophic productivity
Preservation: moderate to good

- | | |
|-------------------------|--------------------------|
| 1. <i>Coscinodiscus</i> | 2. <i>Thalassiothrix</i> |
| 3. <i>Thalassionema</i> | |

Phase 4: "normal" continental margin productivity
Preservation: moderate

Note: these stages apply only to a true "Peruvian" coastal-upwelling sedimentary environment of Quaternary age; older assemblages (Miocene/Pliocene) can be placed in this system, but some Holocene species must be replaced by their fossil counterparts. These are modified in other coastal-upwelling areas and differ from oceanic convergence-divergence belts).

in most samples; these indicate cool water. *Globigerinoides im-maturus* was found in Section 112-687A-1H, CC (7.41 mbsf), *Orbulina universa* and *O. suturalis* were found in Section 112-687A-3H, CC (26.60 mbsf), and *Globorotalia hirsuta* was recognized in Section 112-687A-6H, CC (55.07 mbsf). These species are indicative of warm water. Therefore, the faunal assemblage is transitional from cold to warm waters (Bé, 1977). Planktonic foraminifers in all samples are Quaternary.

Hole 687B

Above Section 112-687B-7H, CC (61.13 mbsf), planktonic foraminifers do not occur except in Sections 112-687B-2H, CC (5.20 mbsf) and 112-687B-5H, CC (37.34 mbsf). Below Section 112-687B-8H, CC (65.20 mbsf), planktonic foraminifers were found in most samples. *Globigerina bulloides*, *G. quinqueloba*, and *Neoglobobulimina pachyderma* occurred in most samples. These species indicate cool water and also are known from the temperate coastal upwellings. *Orbulina universa* occurred in one sample, Section 112-687B-11X, CC (90.70 mbsf); this species indicates warm water. Planktonic foraminifers in all samples are Quaternary.

Benthic Foraminifers

Benthic foraminifers are common to abundant and well preserved in all core-catcher samples of Hole 687A, except for the following. Section 112-687A-2H, CC (17.2 mbsf) is barren of benthic foraminifers, and Sections 112-687A-7X, CC, 112-687A-

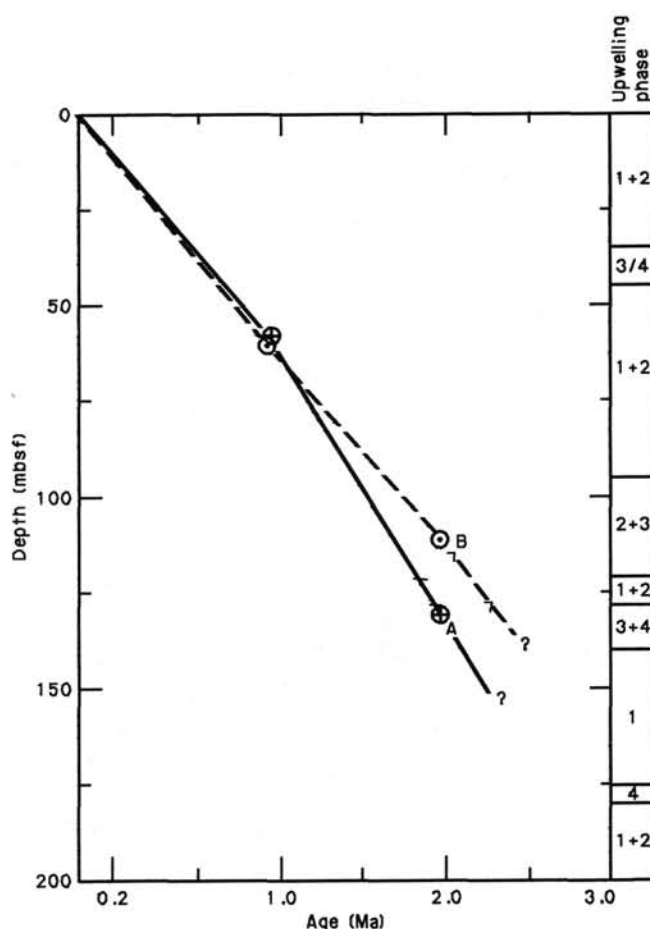


Figure 20. Age vs. depth plots of Hole 687A (circles with crosses) and Hole 687B (circles with points). Upwelling phases combined for the two holes, see right column.

8X, CC (57-64.5 mbsf) and 112-687A-11X, CC (93 mbsf) contain only rare, moderately preserved specimens. Core 112-687A-16X retained no sediment in the core catcher.

The *Bolivina seminuda humilis* Assemblage occurs in the upper 26.6 m of the section (Sections 112-687A-1H, CC and 112-687A-3H, CC). *Bolivina rankini* occurs with or replaces *B. seminuda humilis* in some of the samples. This assemblage is indicative of the modern upper-bathyal, low-oxygen environment found in the site's water depth of 300 m. In Section 112-687A-1H, CC (7.4 mbsf) some specimens of the *Cancris inflatus-Tri-farina carinata* Assemblage occur, but this species does not dominate. This assemblage occurs at the surface of Site 686 and the subsurface elsewhere, as discussed in the Site 686 chapter (this volume). These specimens may be reworked from older zones.

A transitional upper-bathyal/outer-shelf environment is indicated for the interval between Sections 112-687A-4H, CC and 112-687A-6H, CC (36.1-55.1 mbsf), which contains a *B. seminuda humilis* Assemblage, but with abundant *Nonionella* (a shelf-dwelling genus). Outer- to middle-shelf depths are suggested by the *Nonionella* Assemblages of Sections 112-687A-9X, CC through 112-687A-12X, CC (74-104 mbsf), which also contain such inner-shelf forms as *Buccella* and *Quinqueloculina*. Transitional outer-shelf/upper-bathyal assemblages occur from Section 112-687A-13X, CC to the bottom of the cored section (121.2-202 mbsf). These environmental changes probably reflect eustatic sea-level fluctuations, as well as subsequent subsidence of the seafloor from the middle-shelf depth of about 50 m indicated for Section 112-687A-10X, CC (83.5 mbsf).

The restriction of a large, robust species of *Buliminella* to the interval below Section 112-687A-14X, CC (128 mbsf) and its occurrence with a large member species of the *Bolivina seminuda* Group may be evolutionary, as this part of the section is of Pliocene age, according to diatom markers. The association of the *Bolivina seminuda* Group with low-oxygen environments along this coast suggests that these lower strata were also deposited under low-oxygen conditions.

Biogenic Groups—Coarse Fraction Analysis

The relative percentage of distribution of the biogenic groups encountered in the coarse fraction is shown in Figure 21. Benthic foraminifers are dominant throughout the cored section; percentages increase downward from Section 112-687A-17X, CC (138.4 mbsf) toward the bottom of the interval.

Diatoms and radiolarians exhibit a uniform percentage of distribution downhole, and fish remains are significant in Sections 112-687A-8X, CC (65.2 mbsf) and 112-687A-15X, CC (122.3 mbsf).

The planktonic foraminifer species recognized are *Neoglobobulimina dutertrei*, *N. pachyderma*, *Globigerinoides ruber*, *G. sacculifer*, *Globigerinita glutinata*, *Globorotalia menardii*, and *G. (Hirsutella) scitula*; most of these range from Miocene to Holocene. The first appearance of *G. dutertrei* is in the late Pliocene Zone N21 (Section 112-687A-15X, CC, 133.39 mbsf).

ORGANIC GEOCHEMISTRY

Site 687 was located in shallow water (306.8 m) at the southernmost edge of the Lima Basin, an area of tectonic stability adjacent to the Lima Platform. Two holes were drilled to sample Quaternary and Neogene sediments. Organic geochemical analyses were conducted on samples from Hole 687A to 200.5 mbsf and from Hole 687B to 195.0 mbsf. Hydrocarbon gases were monitored in both holes, and organic-carbon and organic-matter characteristics were measured initially on only seven samples from Hole 687B. Organic-matter characteristics were later determined on 22 samples from Hole 687A to develop a higher-resolution depth profile. Details of methods and procedures are given in "Organic Geochemistry" sections, Site 679 and 682 chapters; instruments are described in the "Explanatory Notes" (this volume).

Hydrocarbon Gases

Vacutainer Gases

We observed gas pockets in only a few of the core liners. In Hole 687A, vacutainer gas was collected from six cores; in Hole 687B, only three cores could be sampled (Table 6). The first sample from Hole 687A (Section 112-687A-3H-4) contained mostly air. C_1 concentrations in the other vacutainer samples from both holes ranged from 21.9% to 91.0%. C_2 concentrations in these same samples differed in the two holes. In Hole 687A, C_2 contents ranged from 200 to 260 ppm, and in Hole 687B from 55 to 95 ppm. The gas samples from Hole 687B are more diluted with air from the drilling and sampling procedures, thus reducing the amount of C_2 that is retained for measurement. The amount of C_2 was anomalously large for shallow Quaternary sediments, as it was at the previous site (see "Organic Geochemistry" section, Site 686 chapter); also, except for the shallowest sample, C_1/C_2 ratios are of the same magnitude and decrease at about the same rate (compare Fig. 22 with Fig. 29, "Organic Geochemistry" section, Site 686 chapter).

Extracted Gases

The amount of extracted C_1 (Table 7) increases with depth from the surface to about 50 mbsf, where these concentrations reach sediment values of $> 30,000 \mu\text{L/L}$ of wet sediment and then increase slowly downhole. Figure 23 demonstrates this con-

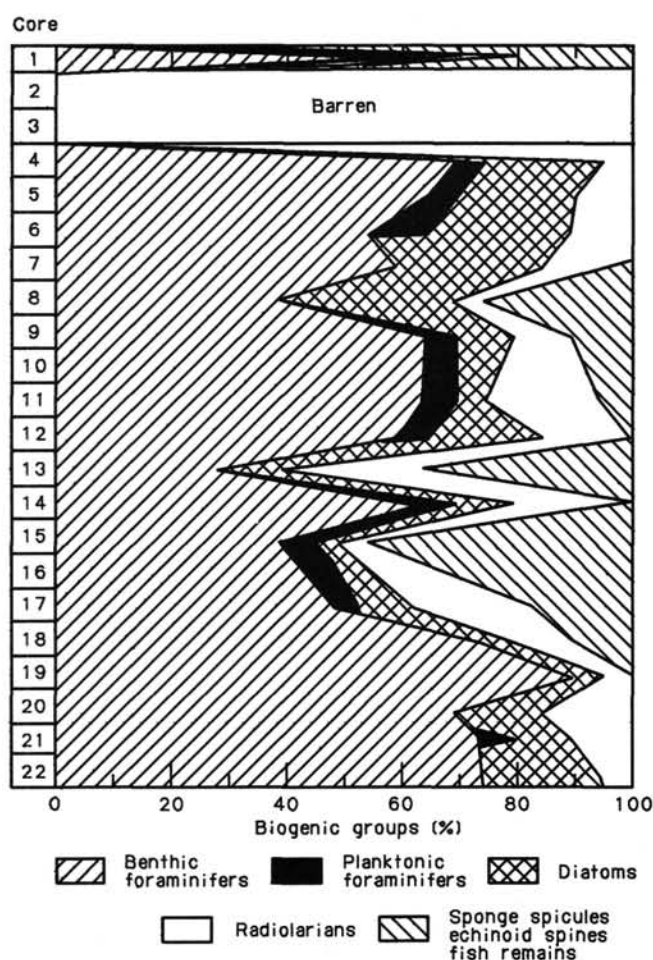


Figure 21. Biogenic groups in the coarse fraction of core-catcher samples, Hole 687A.

Table 6. Vacutainer gases at Site 687.

Core-section interval (cm)	Depth (mbsf)	C_1 (%)	C_2 (ppm)	C_1/C_2
112-687A-3H-4, 35	21.9	0.044	3.6	120
15X-1, 83	131.8	74.2	200	3800
17X-4, 78	155.3	91.0	260	3500
18X-1, 131	160.8	77.2	200	3900
19X-3, 52	172.5	80.6	230	3600
21X-3, 83	191.8	82.9	240	3400
112-687B-6H-6, 118	51.8	21.9	55	4000
10H-1, 50	81.7	45.3	95	4800
20X-1, 45	167.3	26.2	68	3900

Units of (%) and (ppm) are in volume of gas component per volume of gas mixture. All measurements were performed on the Hach-Carle Gas Chromatograph.

centration profile and also shows the similarity of results for the two procedures applied at Site 687. At about this same depth, sulfate concentrations decrease to zero and remain at this value to the bottom of the hole (see "Inorganic Geochemistry" section, this chapter). Again, as at previous sites, this inverse correlation between sulfate and C_1 concentrations indicates that the C_1 derives from microbial methanogenesis. This becomes important when microbial sulfate reduction stops because there are no more sulfate ions (Claypool and Kaplan, 1974).

C_2 concentrations in the extracted gas are anomalously large and range from 14 to 63 $\mu\text{L/L}$, with one exception; C_3 and C_{2+1} could not be detected. These observations were the same as

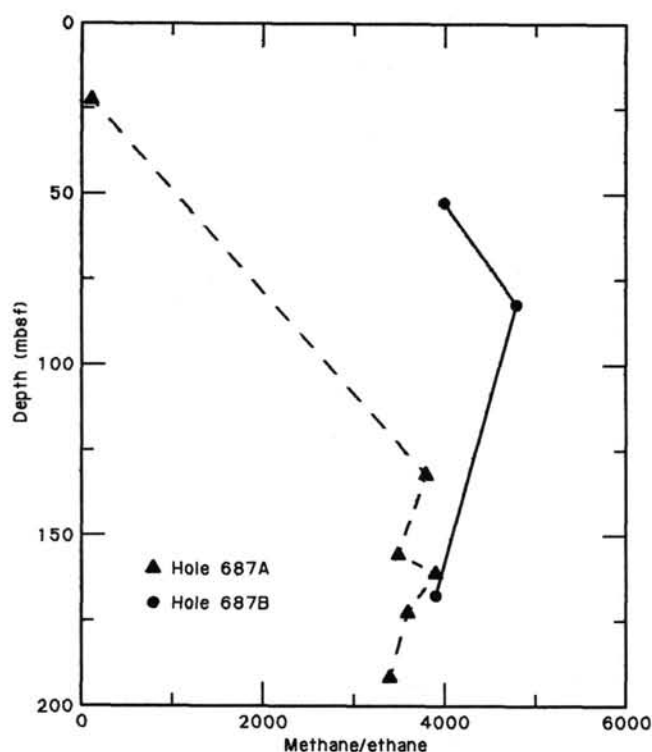


Figure 22. Methane/ethane ratios in gas pockets formed in cores from Holes 687A and 687B.

those we noted at the previous site (see "Organic Geochemistry" section, Site 686 chapter). We believe that the C_2 can be accounted for by intense microbial hydrocarbon generation at Sites 686 and 687. These are the first of the shallow-water sites where sufficient C_1 concentrations were available to cause the formation of gas pockets, which suggests that methanogenesis is more active at these two sites than at the previous shallow-water sites. Although methanogenesis and microbial ethane generation probably require different substrates, the environmental conditions necessary for both processes may be particularly favorable at Sites 686 and 687.

Carbon

Total-carbon, carbonate-carbon and organic-carbon (OC) values were determined for seven samples of "squeeze-cakes" remaining after squeezing pore water for inorganic-geochemistry studies (see "Inorganic Geochemistry" section, this chapter). The carbon contents of these samples are listed in Table 8, and OC and TOC values are compared with depth in Figure 24. In addition, Rock-Eval pyrolysis parameters, including total organic carbon (TOC), were determined using parts of these same samples (Tables 9 and 10). The OC content of these samples varies widely and ranges from 0.32% to 6.20% for OC and from 0.37% to 5.88% for TOC; OC and TOC values are comparable, but TOC is generally lower (Fig. 24). The variability in OC concentrations can be attributed to a significant part of the sediment drilled at this site being fine silt and sand that have an expected low carbon content.

Rock-Eval pyrolysis parameters in Table 9 are shown graphically in Figure 25. The trends with depth of the hydrogen and oxygen indices (HI and OI) and TOC are similar to the trends observed at the previous site (see "Organic Geochemistry" section, Site 686 chapter). Samples with higher amounts of organic carbon have higher HI and lower OI values. The opposite is true for samples with lower amounts of organic carbon. One expla-

Table 7. Extracted gases at Site 687.

Core-section interval (cm)	Depth (mbsf)	C_1 ($\mu\text{L/L}$)	C_2 ($\mu\text{L/L}$)	C_1/C_2
Headspace gases				
112-687A-2H-5, 0-1	13.5	160		
4H-5, 0-1	32.5	230		
6H-5, 0-1	51.5	43,000	24	1800
10X, CC, 0-1	93.0	110,000	28	4100
12X-1, 149-150	105.5	54,000	24	2100
14X-3, 0-1	124.5	74,000	29	2500
18X-1, 149-150	161.0	140,000	50	2800
21X-2, 149-150	191.0	210,000	69	3000
22X-3, 0-1	200.5	150,000	36	4200
112-687B-1H-3, 139-140	4.4	50		
3H-4, 0-1	19.2	220		
5H-2, 0-1	35.2	250		
7H-1, 139-140	54.1	41,000	27	1500
10H-1, 144-145	82.7	44,000	14	3100
13X, CC, 0-1	109.0	33,000	22	1500
15X-2, 0-1	120.8	41,000	27	1500
16X-1, 10-11	128.9	140,000	63	2200
19X-3, 0-1	160.3	120,000	39	3100
22X, CC, 29-30	195.0	140,000	28	5000
Canned gases				
112-687B-1H-3, 140-145	4.5	27		
3H-3, 135-140	19.1	84	2.4	36
6H-5, 135-140	50.6	34,000	13	2600
10H-1, 145-150	82.7	41,000	14	2900
16X-1, 111-121	130.0	40,000	34	1200

Units are in microliters (μL) of gas component per liter (L) of wet sediment. All measurements were made on the Hach-Carle Gas Chromatograph.

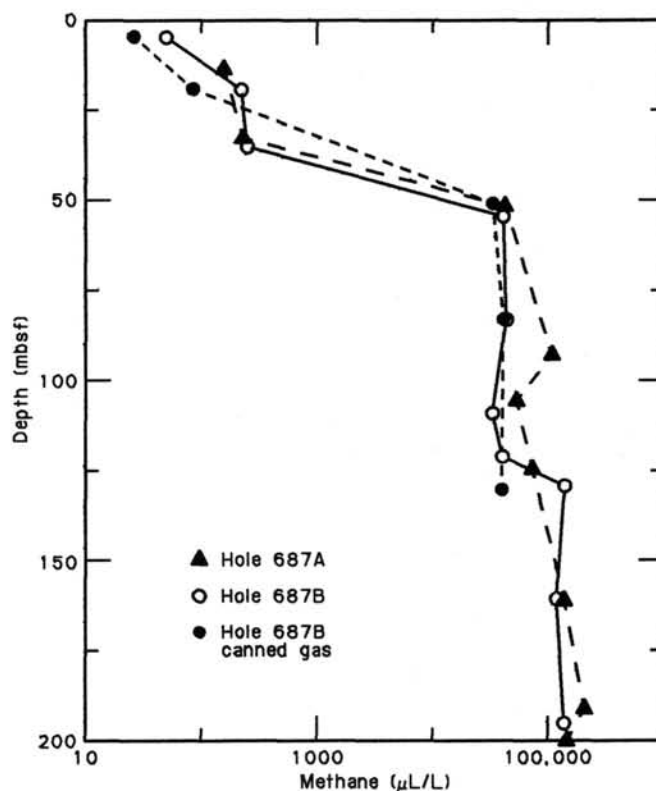
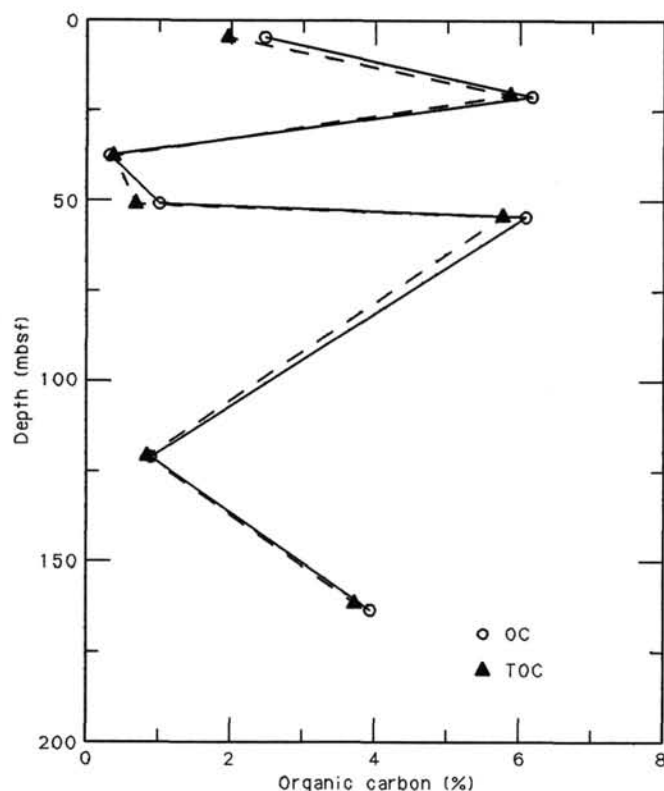


Figure 23. Comparison of extracted methane concentrations with depth determined by the headspace procedure at Holes 687A and 687B. The dots are the results from the can procedure applied to samples from Hole 687B.

Table 8. Organic carbon and carbonate carbon for Hole 687B.

Core-section interval (cm)	Depth (mbsf)	Total carbon (%)	Inorganic carbon (%)	Organic carbon (%)	TOC (%)
112-687B-1H-3, 145-150	4.5	2.71	0.25	2.46	1.95
3H-4, 140-150	20.6	6.24	0.04	6.20	5.88
5H-3, 54-64	37.2	2.52	2.21	0.31	0.37
6H-5, 140-150	50.6	2.15	1.16	0.99	0.68
7H-1, 140-150	54.1	6.81	0.71	6.10	5.78
15X-1, 140-150	120.7	1.71	0.82	0.89	0.84
19X-3, 103-113	161.3	4.10	0.15	3.95	3.73

TOC = total organic carbon from Rock-Eval pyrolysis.

**Figure 24.** Comparison of organic carbon (OC) with total organic carbon (TOC) from Rock-Eval pyrolysis at Site 687.

nation is that the small amounts of organic carbon in the fine silts and sands at this site came mainly from terrigenous sources. Thus, the three samples with the lowest TOC values straddle the type III field of the van Krevelen-type diagram (Fig. 26). The other samples are closer to type II. This is considered indicative of marine organic matter (Tissot and Welte, 1984). These inter-

pretations of Rock-Eval data follow from conventions based on studies related to sources of petroleum rocks. With the immature organic matter in Quaternary oceanic sediments, these conventions may no longer be totally valid. For example, the HI and OI fields of type I, II, and III may not be indicative of specific sources of organic matter. It is well known that immature, marine organic matter contains many oxygenated species. Thus, OI values of immature marine organic matter should be higher than OI values in mature marine organic matter that has lost oxygen through diagenesis.

As one test of the nature of the organic matter in the samples containing the lowest amounts of organic carbon, we investigated the visible organic matter on smear slides of parts of these samples. The sediments were boiled in NaOH, washed, and centrifuged. The residue was treated with alcohol, separated with bromoform, and the lower-density material was washed with alcohol and water and mounted in glycerin-gelatin on a glass slide. Although this treatment destroys some organic matter, the more chemically resistant organic material should remain. Observations about these samples are as follows:

1. Sample 112-687B-1H-3, 145-150 cm, has organic carbon contents of 2.46%; abundant amorphous organic matter; very few cysts, brownish/grayish sacks; no other detectable structural matter.

2. Sample 112-687B-5X-3, 54-64 cm, has organic contents of 0.31%; amorphous organic matter; some dinoflagellate cysts and very few pollen grains; elongate brownish organic tissue.

3. Sample 112-687B-6X-5, 140-150 cm, has organic carbon contents of 0.99%; extremely rare, brown, organic aggregates; no other detectable organic matter.

4. Sample 112-687B-15X-1, 140-150 cm, has organic carbon contents of 0.89%; extremely rare, dark brown, perforated plates; few blackish phytoliths; no other structures.

The results of this survey indicate that the residual organic matter in these samples is mainly marine in origin with only a minor terrigenous component. Thus, determining the source of organic matter in these samples, based on a strict interpretation of the van Krevelen-type diagram, must be evaluated carefully.

The profiles of organic-matter characteristics (Fig. 25), based on only seven samples, give the impression of extreme fluctuations of the various parameters. To determine how these low-resolution profiles compare with high-resolution profiles, we analyzed 22 samples from Hole 687A (Table 10). These samples came from sediments that had been tested for carbonate carbon earlier (see "Lithostratigraphy" section, this chapter). The results are shown in Figure 27. TOC values are generally low (<1.0%) below about 25 mbsf. The silt and sandy units between this depth and about 90 mbsf contain little organic matter that yields low amounts of pyrolysis products (S_1 , S_2 , and S_3). Sections 112-687A-10X, CC (11-12 cm) and 112-687A-11X, CC (13-14 cm) have such low values of S_1 , S_2 , S_3 , and TOC that any parameters derived from or related to these values, such as HI,

Table 9. Summary of Rock-Eval pyrolysis data from Hole 687B.

Core-section interval (cm)	Depth (mbsf)	Weight (mg)	T_{max}	S_1	S_2	S_3	PI	S_2/S_3	PC	TOC (%)	HI	OI
112-687B-1H-3, 145-150	4.45	100.5	404	1.08	6.92	2.43	0.13	2.84	0.66	1.95	354	124
3H-4, 140-150	20.60	99.5	393	3.62	25.36	3.23	0.12	7.85	2.41	5.88	431	54
5H-3, 54-64	37.24	101.7	391	0.04	0.21	0.58	0.17	0.36	0.02	0.37	56	156
6H-5, 140-150	50.60	96.3	384	0.26	1.02	0.88	0.20	1.15	0.10	0.68	150	129
7H-1, 140-150	54.10	99.4	397	4.29	27.80	3.31	0.13	8.39	2.67	5.78	480	57
15X-1, 140-150	120.70	101.0	385	0.30	1.42	1.26	0.17	1.12	0.14	0.84	169	150
19X-3, 130-113	161.33	96.6	393	3.06	16.42	2.08	0.16	7.89	1.62	3.73	440	55

Rock-Eval parameters are defined in "Organic Geochemistry" Section, Site 679 chapter.

Table 10. Summary of Rock-Eval pyrolysis data from Hole 687A.

Core-section interval (cm)	Depth (mbsf)	Weight (mg)	T _{max}	S ₁	S ₂	S ₃	PI	S ₂ /S ₃	PC	TOC (%)	HI	OI
112-687A-1H-1, 61-62	0.61	80.8	397	14.59	54.13	8.56	0.21	6.32	5.72	11.55	468	74
1H-4, 61-62	5.11	61.0	391	8.49	28.09	4.55	0.23	6.17	3.04	6.46	434	70
2H-2, 55-56	9.55	94.0	400	1.85	12.86	2.18	0.13	5.89	1.22	2.94	437	74
2H-3, 142-143	11.92	100.7	411	0.71	7.36	1.91	0.09	3.85	0.67	1.74	422	109
3H-3, 86-87	20.86	101.1	396	2.28	17.66	2.78	0.11	6.35	1.66	4.11	429	67
4H-1, 58-59	27.08	99.4	406	0.35	2.18	1.62	0.14	1.34	0.21	0.77	283	210
4H-3, 58-59	30.08	102.1	397	0.09	0.43	1.12	0.17	0.38	0.04	0.41	104	273
5H-2, 82-83	38.32	93.5	388	0.35	1.37	1.35	0.20	1.01	0.14	0.52	263	259
5H-4, 82-83	41.32	96.8	383	0.10	0.37	1.37	0.22	0.27	0.03	0.72	51	190
10H, CC, 11-12	83.61	100.8	398	0.05	0.16	1.19	0.25	0.13	0.01	0.14	114	850
11H, CC, 13-14	93.13	102.2	309	0.02	0.09	0.90	0.20	0.10	0.00	0.05	180	1800
13X-1, 75-76	112.75	66.8	406	2.44	12.81	2.88	0.16	4.44	1.27	2.83	452	101
13X-3, 75-76	115.75	71.0	391	1.08	3.52	1.85	0.23	1.90	0.38	0.88	400	210
14X-1, 47-48	121.97	96.4	386	0.35	1.25	1.00	0.22	1.25	0.13	0.42	297	238
14X-4, 47-48	126.47	80.0	387	1.11	3.57	1.18	0.24	3.02	0.39	0.95	375	124
15X-2, 44-45	132.94	97.0	392	1.03	3.76	1.61	0.22	2.33	0.39	1.03	365	156
17X-2, 30-31	151.80	100.2	396	0.19	0.70	1.34	0.22	0.52	0.07	0.41	170	326
17X-5, 30-31	156.30	101.3	395	0.47	1.52	2.03	0.24	0.74	0.16	0.86	176	236
18X-2, 35-36	161.35	61.0	400	3.21	11.95	2.81	0.21	4.25	1.26	2.66	449	105
19X-3, 46-47	172.46	82.2	395	1.36	4.58	2.09	0.23	2.19	0.49	1.29	355	162
21X-3, 103-104	192.03	97.1	401	2.96	14.93	3.11	0.17	4.80	1.49	3.62	412	85
22X-3, 61-62	201.11	73.5	390	0.57	1.52	1.76	0.27	0.86	0.17	0.47	323	374

Rock-Eval parameters are defined in "Organic Geochemistry" section, Site 679 chapter.

OI, and T_{max}, are probably meaningless and should be discounted. In Figure 27, these profiles (less the two samples mentioned above) provide a more realistic appraisal of the organic matter in the sediments at Site 687 than do the profiles shown in Figure 25, as would be expected for the larger data base. Figure 28 shows the distribution of HI and OI values and emphasizes the high oxygen content of many of the samples from this site. Before we can be confident of applying Rock-Eval data to young, oceanic sediments, more studies will be needed to define the ranges of values of the various parameters for organic matter from different sources.

INORGANIC GEOCHEMISTRY

Introduction and Operation

At Site 687, the shallower site in the southernmost transect at ~13°S, two holes were cored in a water depth of 306.8 m. Except for one *in-situ* water sample at 169.0 m from Hole 687A, all interstitial-water samples analyzed were squeezed from whole-round samples of sediment. Because sediments recovered in Hole 687B were extremely poor and disturbed, mainly 10-cm whole-round samples were retrieved, beginning with Section 112-687B-3H-4 downhole. Results are shown in Figures 29 through 38.

As with the adjacent Site 686, the *in-situ* water sampler recovered pristine interstitial waters from the rather soft sediments. Large systematic downhole increases in chloride, salinity, calcium, magnesium, ammonia, and phosphate were observed at this site (Figs. 29 and 32 through 38). As was the case at Sites 684 and 686, sulfate concentrations did not increase with depth below the methanogenesis zone. The deepest sample analyzed (at 169 mbsf) was still within the sulfate-depleted zone. Sedimentation rates in the Quaternary section of Site 687 are considerably lower (~65 m/m.y.) than those at the nearby Site 686, where Quaternary sedimentation rates are ~160 m/m.y. (see "Biostratigraphy" section, Site 686 and 687 chapters).

Chloride and Salinity

Chloride and salinity gradients were more than twice as steep at this shallow site as at adjacent Site 686 (Fig. 29 and Table 11) in somewhat deeper water (446.8 m water depth). The average chloride concentration gradient at Site 687 is 13.7 mmol/L/10 m vs. 6.0 mmol/L/10 m at Site 686 (see Fig. 36, Site 686 chapter). At 169 mbsf, chloride concentrations are ~138‰ of seawater.

Although not as distinct as at Site 686, a salinity minimum was again observed, however, at a different depth interval in Samples 112-687B-3H-4, 140-150 cm, and 112-687B-5H-3, 54-64 cm, between ~20 and 40 mbsf. The depth of the salinity minimum at Site 686 does not coincide with the sulfate minimum but does occur at the same depth as the Ca²⁺ minimum and Mg²⁺/Ca²⁺ maximum at Site 687 (Fig. 35). For a discussion of salinity minimum see "Inorganic Geochemistry" section, Site 686 chapter.

Sulfate and Alkalinity

The sulfate-reduction zone at Site 687 is almost 40 m thick, compared with only ~15 m at Site 686 (Figs. 30 and 31 and Table 11). The different and slower sedimentation regime at this site is responsible for the thicker sulfate-reduction zone (see "Lithostratigraphy" section, this chapter). A discussion about sulfate and alkalinity can be found in the "Inorganic Geochemistry" section, Site 686 chapter.

The alkalinity maximum can be seen in Figure 30, at 10 to 15 m shallower than the sulfate minimum. This is an "apparent" maximum controlled by carbonate diagenesis between 20 and 40 mbsf. Methane concentrations increase steeply at about 40 mbsf, below the sulfate-reduction zone (Fig. 31).

Ammonia and Phosphate

A general trend of increasing concentrations with depth can be seen for both ammonia and phosphate (Figs. 32 through 34 and Table 11). The NH₄⁺ maximum occurs approximately 15 m deeper (37.2 mbsf; Sample 112-687B-5H-3, 54-64 cm) than the phosphate maximum (20.6 mbsf; Sample 112-687B-3H-4, 140-150 cm). Figures 33 and 34 show the positive correlations between the systematic downhole increases in chloride and ammonia and phosphate concentrations, respectively. For a discussion, see the Site 686 chapter.

Silica

Silica concentrations are high and reach values between 944 and 1104 μmol/L (Table 11). The small fluctuations in silica concentrations with depth (e.g., 1038 μmol/L at 20.6 mbsf, 951 μmol/L at 37.2 mbsf, and 1072 μmol/L at 54.1 mbsf), may reflect the fluctuations between more diatomaceous, sandier zones. In the sandier intervals, preservation of diatoms is only moderate to poor (see "Biostratigraphy" section, this chapter).

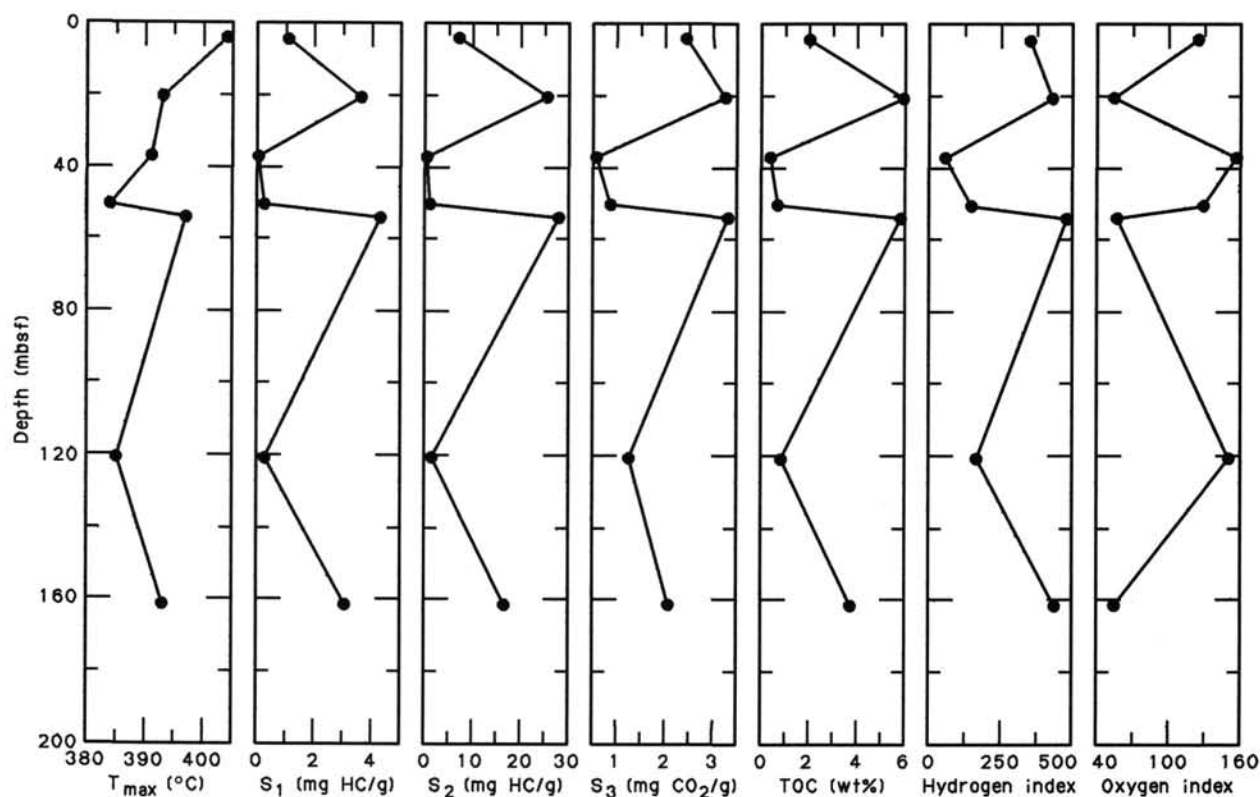


Figure 25. Comparison of Rock-Eval parameters T_{max} , S_1 , S_2 , S_3 , TOC, HI, and OI in seven samples from Hole 687B.

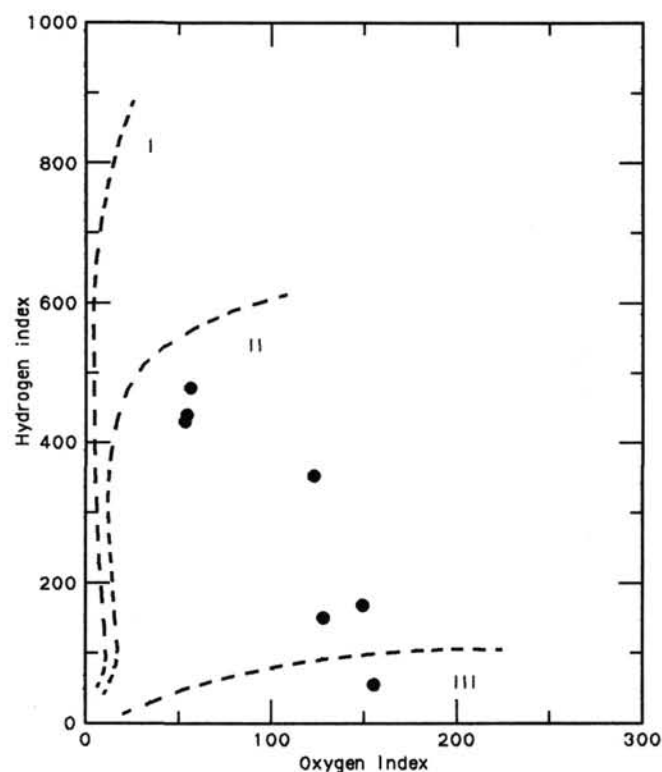


Figure 26. Hydrogen and oxygen indices (HI and OI) obtained from Rock-Eval pyrolysis of seven samples from Hole 687B and plotted on a van Krevelen-type diagram (Tissot and Welte, 1984).

Calcium and Magnesium

The main differences among the profiles of Ca^{2+} , Mg^{2+} , and Mg^{2+}/Ca^{2+} that we observed at Sites 687 and 686 are as follows:

	Site 687 (mmol/L/10 m)	Site 686 (mmol/L/10 m)
Ca^{2+} concentration downhole increases	0.96	0.17
Mg^{2+} concentration downhole gradient	1.90	Constant value of gradient ~ 27 mmol/L between 106 and 296 mbsf
Mg^{2+}/Ca^{2+} downhole decreasing ratio	0.27	0.16

Despite the rather extensive dolomitization at this site, Mg^{2+} concentrations increase with depth. Because of slower sedimentation rates, the rate of magnesium diffusion from the subsurface brine is greater than the rate of Mg^{2+} consumption by dolomitization at this site (see Fig. 38). In contrast, at Site 686 the magnesium diffusion rate seems to equal the rate of dolomite formation. For the sequence of diagenetic reactions of carbonate, see the discussion in Site 686 chapter.

PALEOMAGNETICS

Introduction

The shipboard paleomagnetic studies were conducted to obtain a detailed magnetostratigraphy of the sediment cores. The upper 21 m of Hole 687A possessed a strong magnetic signal

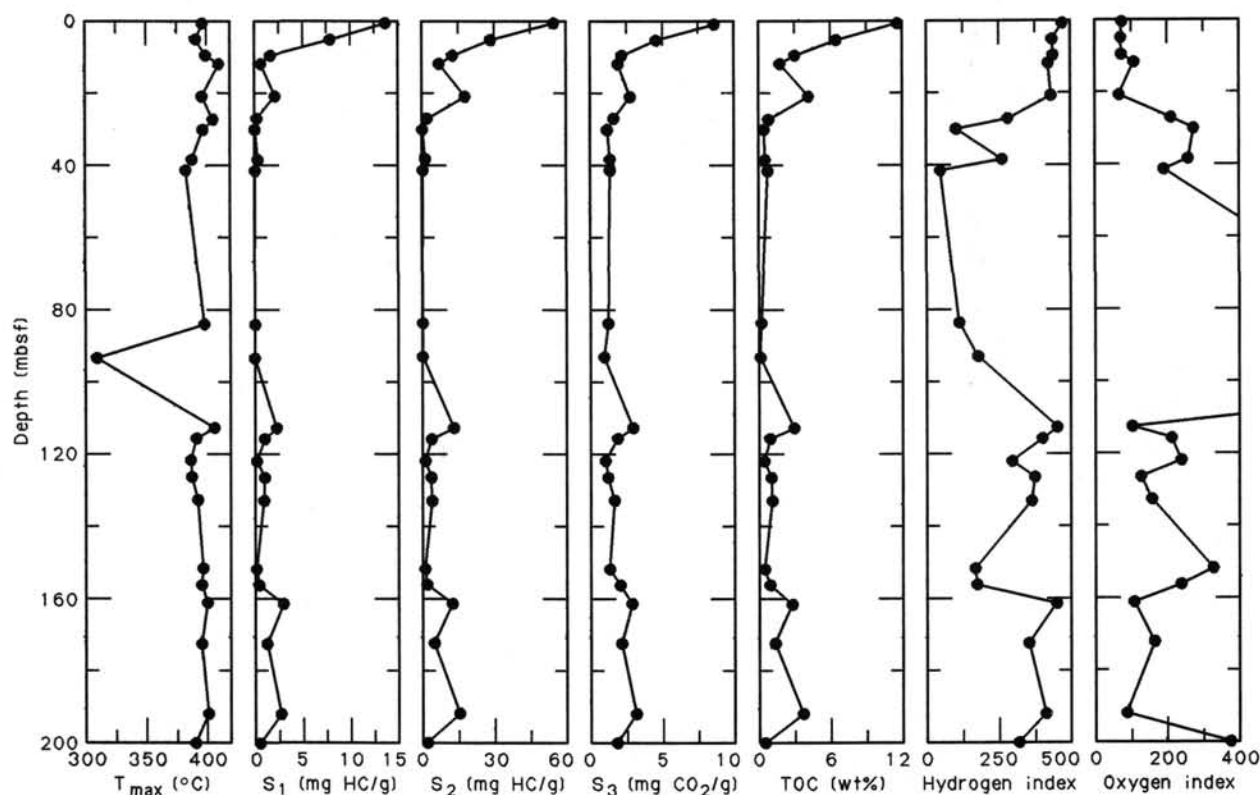


Figure 27. Comparison of Rock-Eval parameters T_{max} , S_1 , S_2 , S_3 , TOC, HI, and OI in 22 samples from Hole 687A.

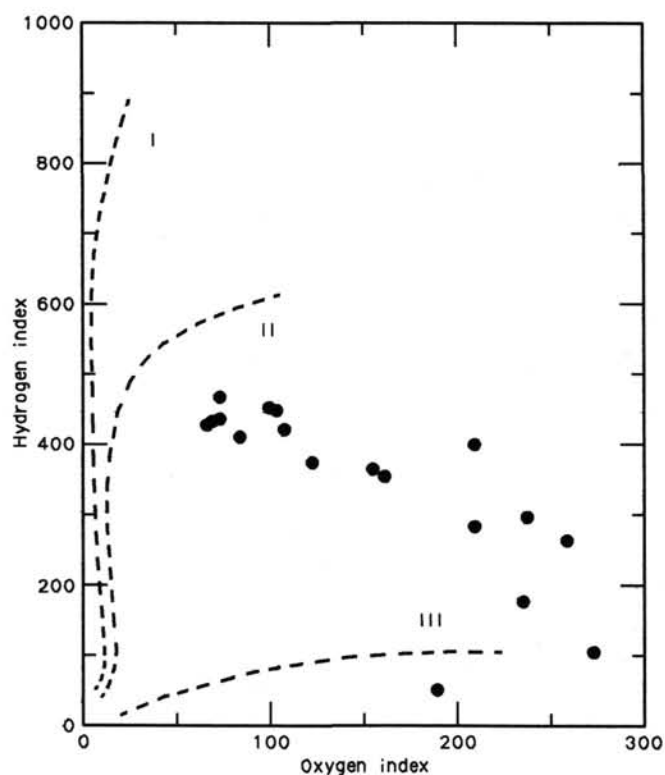


Figure 28. Hydrogen and oxygen indices (HI and OI) obtained from Rock-Eval pyrolysis of 22 samples from Hole 687A.

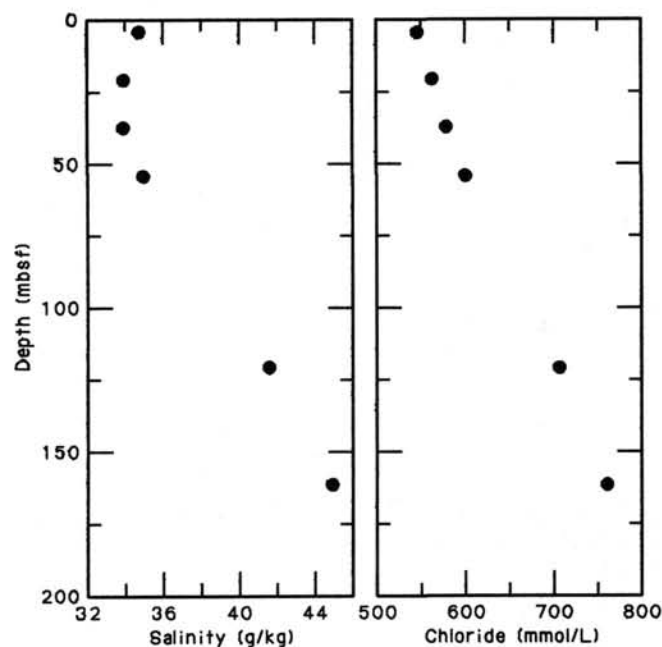


Figure 29. Profiles of salinity and chloride for Site 687.

that was easy to measure with the shipboard spinner magnetometer. The deeper sediment cores were characterized by weak magnetic moments (< 0.2 mA/m). This rapid decay in the magnetic moments of the samples is easily seen in Figure 39. This behavior is similar to results from all sites collected during Leg 112

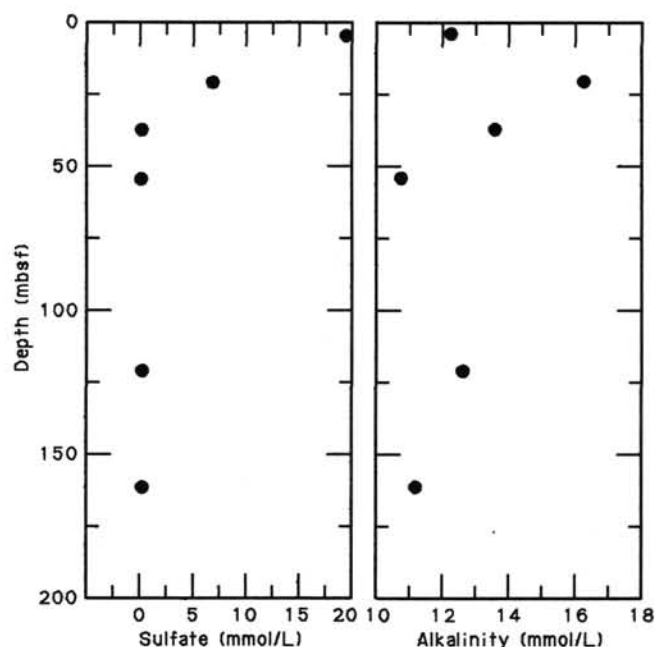


Figure 30. Profiles of sulfate and alkalinity for Site 687.

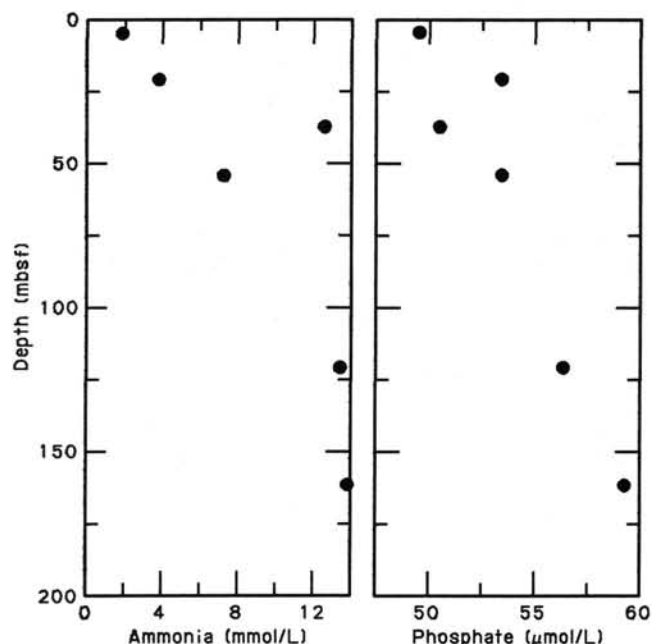


Figure 32. Interstitial ammonia and phosphate at Site 687.

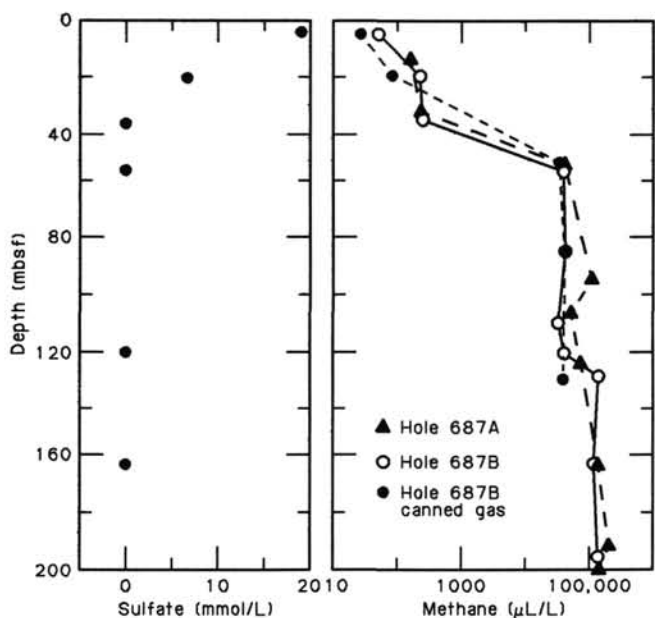


Figure 31. Profiles of sulfate and extracted methane for Site 687. (Extracted methane profile is from the "Organic Geochemistry" section, this chapter).

and reported here. Past DSDP Legs (e.g., Barton and Bloemendal, 1986) reported a similar loss of magnetic intensity with depth from other sedimentary sections. Although the cause of this decrease in magnetic intensity is not known, it probably is related to a diagenetic effect in the sediments after burial. This diagenetic effect probably results in the chemical reduction of the magnetic carrier and transfer of iron into a more reduced state, that is, a nonmagnetic or weakly magnetic sulfide phase. Both the weakness of the magnetic moments and the large cir-

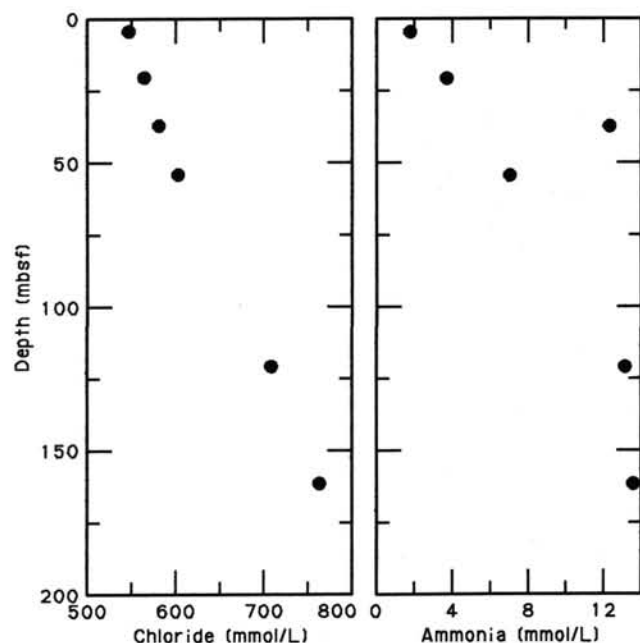


Figure 33. Interstitial chloride and ammonia at Site 687.

cular standard deviation for the cores below Core 112-687A-3H, eventually forced us to end our sample measurements below Core 112-687A-6H. These deeper cores will be sampled and measured in shore-based studies with a cryogenic magnetometer.

Results

Vector plots of these samples show that beginning demagnetization with 150 Oe did not destroy the valuable primary signal. In fact, most samples showed unidirectional decay of their magnetic behavior between 100 to 300 Oe. Figure 39 shows the decli-

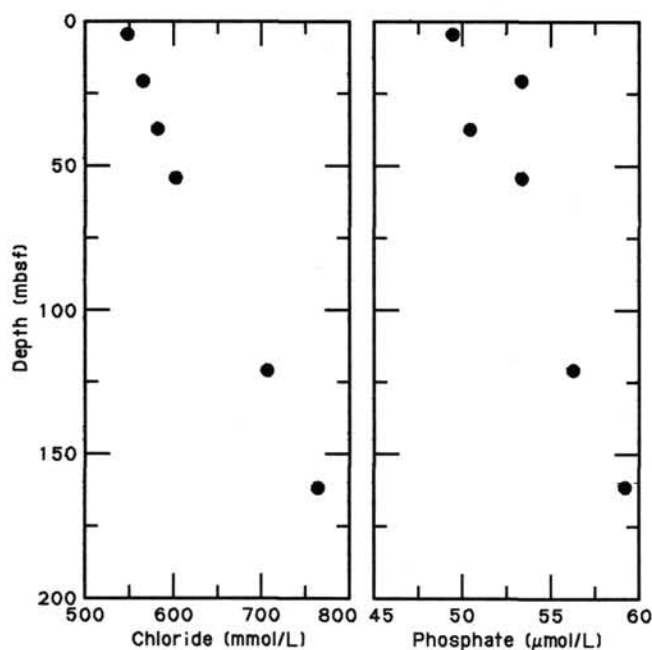


Figure 34. Interstitial chloride and phosphate at Site 687.

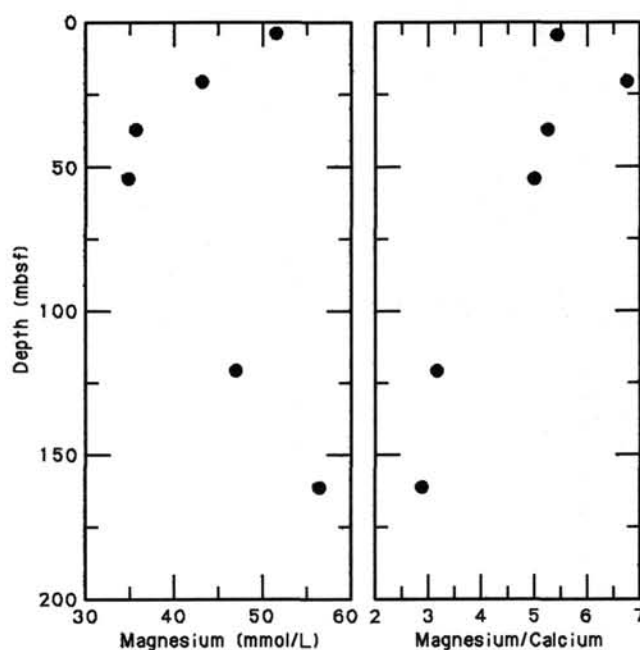
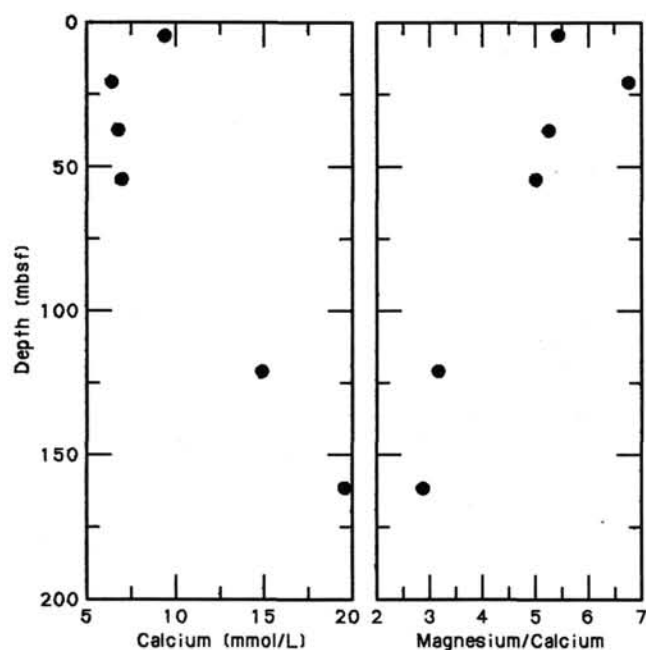
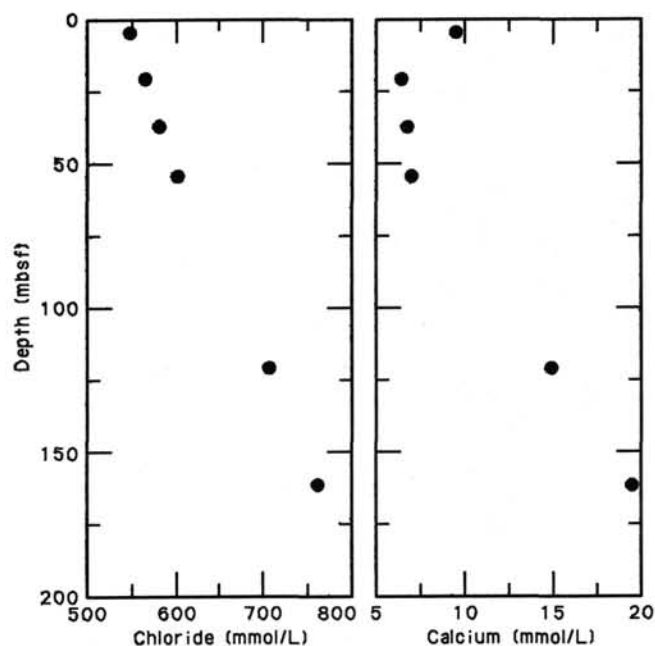
Figure 36. Interstitial magnesium and Mg^{2+}/Ca^{2+} at Site 687.Figure 35. Interstitial calcium and Mg^{2+}/Ca^{2+} at Site 687.

Figure 37. Interstitial chloride and calcium at Site 687.

nation, inclination, and intensity values of the analyzed samples at the 150-Oe level of demagnetization. This value of demagnetization was selected on the basis of the vector plots. The figure indicates that a change in the normal-to-reversed inclination value can be found between 35 and 38 mbsf (Section 112-686A-5H-2), which apparently corresponds to the Brunhes/Matuyama boundary. This finding is consistent with shipboard paleontological and sedimentological studies.

Hole 687A

We noted two interesting observations while measuring samples. First, the upper three cores (Cores 112-686A-1H through

112-686A-3H) were characterized by relatively strong (>1 mA/m) samples with stable magnetizations. Samples collected from similar lithologies in deeper cores (below Core 112-686A-3H) showed a marked deterioration in the magnetic signal, as is observed in the plot on the right of Figure 39. This intensity-vs.-depth plot also indicates that the intensity of magnetization shows a cyclic pattern, as seen in Sites 680, 683, and 685.

PHYSICAL PROPERTIES

Physical-properties measurements at Site 687 were performed on split cores, at an approximate interval of two samples per core in good quality APC cores and, where quality of recovery

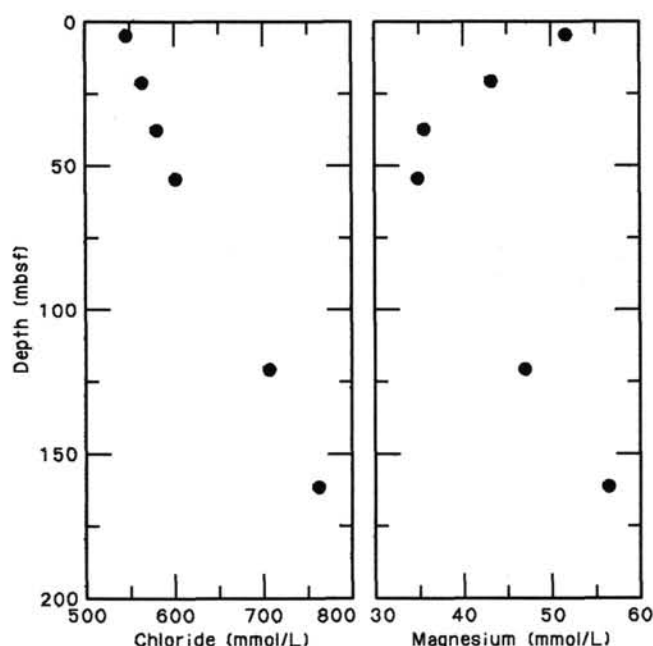


Figure 38. Interstitial chloride and magnesium at Site 687.

permitted, in XCB cores. Lithologic Unit II at this site consisted of fine-grained sand that generally was either highly disturbed or had poor recovery. Cores from this unit were neither sampled, nor run through the GRAPE, which resulted in a large data gap in both holes. A sample of sediment from Section 112-687A-3H-2, which had been split by the saw, was evaluated for freshwater contamination by analyzing the interstitial water. Analysis indicated approximately 2% dilution by freshwater (M. Kastner, pers. comm., 1986), which is consistent with previous analyses at Site 685 (see "Inorganic Geochemistry" and "Physical Properties" sections, Site 685 chapter).

Index Properties

The index properties measured at this site include water content (presented as a percentage of dry sample weight), porosity, bulk density, and grain density (Table 12). Downhole profiles of water content and porosity are shown in Figure 40. These data depict great variability over short distances, with water content ranging from <50% to >250% and porosity from 50% to >90%. This variability is similar to that seen at Site 686, but less data were collected at Site 687 and cycles were not as well defined. Water content and porosity decrease through Subunit IA and the upper part of Subunit IB, but increase again in the lower part of Subunit IB. In Unit III, these properties show no discernible trends.

The bulk-density data (Fig. 41) show similar variability through Units I and III. An increase in bulk density from the

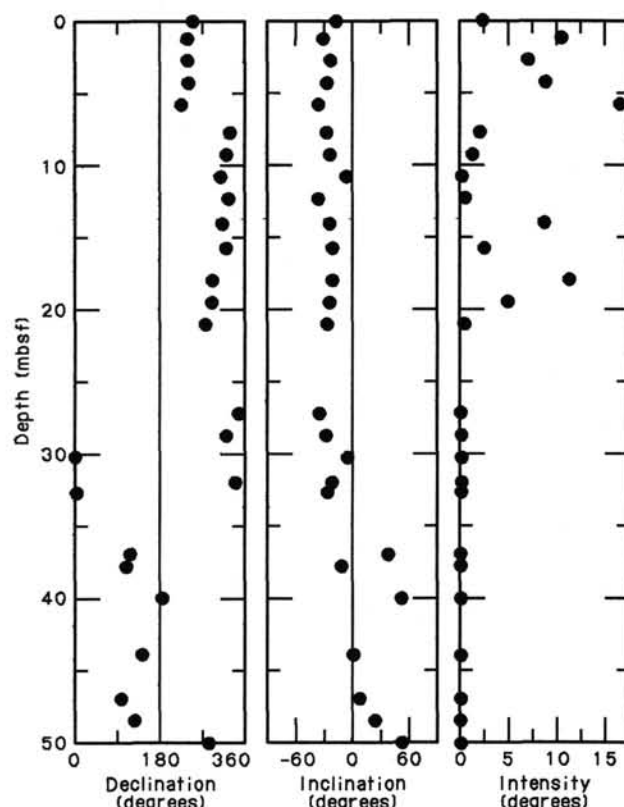


Figure 39. Declination, inclination, and magnetic intensity plots vs. depth below seafloor for Hole 687A. The diagram shows a reversal occurring at 35–38 mbsf. The magnetic intensity vs. depth plot appears to show the cyclicity noted in Sites 680 and 683.

seafloor to the upper part of Subunit IB complements the decrease in water content and porosity over the same interval. More detailed plots of the GRAPE data show the marked variability of the bulk density over distances of only a few centimeters (Fig. 42). The importance of obtaining continuous GRAPE profiles for use to resolve the highly varied sediment facies is evident in Figure 42. The expanded GRAPE profile depicts these variations well, while the sample measurement gives only a rough indication of trends in bulk density.

In Figure 42A, the sediment sequence consists of predominantly diatomaceous mud from 10.5 to 12.3 m, which indicates relatively low and consistent bulk-density values, except for spikes corresponding to graded terrigenous sand and silt beds. Below 12.3 m, the sequence contains a greater proportion of the graded sand and silt beds, which causes bulk density to fluctuate greatly and the GRAPE profile to become even more irregular and broken up (Fig. 42B).

Table 11. Interstitial-water geochemical data for Site 687.

Core-section interval (cm)	Depth (mbsf)	pH	Salinity (g/kg)	Cl ⁻ (mmol/L)	Alkalinity (mmol/L)	SO ₄ ²⁻ (mmol/L)	PO ₄ ³⁻ (μmol/L)	NH ₄ ⁺ (mmol/L)	SiO ₂ (μmol/L)	Ca ²⁺ (mmol/L)	Mg ²⁺ (mmol/L)	Mg ²⁺ /Ca ²⁺
112-687B-1H-3, 145–150	4.45	7.6	34.8	547.55	12.24	19.25	49.48	1.76	944	9.40	51.60	5.49
3H-4, 140–150	20.60	7.8	34.0	564.73	16.25	6.77	53.37	3.68	1038	6.36	43.13	6.78
5H-3, 54–64	37.24	7.9	34.0	580.94	13.57	0.0	50.45	12.54	951	6.71	35.54	5.30
7H-1, 140–150	54.10	7.6	35.0	601.93	10.74	0.0	53.37	7.12	1072	6.93	34.76	5.02
15X-1, 140–150	120.70	7.4	41.6	706.86	12.62	0.0	56.28	13.36	1049	14.82	46.91	3.17
19X-3, 103–113	161.33	7.5	44.9	762.19	11.20	0.0	59.20	13.77	1104	19.44	56.45	2.90
112-687A <i>In-situ</i> 1	169.0	7.3	46.1	769.91	12.77	0.0	51.42	13.83	1089	20.66	58.76	2.84

Table 12. Summary of index-properties data for Holes 687A and 687B.

Core-section interval (cm)	Depth (mbsf)	Water content (% dry wt)	Porosity (%)	Bulk density (g/cm ³)	Grain density (g/cm ³)
112-687A-1H-1, 61	0.61	260.79	89.82	1.27	2.32
1H-3, 110	4.10	229.70	89.70	1.32	2.39
2H-2, 35	9.35	144.97	81.28	1.41	2.50
2H-4, 79	12.79	86.61	74.29	1.64	2.62
3H-2, 74	19.24	146.53	79.65	1.37	2.32
4H-2, 95	28.95	72.90	67.53	1.64	2.69
4H-4, 111	32.11	73.94	67.42	1.63	2.52
5H-2, 80	38.30	68.61	65.41	1.65	2.54
5H-4, 83	41.33	56.50	61.33	1.74	2.68
5H-6, 135	44.85	73.01	68.53	1.66	2.70
6H-1, 60	46.10	120.04	77.44	1.45	2.42
6H-3, 99	49.49	135.81	79.56	1.42	2.30
7X-2, 10	56.60	125.04	77.16	1.42	2.37
12X-1, 103	103.53	45.69	58.04	1.90	2.72
13X-2, 88	114.38	125.38	77.74	1.43	2.46
13X-4, 92	117.42	87.75	74.35	1.63	2.70
13X-6, 77	120.27	154.57	79.96	1.35	2.07
14X-1, 33	120.83	68.51	65.82	1.66	2.58
14X-3, 110	125.60	86.29	71.65	1.58	2.55
14X-5, 23	127.73	164.41	83.47	1.38	2.42
15X-2, 34	132.84	88.86	72.71	1.58	2.41
17X-2, 117	152.67	49.53	57.86	1.79	2.60
17X-4, 122	155.72	67.28	66.38	1.69	2.58
17X-6, 37	157.87	196.75	86.55	1.34	2.39
18X-2, 50	161.50	132.68	78.03	1.40	2.15
19X-2, 120	171.70	125.59	77.45	1.43	2.27
19X-4, 36	173.86	74.84	67.55	1.62	2.43
21X-2, 128	190.78	141.03	79.93	1.40	2.34
21X-4, 34	192.84	109.89	76.99	1.51	2.57
22X-1, 133	198.83	33.37	49.87	2.04	2.75
22X-3, 80	201.30	102.07	75.75	1.54	2.50
112-687B-1H-3, 114	4.14	179.58	82.40	1.31	2.28
3H-2, 115	17.35	122.20	92.72	1.73	2.36
3H-4, 65	19.85	194.86	72.73	1.13	2.15
5H-2, 78	35.98	51.59	59.80	1.80	2.66
6H-2, 84	45.54	63.69	65.40	1.72	2.62
6H-4, 64	48.34	127.20	79.15	1.45	2.31
6H-6, 67	51.37	124.45	78.44	1.45	2.36
7H-1, 50	53.20	183.62	82.74	1.31	2.12
15X-2, 107	121.87	147.14	82.65	1.42	2.44
16X-1, 63	129.43	194.07	87.80	1.36	2.18
19X-3, 42	160.72	222.52	86.62	1.29	1.99

Compressional-Wave Velocity

As at previous sites, velocities were obtained using the *P*-wave logger, which only functions well with high-quality APC cores. At Site 687, reliable data were obtained only from the top 30 m of Holes 687A and 687B. A profile of velocities from Section 112-687A-1H-1 is shown in Figure 43. The marked spikes at approximately 75 and 85 cm probably correspond to dolomite nodules found at these levels.

Vane Shear Strength

Vane shear strengths were measured with the Wykham-Farrance shear vane device and are listed in Table 13. As was expected from the variable lithology at Site 687, vane shear strength measurements are highly scattered (Fig. 44). Some draining during testing also occurred in the coarser or highly diatomaceous sediments, contributing to the scatter we observed. The profile shows shear strength broadly increasing with depth; that is, from a near-surface value of 12 kPa to values as high as 175 kPa at depth.

We calculated the total and effective overburden stresses using bulk-density measurements and by assuming hydrostatic pore-pressure conditions. The ratio of peak undrained vane shear strength to effective overburden pressure (C_u/P') is plotted vs. depth below seafloor for Hole 687A (Fig. 45). Some of the variation imposed by cyclic behavior of the physical properties is apparent in the profile. The high vane shear strength (166 kPa) and corresponding low bulk density at 49.5 mbsf are emphasized.

Thermal Conductivity

Thermal conductivity was measured by the needle-probe method on samples from Hole 687B. Measurements were usually performed before splitting the cores. For Core 112-687B-3H, the probes were inserted into the ends of the split sections. After Core 112-687B-7H, few measurements were possible because cores were either highly disturbed or recovery was poor. Results are presented in Table 14 and Figure 46.

Thermal conductivity was greater than 1.2 W/m·K between 25 and 40 mbsf, although the highest two values may be questionable because these samples were slightly disturbed. As observed at Site 686, the high values correspond to the sandy layers. Below these layers, thermal conductivity rapidly decreases to 0.78 W/m·K at 54 mbsf. As a whole, variations in thermal conductivity are consistent with the variations in index properties (Figs. 40 and 41).

Discussion

All physical-properties data at Site 687 vary greatly because of lithologic changes similar to those observed at Site 686. Zones containing abundant diatoms have high water contents, high porosities, and low bulk densities. Zones containing higher silts have lower water contents, lower porosities, and higher bulk densities. At Site 687, the presence of numerous sand- and silt-based graded beds causes greater variability of the physical properties than we observed at Site 686. Thus, climate-related cycles are more difficult to identify.

The value of continuous GRAPE profiles becomes clear when such variations are present. As can be seen from Figure 42, the relatively few data points obtained from sample measurements (represented by open circles in Fig. 42) do not represent the sequence as a whole. Combined use of both GRAPE and sample data provide the best basis for understanding the physical properties at Site 687.

GEOPHYSICS

Structure and Seismic Records

Site 687 was located on the gently dipping, landward flank of the southern end of the Lima Basin (Fig. 47). This landward boundary, the Lima Platform, is a block-faulted basement structure that runs along the outer shelf. Many scientists believe that tensional faulting breaks down the Lima Platform and that the fault blocks subside and constitute the floor of the Lima Basin proper (Thornburg and Kulm, 1981). The center of thickest sediment cover of this basin has shifted, indicating a seaward shift in subsidence of these blocks to a water depth of >2000 m. An upper-slope rise marks the seaward boundary of the Lima Basin. In the area where Site 687 was drilled (southeast corner of the basin), the Lima Platform is a broad structural feature that is oriented transversely to the margin, thereby marking the boundary between the southern end of the Lima Basin and the northern end of the West Pisco Basin (see Site 686 Chapter). Site 687 lies in shallow water (307 m) over a tectonically stable portion of the westernmost part of the Lima Platform. About 15 km west of the site, flat-lying reflectors are truncated by the seafloor, which forms scarps and indicates removal of several hundreds of meters of sediment from the upper slope. Such scarps are also present in the subsurface. Drilling at Site 687 penetrated 200 m into these flat-lying reflectors.

Selection of Site 686 was initially based on SCS Line YALOC 13-03-74, obtained during the Nazca Plate Project (Kulm et al., 1981). An interpreted section of this line is shown in Figure 47, and part of the original single-channel record is depicted in Figure 48. These data were supplemented during approach to the site by a seismic survey shot with an 80-in.³ water gun and concurrent 3.5-kHz profiling from *JOIDES Resolution*. This combined information delineates these flat-lying packets that con-

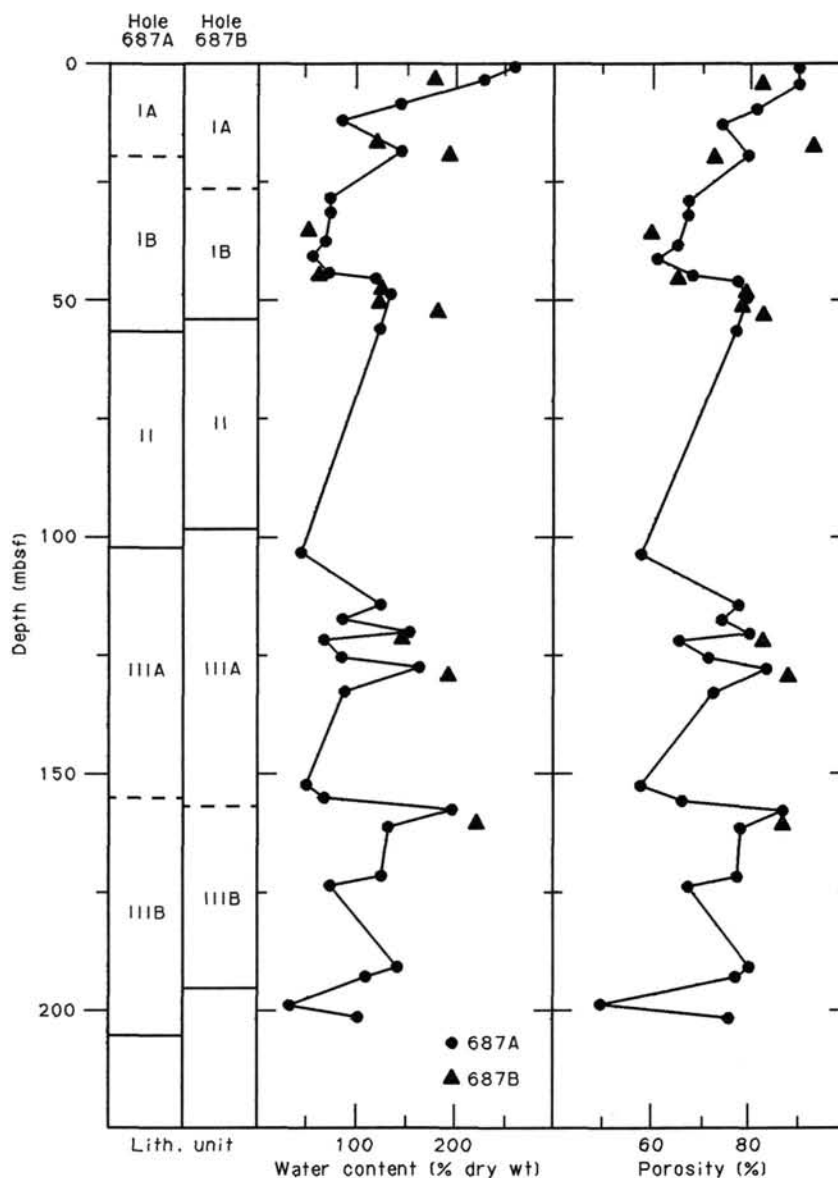


Figure 40. Profiles of water content and porosity for Site 687.

formably overlie the gently dipping flank of the Lima Platform. As we observed previously in the West Pisco Basin, two sequences can be distinguished at Site 687: (1) a lower sequence (lithologic Units II and III) that thickens seaward and (2) an upper sequence (lithologic Unit I) that thickens landward. The upper sequence forms a downlapping contact with the lower one. Apparently, farther landward of Site 687, this interface may be erosional. The interface between both units occurs at 60 ± 10 mbsf, which coincides with the boundary between lithologic Units I and II. Unit II consists of 50 m of dominantly sandy beds, which either represents the early parts of the downlapping sequence or is reworked material from the top of Unit III. Just above the Unit I/II boundary (47.8 mbsf), we found a distinct ash bed that consisted of a 2-cm-thick, light-colored lower part and a 6-cm-thick, dark gray upper part. This marker was tentatively identified at Site 686 in the same seismic stratigraphic position (i.e., near the base of the landward-thickening sequence; however, at 153.6 mbsf. Thus, we believe that the landward-thickening seismic sequences at Sites 686 and 687 are coeval and that during the late Quaternary (<0.9 Ma), the sedimentation rates in the neighboring basins differed by almost a factor of

three. Similarly, the lower seismic sequences, which at Site 687 contain the Pliocene/Pleistocene boundary at 120 mbsf but which at Site 686 do not reach that age, represent comparable geologic intervals. However, the time resolution of this sequence is quite different for the Lima and the West Pisco basins, at least for the upper part. The 3.5-kHz record shows the uppermost part of the landward-thickening sequence in greater detail (Fig. 49). Several sub-bottom reflectors can be correlated with lithologic changes in the recovered section. A series of sandy beds at 12–14 mbsf and 22–24 mbsf correlate well.

Heat Flow

Temperature Measurements

Temperatures were measured at Hole 687A using the APC tool and the T-probe. The APC tool was run while retrieving Cores 112-687A-4H and 112-687A-6H. In both measurements, frictional heating from penetration was high. Moreover, on the second run, the decay curve was somewhat irregular (Fig. 50), which suggests that the APC shoe may not have been stable in the sediments. These factors account for large errors in temper-

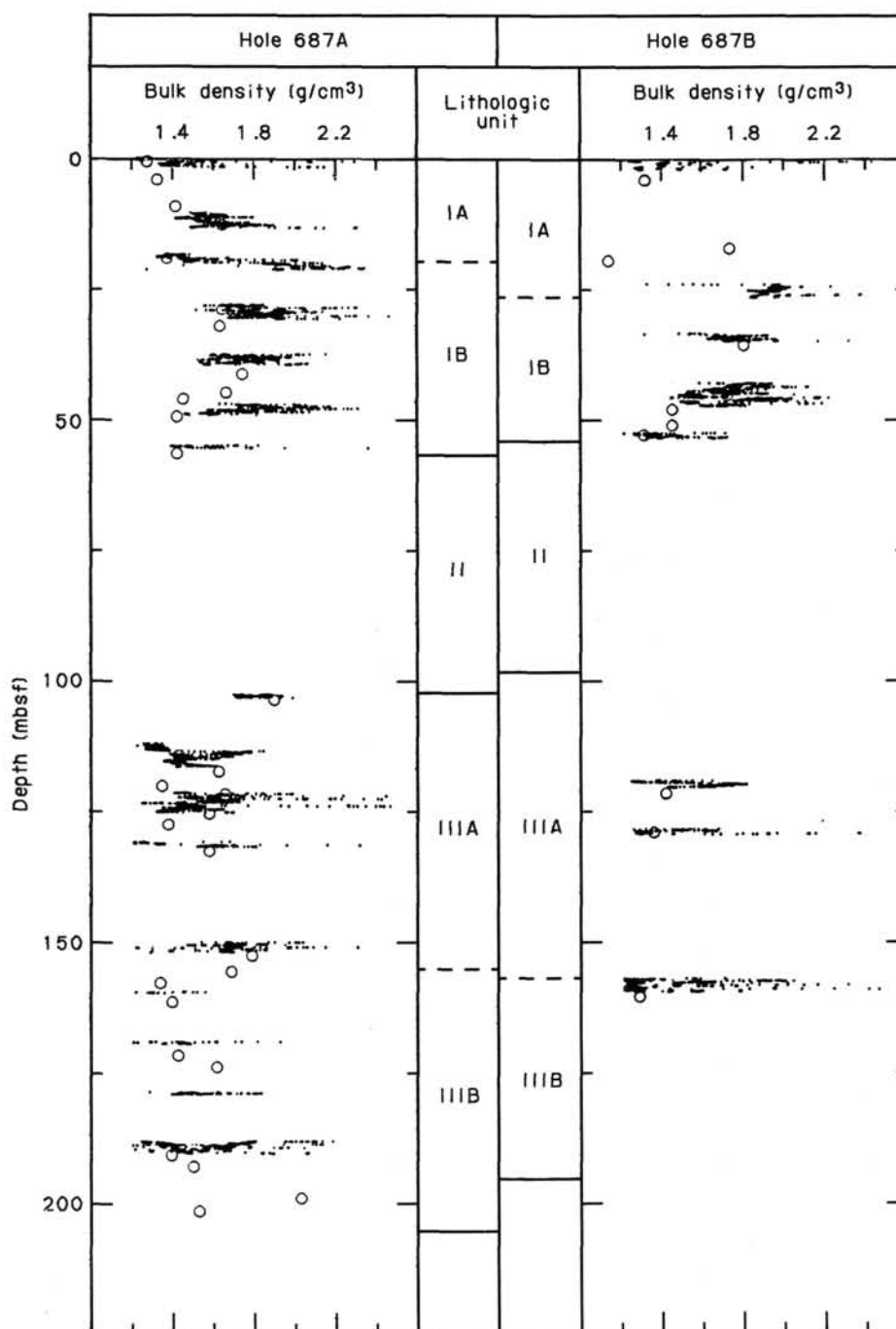


Figure 41. Bulk-density profiles for Site 687. Small dots are the GRAPE data; open circles indicate sample measurements.

ature extrapolation. Equilibrium temperatures were estimated as $11.0 \pm 0.5^\circ\text{C}$ at 36.0 mbsf and $11.8 \pm 0.5^\circ\text{C}$ at 55.0 mbsf.

The T-probe was deployed with the pore-water sampler after Core 112-687A-18X. The APC tool was run by attaching the APC shoe to the pore-water sampler, and then mud-line water temperature was measured for calibration. Figure 51 shows the temperature record obtained with the T-probe after correction with the mud-line temperature. A problem in the connection between the temperature sensor and connector could indicate an error in temperature of 0.5°C (see "Explanatory Notes" chapter, this volume). The temperature record was stable in the sedi-

ment, and the equilibrium temperature was calculated as 18.8°C at 169.0 mbsf.

Estimating Heat Flow

Formation temperatures obtained with the APC tool and the T-probe are plotted vs. depth in Figure 52. The geothermal gradient determined by the least-squares fitting is $58 \text{ m}^2 \cdot \text{K}/\text{m}$ (solid line in Fig. 52). However, thermal-conductivity measurements indicate that the sand layers have much higher thermal conductivity than the mud layers (see "Physical Properties" section, this chapter). Hence, the temperature-vs.-depth profile cannot

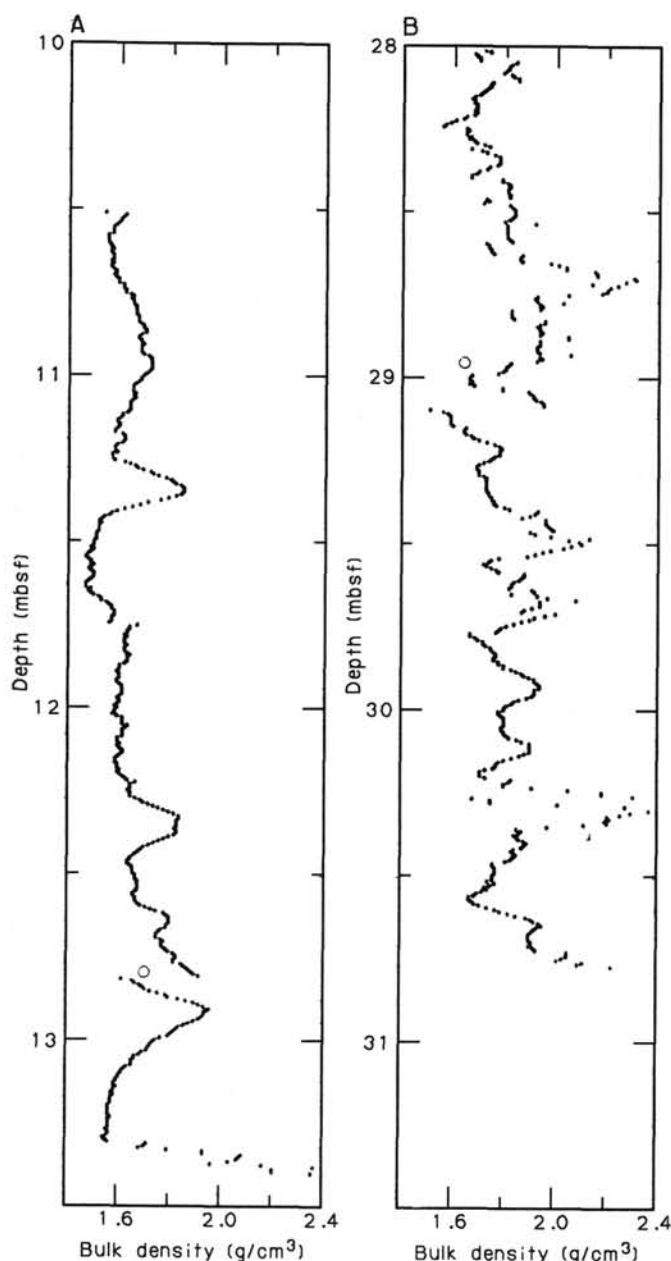


Figure 42. Detailed profiles of bulk-density data for two intervals in Hole 687A. A) Sections 112-687A-2H-3 and 112-687A-2H-4. B) Sections 112-687A-4H-2 and 112-687A-4H-3. Small dots denote GRAPE data; open circles indicate sample measurements.

be a straight line, and heat flow should be calculated by taking into account the variation of thermal conductivity. Because few thermal-conductivity data were obtained from lithologic Units II and III, we assumed that the thermal conductivity was $1.3 \text{ W/m} \cdot \text{K}$ in Unit II (57 to 103 mbsf) and $0.9 \text{ W/m} \cdot \text{K}$ in Unit III (below 103 mbsf). The latter value is based on the relationship between thermal conductivity and water content for the Leg 112 samples (see "Physical Properties" section, Site 688 chapter). These values were corrected for temperature and pressure effects and then converted into the thermal resistance between the temperature measurement points. Using the least-squares method, we calculated the heat flow as 60 mW/m^2 . This value is higher than a heat flow of 45 mW/m^2 at Site 686; however, this difference may not be significant when one considers the uncertainty of all the thermal-conductivity data.

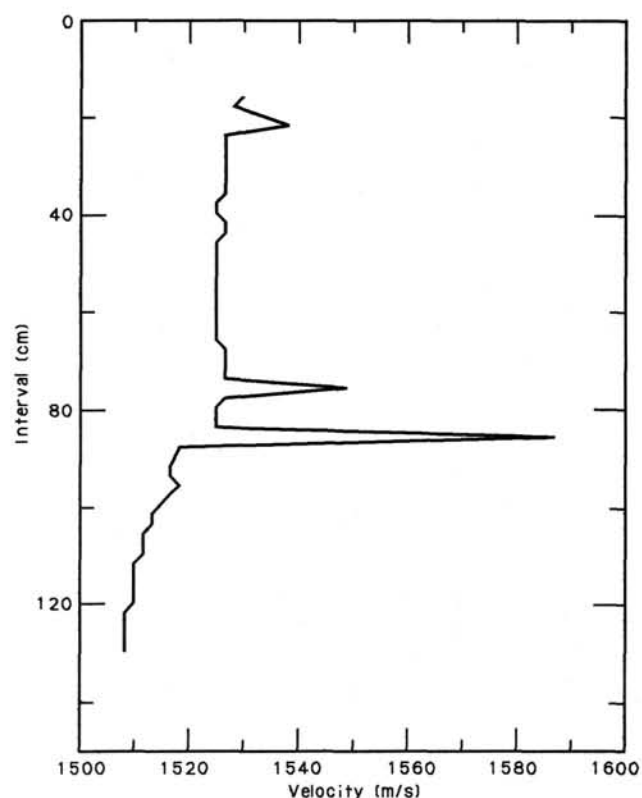


Figure 43. P-wave-velocity profile for Section 112-687A-1H-1.

SUMMARY AND CONCLUSIONS

Site 687 and the companion Site 686 straddle the critical water depths between 300 and 450 m near the lower boundary of the oxygen-minimum zone in the Peru coastal upwelling regime. These sites were selected (1) to obtain a high-resolution record of the upwelling and climatic histories from Quaternary and possibly Neogene sediments, (2) to evaluate further the role of the oxygen-minimum zone on organic matter burial, and (3) to document in detail early diagenetic reactions and products specific to the coastal upwelling environment. Site 687 is located on the seaward flank of the Lima Platform, which in this area forms the eastern and southern boundaries of the Lima Basin.

Two holes were drilled at Site 687. Hole 687A was cored to a total depth of 207.0 mbsf, using the APC tool to 55.0 mbsf and then followed by XCB coring. Hole 687B was cored using the same combination of drilling tools to 195.3 mbsf. Overall core recovery was moderate (50%) in both holes; however, recovery was poor (<20%) in the thick sand intervals. Cores from both holes could be correlated readily, based on lithostratigraphic and biostratigraphic markers. A distinct ash bed marker was located at 47.8 mbsf; it consisted of a 2-cm-thick white layer and 10-cm-thick gray layer above. We also found this marker at Site 686 in the same stratigraphic position (i.e., near the base of the lower sequence; however, located at 153.6 mbsf. Clearly, these landward-thickening sequences, which occur at both Sites 686 and 687, are coeval. During the late Quaternary, the sedimentation rates in these neighboring basins differed by a factor of almost three.

The sediments at Site 687 consisted of diatomaceous mud having wide variations in texture and composition. These variations served to subdivide the sections into three lithologic units and four subunits (i.e., Subunits IA, IB, Unit II, Subunit IIIA, and Subunit IIIB). The variation in composition is caused by calcareous intervals and reflects different proportions of authi-

Table 13. Summary of vane-shear-strength data for Holes 687A and 687B.

Core-section interval (cm)	Depth (mbsf)	Peak (kPa)
112-687A-1H-1, 61	0.61	11.86
1H-3, 110	4.10	38.08
2H-2, 35	9.35	51.67
2H-4, 79	12.79	54.44
3H-2, 74	19.24	65.97
4H-2, 96	28.96	48.90
4H-4, 112	32.12	78.43
5H-2, 81	38.31	77.05
5H-4, 84	41.34	71.05
5H-6, 136	44.86	93.66
6H-1, 61	46.11	86.60
6H-3, 100	49.50	165.74
7X-2, 11	56.61	50.02
13X-2, 89	114.39	85.85
13X-4, 93	117.43	80.63
13X-6, 78	120.28	98.55
15X-2, 35	132.85	84.36
17X-2, 118	152.68	69.43
17X-4, 122	155.72	64.95
17X-6, 38	157.88	91.83
19X-2, 121	171.71	53.75
21X-2, 129	190.79	67.94
21X-4, 35	192.85	165.74
22X-3, 80	201.30	129.90
112-687B-1H-3, 115	4.15	44.75
3H-4, 65	19.85	88.84
5H-2, 78	35.98	68.68
6H-2, 84	45.54	64.95
6H-4, 64	48.34	135.13
6H-6, 67	51.37	174.70
7H-1, 50	53.20	95.56
15X-2, 107	121.87	88.84

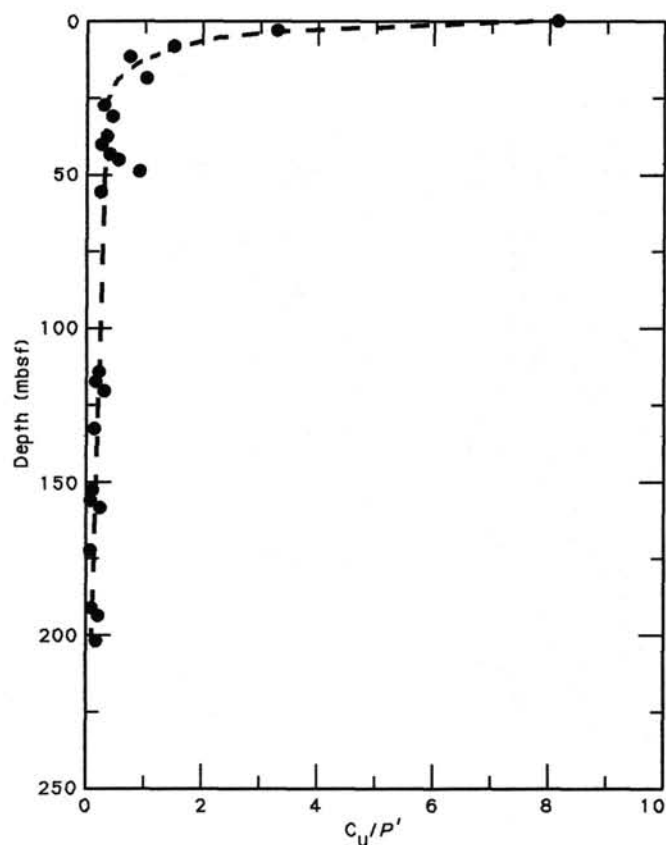


Figure 45. Ratio of peak undrained vane shear strength to effective overburden pressure vs. depth for Hole 687A.

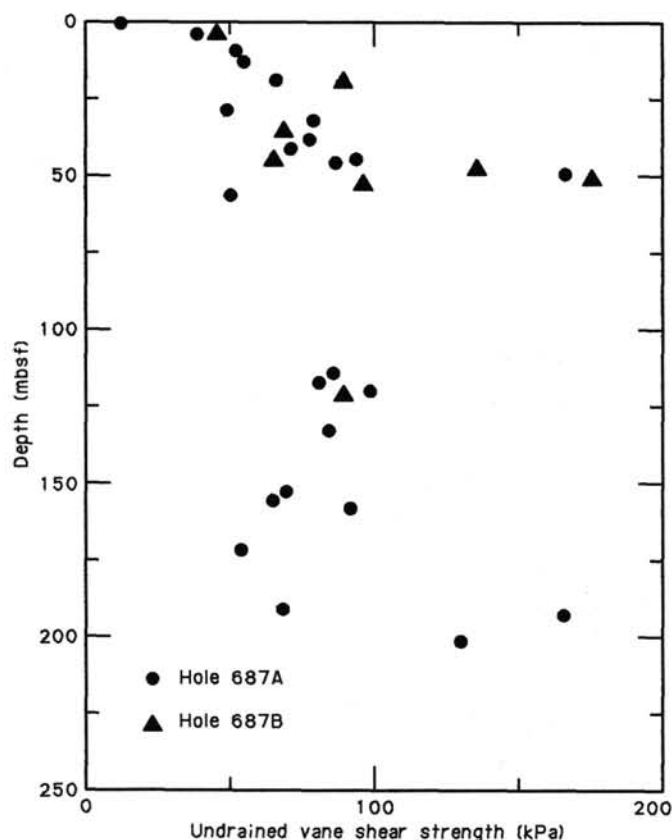


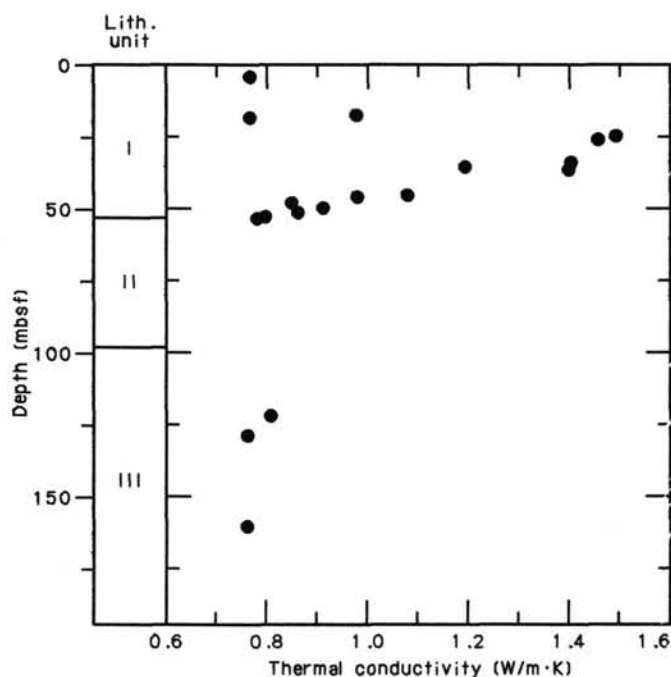
Figure 44. Profile of vane shear strength for Site 687.

genic dolomite and calcite as well as biogenic (mainly foraminifer and mollusk) calcium carbonate. The variation in texture results from sand and silt contents, which are higher at Site 687 than anywhere else along the paleoceanographic transect off Peru. Indeed, units are subdivided by frequent sand and silt beds interlayered with laminated diatomaceous mud. These units display a large-scale trend from laminated intervals having little textural variation and rare bioturbation (Subunit IIIB) to laminated intervals containing more frequent sand beds (Subunit IIIA) to those that consist largely of fine sand (Unit II). The youngest unit, which overlies the fine sand, changes back again from bioturbated diatomaceous mud having frequent sand intervals (Subunit IB) to a more laminated diatomaceous mud having fewer sand intervals (Subunit IA). Thus, the deposition environment at Site 687 has changed over the past 2.5 m.y. from one of upper-slope water depths to a shallower shelf environment and back again to upper-slope water depths. The influence of the nearby shelf can be seen in the many graded beds of well-sorted sands. The most likely cause for these beds is sporadic sand flows over the shelf break in the form of current-generated sand sheets. This mechanism could produce the sharp contacts to the underlying diatomaceous mud typical for the sand beds at Site 687. Benthic foraminifers support the changes in water depth inferred from the lithostratigraphy and also indicate low oxygen conditions for the deep habitats (300 m). These changes probably reflect eustatic sea-level fluctuations in the Pliocene-lower Pleistocene section and basin subsidence for the middle and upper Quaternary sections.

In all sections, diatom floras were found that indicated different intensities of coastal upwelling and fertility. These were classified to represent (1) strong, (2) sporadic, (3) no upwelling but high productivity, and (4) normal continental margin pro-

Table 14. Thermal-conductivity data from Hole 687B.

Core-section interval (cm)	Depth (m)	Thermal conductivity (W/m·K)
112-687B-1H-4, 20	4.70	0.763
3H-2, 147	17.67	0.972
3H-4, 3	19.23	0.762
4H-1, 80	25.00	1.490
4H-2, 40	26.10	1.457
5H-1, 70	34.40	1.401
5H-2, 80	36.00	1.191
5H-2, 130	36.50	1.397
6H-2, 80	45.50	1.076
6H-3, 80	46.00	0.975
6H-4, 60	48.30	0.845
6H-5, 70	49.90	0.907
6H-6, 100	51.70	0.858
7H-1, 70	53.40	0.792
7H-1, 120	53.90	0.776
15X-2, 118	121.98	0.806
16X-1, 53	129.33	0.759
19X-3, 46	160.76	0.756

**Figure 46. Thermal conductivity vs. depth below seafloor for Hole 687B.**

ductivity. At least five prolonged phases of intense coastal upwelling and high productivity occur during shallow- and deep-water periods at Site 687. This provides ample resolution and a repeated record of different facies development to document changes in the zonal structure of upwelling centers.

Diagenetic products are common throughout the cores of Site 687. Of these, friable phosphates occur only in the diatomaceous mud of Subunit IA. Dense phosphate peloids are present throughout the lithologic units. Phosphate conglomerates are common at erosional contacts, and phosphate-cemented shells or bones were found in several cores. Both authigenic calcite and dolomite are abundant in the sediment as disseminated crystals in unlithified sands, silts, or muds and as fully lithified nodules and beds. The first dolomite bed occurs below the sulfate-

depletion zone and coincides with high methane concentrations. In this zone, biogenic methane again is accompanied by persistent and anomalously high ethane contents, as we found previously at Site 686. The source of the ethane is unclear; microbial production may be one mechanism and another might be the influx of ethane from a subsurface brine. This brine can be seen clearly in a chloride anomaly equivalent to 140% of normal seawater salinity, similar to other shelf sites. Besides potentially supplying ethane, the brine continually replenishes calcium and magnesium depleted by carbonate mineral formation. We found subtle differences in the Ca^{2+} , Mg^{2+} , alkalinity, NH_4^+ , and PO_4^{3-} profiles between Sites 686 and 687, which we believe are related to the rate of sedimentation, rate of authigenic mineral formation, and to loading of the brine with unreactive metabolites. The loading of metabolites probably reflects the brine's subsurface passage through organic-rich sediments that undergo decomposition by sulfate reduction.

REFERENCES

- Akiba, F., 1985. Middle Miocene to Quaternary diatom biostratigraphy in the Nankai Trough and Japan Trench, and modified lower Miocene through Quaternary diatom zones for the middle-to-high latitudes of the north Pacific. In Kagami, H., Karig, D. E., Coulbourn, W. C., et al., *Init. Repts. DSDP*, 87: Washington (U.S. Govt. Printing Office), 393-481.
- Backman, J., and Shackleton, N. J., 1983. Quantitative biochronology of Pliocene and early Pleistocene calcareous nannoplankton from the Atlantic, Indian and Pacific oceans. *Mar. Micropaleontol.*, 8: 141-170.
- Barton, C. E., and Bloemendal, J., 1986. Paleomagnetism of sediments collected during Leg 90, Southwest Pacific. In Kennett, J. P., von der Borch, C. C., et al., *Init. Repts. DSDP*, 90 (Pt. 2): Washington (U.S. Govt. Printing Office), 1273-1316.
- Bé, A. W. H., 1977. An ecological, zoogeographic and taxonomic review of Recent planktonic foraminifera. In Ramsay, A. T. S. (Ed.), *Oceanic Micropaleontol.*, 1: 1-100.
- Claypool, G. E., and Kaplan, I. R., 1974. The origin and distribution of methane in marine sediments. In Kaplan, I. R. (Ed.), *Natural Gases in Marine Sediments*: New York (Plenum Press), 94-129.
- Codispoti, L. A., 1983. On nutrient variability and sediments in upwelling regions. In Suess, E., and Thiede, J. (Eds.), *Coastal Upwelling: Its Sediment Record*: New York (Plenum Press), 125-145.
- Dugdale, R. C., 1983. Effects of source nutrient concentrations and nutrient regeneration on production of organic matter in coastal upwelling centers. In Suess, E., and Thiede, J. (Eds.), *Coastal Upwelling: Its Sediment Record*: New York (Plenum Press), 175-182.
- Jones, B. H., Brink, K. H., Dugdale, R. C., Stuart, D. W., van Leer, J. C., Blasco, D., and Kelly, J. C., 1983. Observations of a persistent upwelling off Point Conception, California. In Suess, E., and Thiede, J. (Eds.), *Coastal Upwelling: Its Sediment Record*: New York (Plenum Press), 37-60.
- Kulm, L. D., Schrader, H., Resig, J. M., Thornburg, T. M., Masias, A., and Johnson, L., 1981. Late Cenozoic carbonates on the Peru continental margin: Lithostratigraphy, biostratigraphy, and tectonic history. In Kulm, L. D., Dymond, J., Dasch, E. J., and Hussong, D. M. (Eds.), *Nazca Plate: Crustal Formation and Andean Convergence*. Geol. Soc. Am. Mem., 154: 469-508.
- Packard, T. T., Garfield, P. C., and Codispoti, L. A., 1983. Oxygen consumption and denitrification below the Peruvian upwelling. In Suess, E., and Thiede, J. (Eds.), *Coastal Upwelling: Its Sediment Record*: New York (Plenum Press), 147-173.
- Quinn, W. H., Zopf, D. O., Short, K. S., and Kuo Yang, R. T. W., 1978. Historical trends and statistics of the southern oscillation, El Niño and Indonesian draughts. *Fishery Bull.*, 76(3): 663-678.
- Shackleton, N. J., and Opdyke, N. D., 1973. Oxygen isotope and paleomagnetic stratigraphy of Equatorial Pacific core V28-238: oxygen isotope temperatures and ice volumes on a 10^5 -year and 10^6 -year scale. *Quat. Res.*, 3: 39-55.
- Thornburg, T. M., and Kulm, L. D., 1981. Sedimentary basins of the Peru continental margin: structure, stratigraphy and Cenozoic tec-

tonics from 6°S to 16°S latitude. In Kulm, L. D., Dymond, J., Dasch, E. J., and Hussong, D. M. (Eds.), *Nazca Plate: Crustal Formation and Andean Convergence*. Geol. Soc. Am. Mem., 154:393-422.

Thornton, S. E., 1984. Basin model for hemipelagic sedimentation in a tectonically active continental margin: Santa Barbara Basin, California Continental Borderland. In Stow, D.A.V., and Piper, D.J.W. (Eds.), *Fine-Grained Sediments: Deep-Water Processes and Facies*. Alexandria, VA (Geol. Soc. Am. Spec. Publ.), 15:377-394.

Tissot, B. P., and Welte, D. H., 1984. *Petroleum Formation and Occurrence* (2nd Ed.). Berlin-Heidelberg (Springer-Verlag).

Walker, R. G., 1984. Shelf and shallow marine sands. In Walker, R. G. (Ed.), *Facies Models* (2nd Ed.). Waterloo (Geosci. Can. Reprint Ser.), 1:141-170.

Ms 112A-118

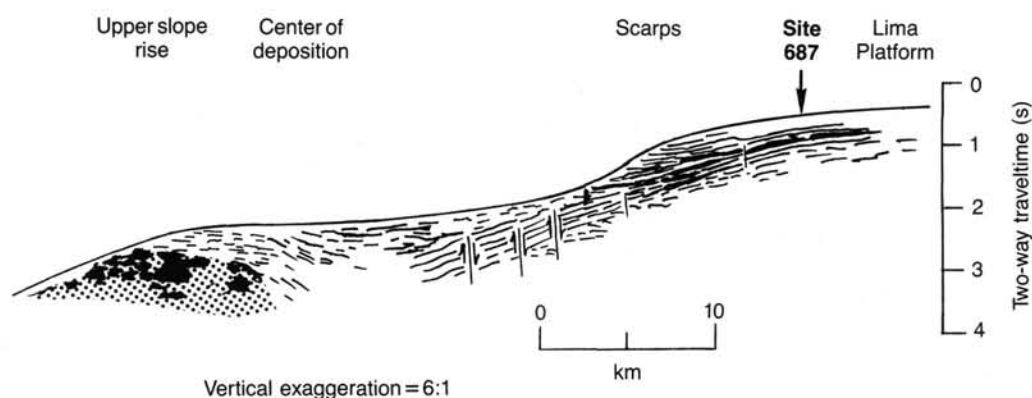


Figure 47. Structure of southern end of Lima Basin at 12.8°S and location of Site 687 (Thornburg and Kulm, 1981).

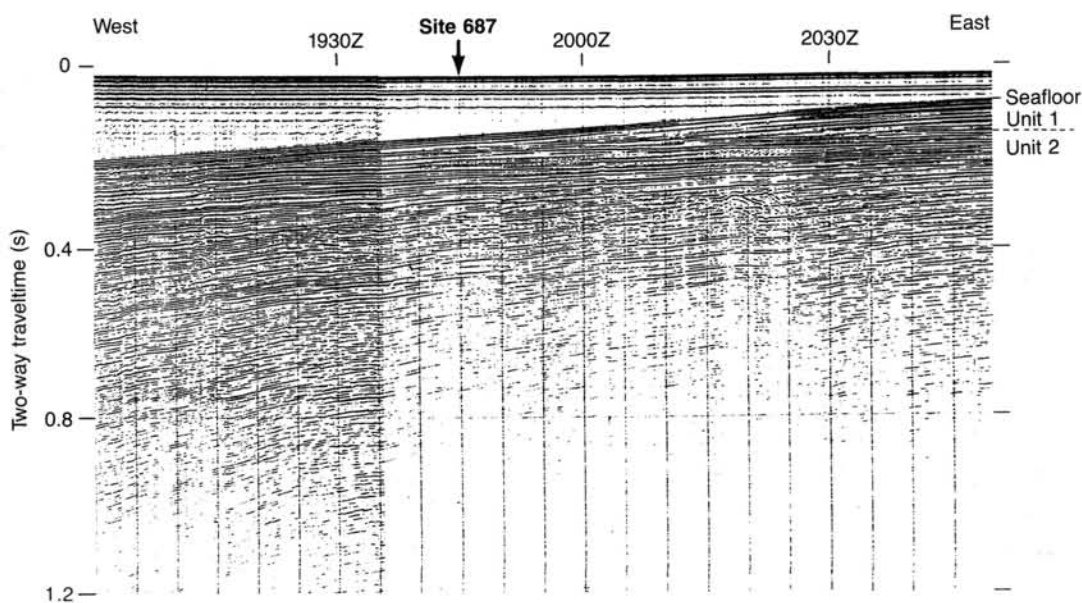


Figure 48. Part of the single-channel seismic line YALOC 12-03-74, showing near flat-lying strata on the seaward flank of the Lima Platform; note the location of Site 687.

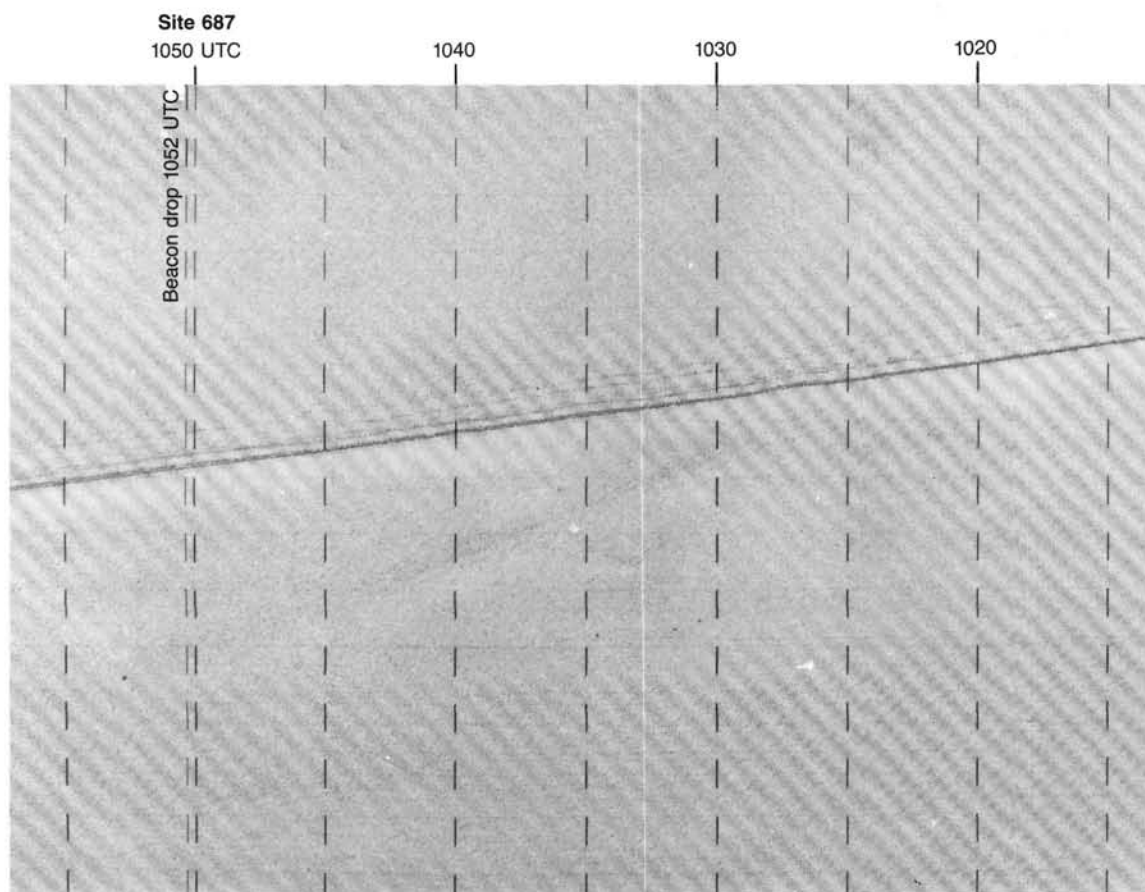


Figure 49. The 3.5-kHz record at Site 687 obtained from *JOIDES Resolution* during approach to the site.

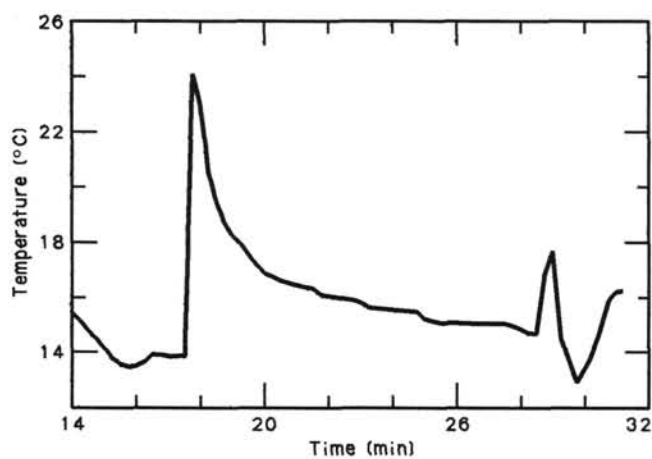


Figure 50. Temperature vs. time record obtained with the APC tool while retrieving Core 112-687A-6H.

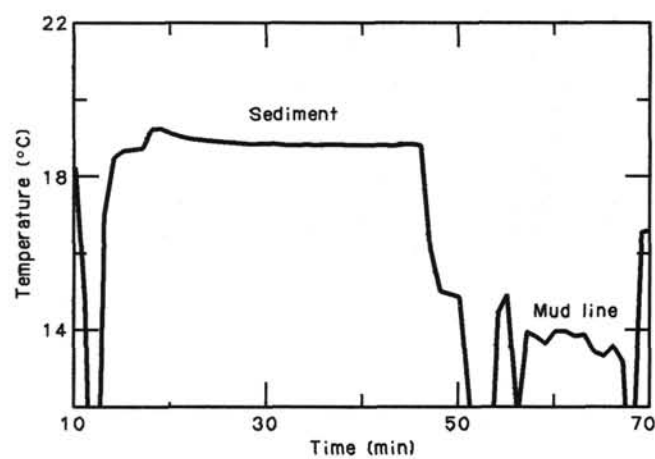


Figure 51. Temperature vs. time record obtained with the T-probe after retrieving Core 112-687A-18X.

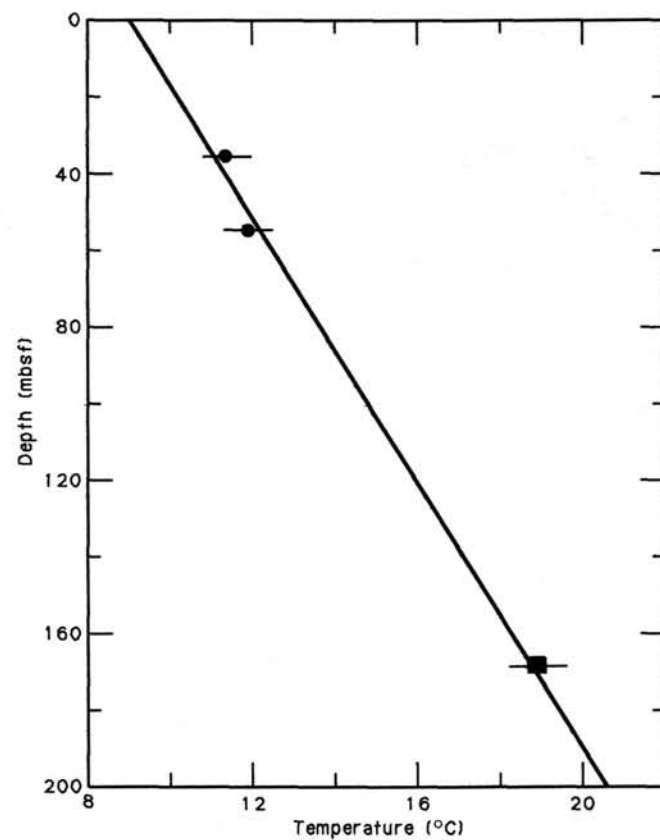
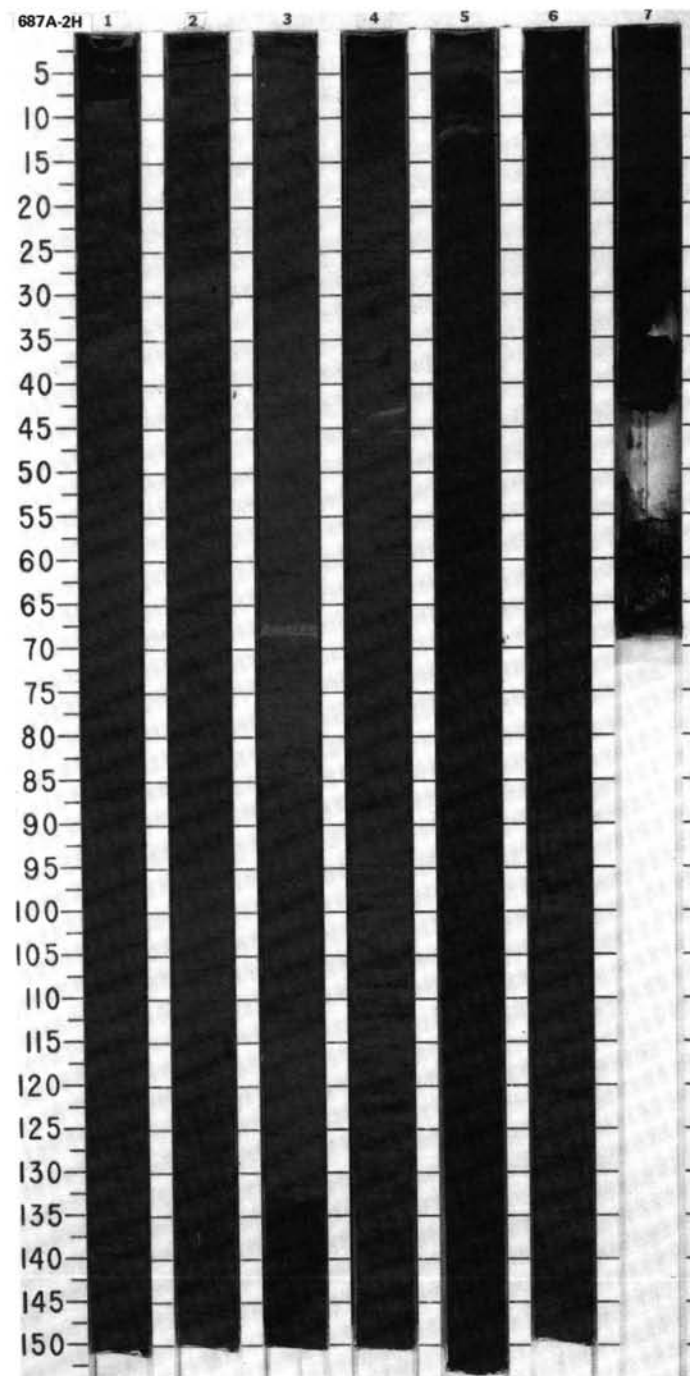


Figure 52. Temperature data from Hole 687A, with error bars plotted vs. depth. Temperatures determined using the APC tool are indicated by dots; T-probe values are indicated by the square. Solid line depicts the geothermal gradient, determined by the least-squares fitting to a straight line.

SITE 687 HOLE A CORE 2H CORED INTERVAL 314.3-323.8 mbsl; 7.5-17.0 mbsf

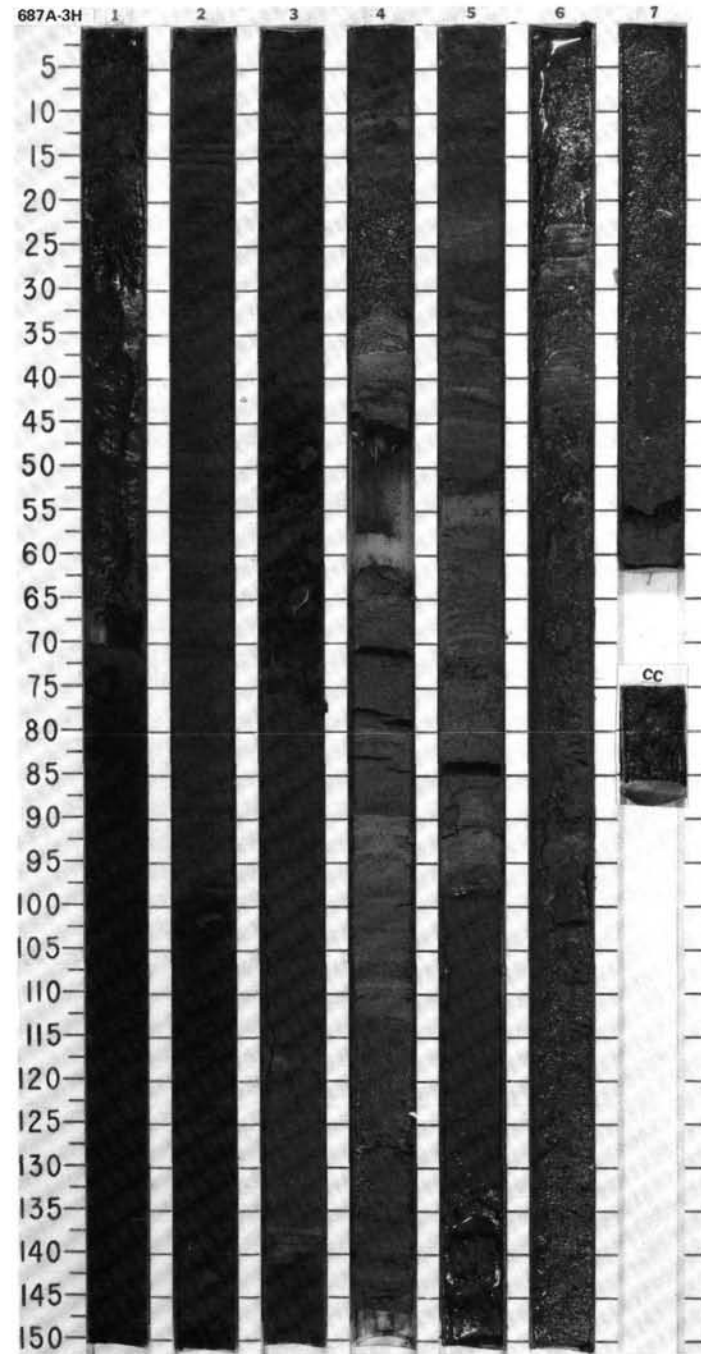
TIME-ROCK UNIT	BIOSTRAT. ZONE/ FOSSIL CHARACTER				PALEOMAGNETICS	PHYS. PROPERTIES	CHEMISTRY	SECTION METERS	GRAPHIC LITHOLOGY	DRILLING DISTURB.	SED. STRUCTURES	SAMPLES	LITHOLOGIC DESCRIPTION
	FORAMINIFERS	NANNOFOSSILS	RADIOLARIANS	DIATOMS									
QUATERNARY													DIATOMACEOUS MUD, SILT, RUBBLE, PHOSPHATE NODULES, and DIATOMACEOUS MUD
								0.5					Major lithology: Section 1, 0-150 cm: diatomaceous mud and silt, very dark gray (5Y 3/1) mud and silt, and dark olive gray (5Y 3/2) to olive gray (5Y 3/3), massive, faintly mottled. Phosphorite blebs at 108 and 122 cm.
								1.0					Section 2, 0-150 cm, diatomaceous mud and silt, dark olive (5Y 3/3) with olive diatom-rich bands, mottled, occasional burrows. Fish bones at Section 2, 80 and 103 cm.
													Section 3, 0-150 cm: diatomaceous mud, olive (5Y 3/3), massive, mottled, vague layering, but evidence for bioturbation. Slump between Section 3, 85 and 113 cm. Dark olive gray (5Y 3/2) sand and silt between 134 and 150 cm.
													Section 4, 0-150 cm: diatomaceous mud, dark olive gray (5Y 3/2) to olive (5Y 3/3), coarsely laminated. Sand layers at Section 4, 50-57, 84-87, and 92-106 cm. Graded beds between Section 4, 98-102, 105-120, 125-131, and 139-143 cm.
													Section 5, 0-150 cm: diatomaceous mud, dark olive gray (5Y 3/2) to black (5Y 2.5/2), with shell fragments, mottled. Graded sand layer at Section 5, 10 cm.
													Section 6, 0-12 cm: rubble and phosphate nodules, black (5Y 2.5/2) to olive (5Y 3/3); 12-150 cm: diatomaceous mud, black (5Y 2.5/2) to dark olive gray (5Y 3/3), bioturbated (12-88 cm) or laminated (88-150 cm). Bone fragment at 98 cm.
													Section 7, 0-70 cm: diatomaceous mud, dark olive gray (5Y 3/2). Bone at 18 cm. Gray (N 5) sand at 20-22 cm. Section 7, 42-68 cm, void.
													SMEAR SLIDE SUMMARY (%):
													1, 79 2, 122 3, 69 4, 120 5, 10 5, 61 D M M M M M
													TEXTURE:
													Sand 2 1 — 80 45 — Silt 61 92 80 20 20 45 Clay 37 7 20 — 35 55
													COMPOSITION:
													Quartz 10 2 35 55 30 13 Feldspar 5 1 23 10 8 5 Rock fragments 2 1 10 25 16 5 Mica Tr — 2 — 2 Tr Clay 37 5 19 — 35 17 Volcanic glass — — — Tr — 1 Calcite/dolomite 2 2 1 — — 2 Accessory minerals 1 — 2 5 — — Pyrite 1 2 3 1 5 10 Phosphate/apatite Tr 2 — — — 37 Glauconite — Tr — — — — Hornblende — — — 2 2 — Foraminifers 10 5 — — — — Nannofossils 2 — — — — — Diatoms 30 80 5 2 2 10
													6, 38 7, 64 D M
													TEXTURE:
													Sand — 100 Silt 25 — Clay 75 —
													COMPOSITION:
													Quartz 1 42 Feldspar — 18 Rock fragments — 30 Clay 75 — Volcanic glass 1 2 Accessory minerals 1 — Pyrite 2 — Hornblende — 8 Diatoms 20 —
													VOID



SITE 687

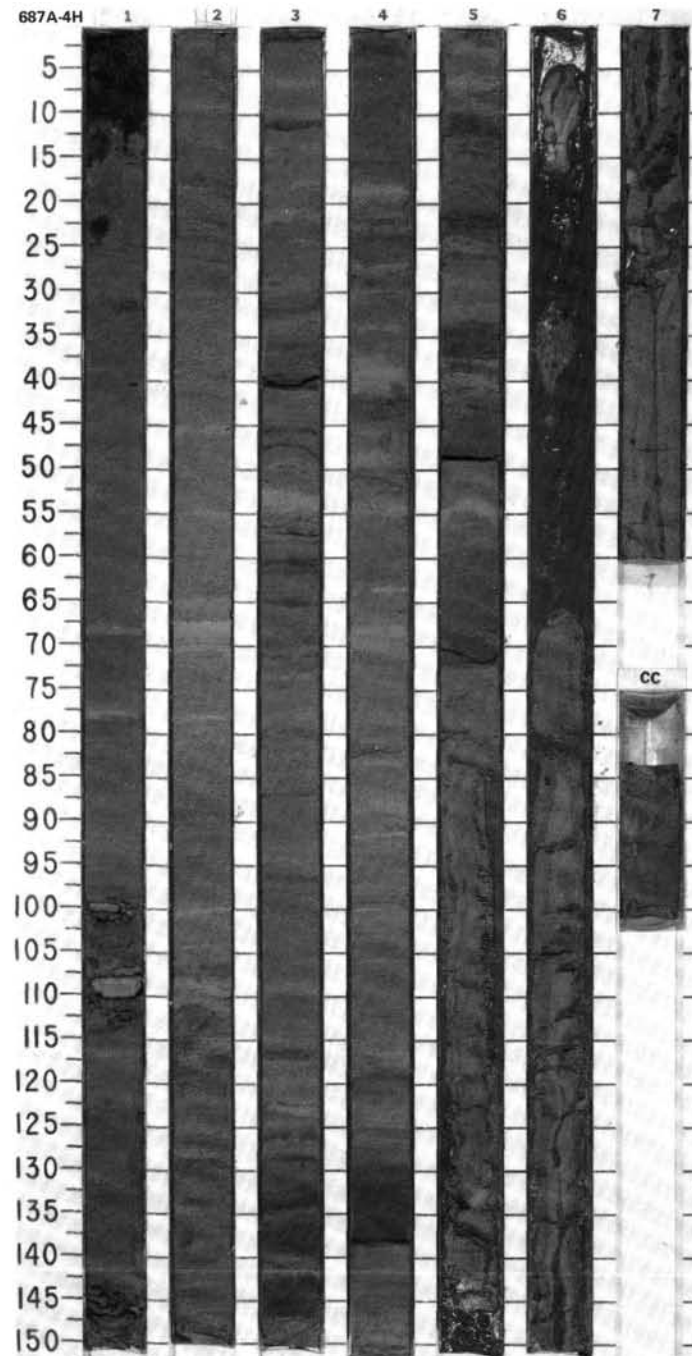
SITE 687 HOLE A CORE 3H CORED INTERVAL 323.8-333.3 mbsf: 17.0-26.5 mbsf

TIME-ROCK UNIT	BIOSTRAT. ZONE/ FOSSIL CHARACTER				PALEOMAGNETICS	PHYS. PROPERTIES CHEMISTRY	SECTION	METERS	GRAPHIC LITHOLOGY	DRILLING DISTURB.	SED. STRUCTURES	SAMPLES	LITHOLOGIC DESCRIPTION
	FORAMINIFERS	NANNOFOSSILS	RADIOLARIANS	DIATOMS									
QUATERNARY	*Quaternary ?	*B	*P. dolioolus Zone		N 1.37 N 1.45								DIATOMACEOUS MUD, SAND, DOLOMITIZED(?) PHOSPHORITE NODULES, DIATOMACEOUS MUD, PHOSPHATIC SAND, SILT, and SILTY SAND Major lithology: Section 1, 0-15 and 76-150 cm: diatomaceous mud, olive gray (5Y 4/2) and dark olive gray (5Y 3/2) with black (5Y 2.5/2) intervals, bioturbated. Small friable phosphates at 103 cm, yellow brown (10 YR 5/6). 15-76 cm: sand, very dark gray (N 4); and 73-76 cm: dolomitized(?) phosphorite nodules, dark brown (10 YR 3/3). Section 2, 0-99 cm: diatomaceous mud, olive gray (5Y 3/2) and dark olive gray (5Y 4/2) with olive (5Y 5/4) laminae rich in diatoms, laminated; 99-104 cm: dark olive gray (5Y 3/2), with yellow brown fish debris and dark olive gray dolomite nodules; and 104-150 cm: diatomaceous mud, dark olive gray (5Y 3/2), with faint olive gray (5Y 4/2) laminae between 127 and 150 cm. Section 3, 0-45 and 77-100 cm: diatomaceous mud, dark olive gray (5GY 3/2), coarsely laminated; 45-77 cm: sand and silt, dark olive (5Y 3/3) with phosphate nodules and large shell fragments; and 100-150 cm: sand and silt, gray (5Y 3/3) and dark greenish gray, bioturbated. Section 4, 0-150 cm: sand and silt, gray (N 5; N 6) and greenish gray (5GY 4/2). Graded beds (base) at 37, 80, 90, 101, 108, and 138 cm; 43-63 cm void. Section 5, 0-150 cm: sand and silty sand, gray (N 5) and dark greenish gray. Graded beds (base) at 45, 50, 74-78, 85, and 90 cm. Section 6, 0-150 cm, Section 7, 0-61, and CC, 0-11 cm: fine sand, gray (N 5/1).
													SMEAR SLIDE SUMMARY (%):
													1, 62 3, 54 3, 88 5, 52 5, 55 D M D D D
													TEXTURE:
													Sand 85 100 — 95 55 Silt 15 — 67 5 30 Clay — — 33 — 15
													COMPOSITION:
													Quartz 50 20 15 30 35 Feldspar 3 15 10 25 5 Rock fragments 20 10 5 — 9 Mica 1 — Tr 1 1 Clay — — 30 — 15 Volcanic glass — — — — 3 Calcite/dolomite — — — 10 — Accessory minerals 3 3 — 3 — Pyrite 15 — — 20 8 Hornblende 8 — Tr 10 — Phosphate — 15 — — — Glaucconite — Tr — 1 — Micrite — — — — 20 Opauques — — 3 — — Green amphibole — 2 — — 4 Diatoms Tr — 35 — 4 Fish remains — 35 — — —



SITE 687 HOLE A CORE 4H CORED INTERVAL 333.3-342.8 mbsl; 26.5-36.0 mbsf

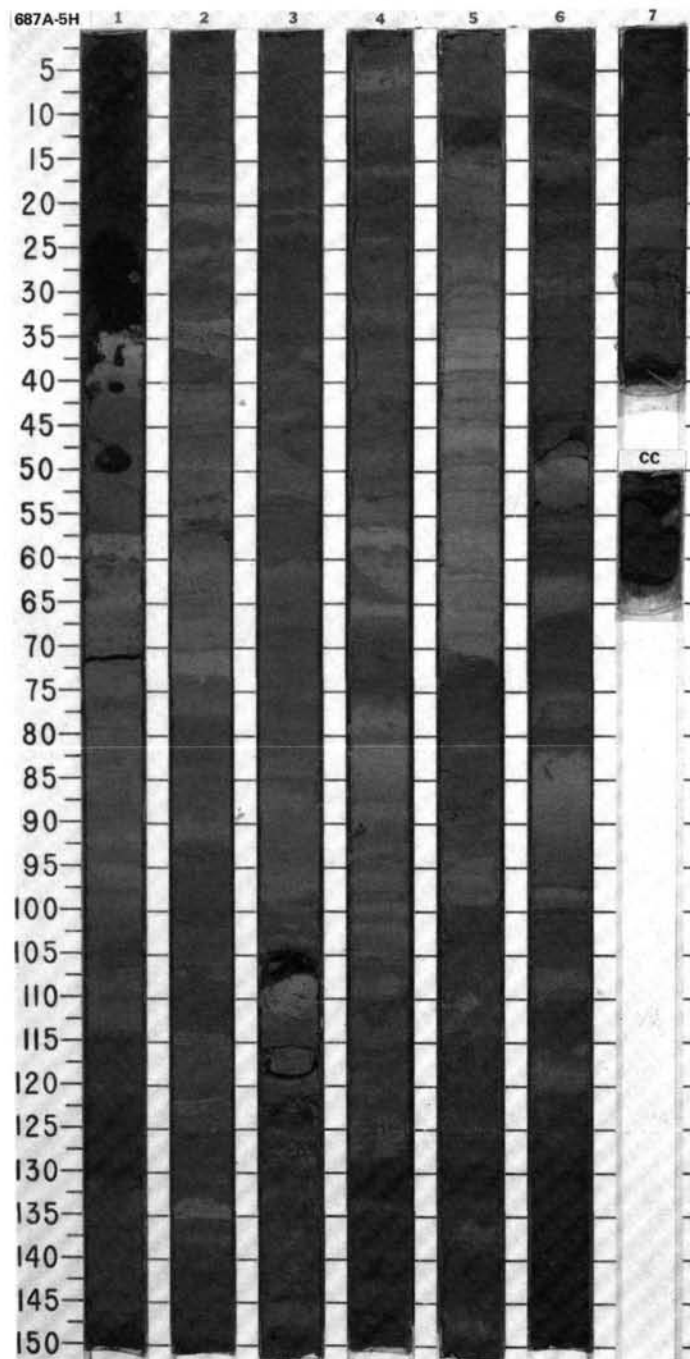
TIME-ROCK UNIT	BIOSTRAT. ZONE/ FOSSIL CHARACTER				PALEOMAGNETICS	PHYS. PROPERTIES	CHEMISTRY	SECTION	METERS	GRAPHIC LITHOLOGY	DRILLING DISTURB.	SED. STRUCTURES	SAMPLES	LITHOLOGIC DESCRIPTION
	FORAMINIFERS	NANNOFOSSILS	RADIOLARIANS	DIATOMS										
QUATERNARY	* B													
	* B													
	* P. dolioles Zone													
	</													

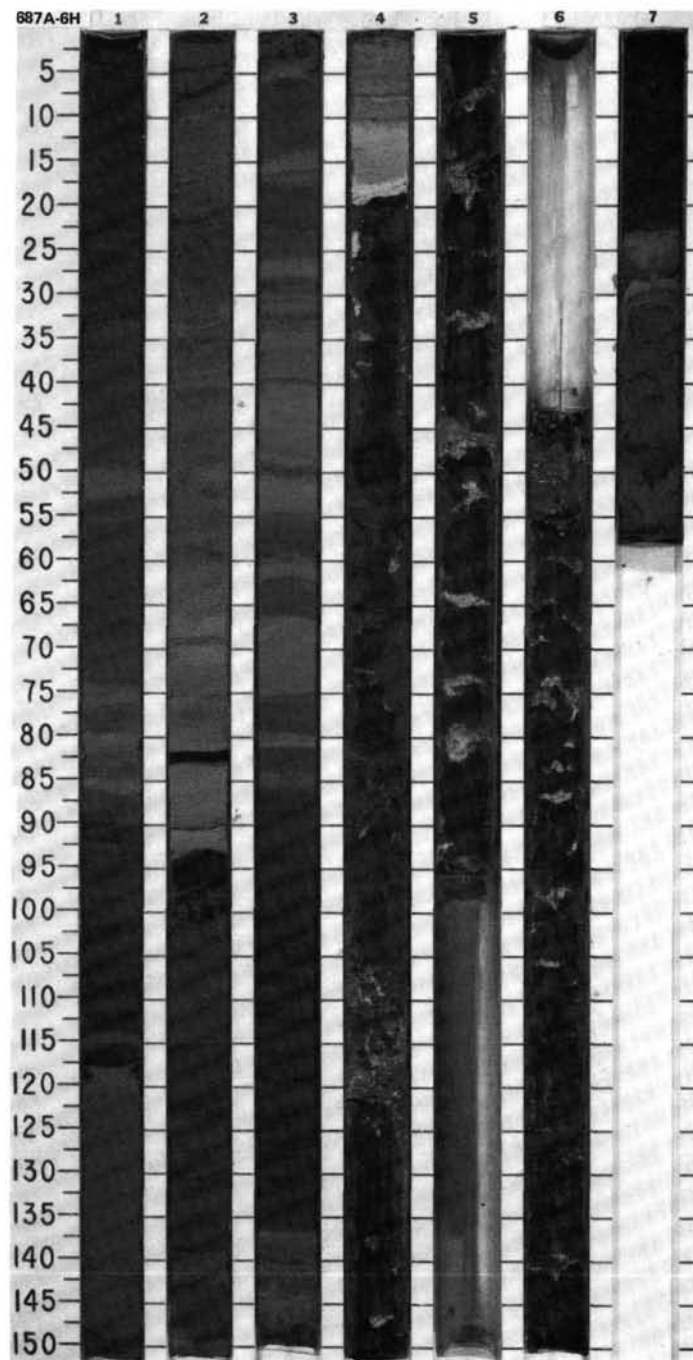


SITE 687

SITE 687 HOLE A CORE 5H CORED INTERVAL 342.8-352.3 mbsl; 36.0-45.5 mbsf

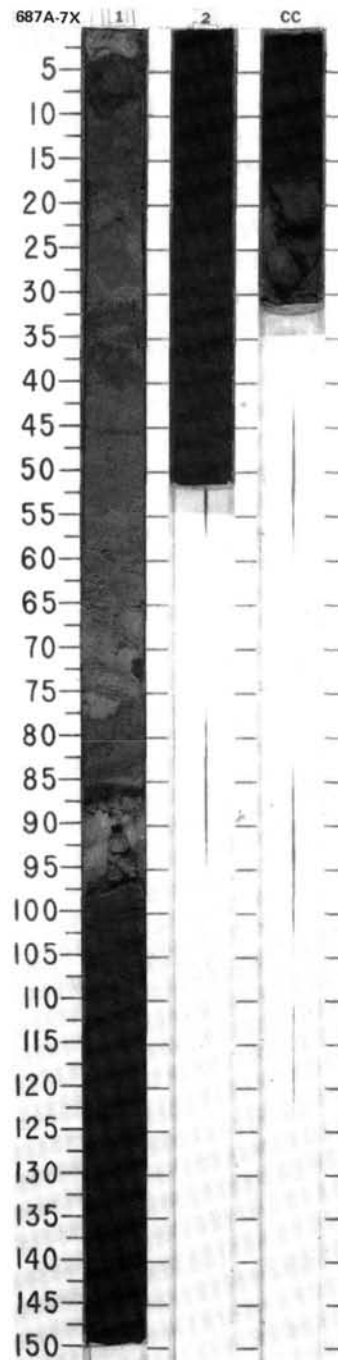
TIME-ROCK UNIT	BIOSTRAT. ZONE/ FOSSIL CHARACTER				SECTION METERS	GRAPHIC LITHOLOGY	DRILLING DISTURB.	SED. STRUCTURES	SAMPLES	LITHOLOGIC DESCRIPTION																																																																																																																																																																	
	FORAMINIFERS	NANNOFOSSILS	RADIOLARIANS	DIATOMS																																																																																																																																																																							
QUATERNARY	* non diagnostic	* B	* <i>P. dolioles</i> Zone	Matuyama	Brunhes					<p>QUARTZO-FELDSPATHIC-LITHIC SAND, DIATOMACEOUS MUD, MUD, DIATOMACEOUS DOLOMITIC SILT, SAND, and SILT</p> <p>Major lithology: Section 1, 0–22 cm: quartz-feldspathic-lithic sand, very dark gray (N 3), graded; 22–34 cm: diatomaceous mud, dark brown (2.5Y 2/2), with black phosphate nodules at base in sandy silt to clay graded bed; 34–150 cm: mud, gray green (5GY 4.5/1) and olive gray (5Y 4/2) interbeds with quartzo-feldspathic-lithic sand. Graded beds at 55, 64, 93, 97, 110, 136, and 147 cm.</p> <p>Section 2, 0–150 cm: diatomaceous mud, olive (5Y 5/1) to dusky green (10Y 3/2), interbedded with gray (N 5) sand. Graded beds at 27, 40, 59, 73, 76, 121, 143, and 145 cm. Locally minor bioturbation.</p> <p>Section 3, 0–150 cm: diatomaceous mud, olive (5Y 5/1) to dusky green (10Y 3/2), interbedded with gray (N 4) sand. Graded beds at 40, 54, and 140 cm. Probable slump fold at 46–52 cm; 105–110 cm void.</p> <p>Section 4, 0–150 cm: diatomaceous mud, olive (5Y 5/1) to dusky green (10Y 3/2), interbedded with gray (N 4) sand and dolomitic silt, thin bedding to mottled. Graded beds at 56, 74, 87, 93, 102, 104, 110, 114, 129, and 143 cm.</p> <p>Section 5, 0–150 cm: diatomaceous dolomitic silt, olive (5Y 4/3), interbedded with dark gray (5Y 4/1) sand. Graded beds at 9, 35, 45, 59, 69, 92, 142, and 148 cm.</p> <p>Section 6, 0–150 cm: dolomitic diatomaceous silt, olive (5Y 4/3), interbedded with gray (5Y 5/1) sand. Graded beds at 66, 80, 97, 102, 113, and 125 cm. Gray (5Y 5/1) dolomitic at 46–54 cm.</p> <p>Section 7, 0–40 cm: diatomaceous silt (0–13 cm), olive (5Y 4/3) and gray (5Y 5/1) sand and mud. Graded beds at 20 and 40 cm.</p> <p>CC, 0–12 cm: sand and silt, olive (5Y 4/3) and dark olive gray (5Y 3/2), massive.</p> <p>SMEAR SLIDE SUMMARY (%):</p> <table> <tr> <td>1, 32 D</td><td>1, 37 M</td><td>2, 57 D</td><td>2, 97 D</td><td>3, 6 M</td><td>3, 114 D</td></tr> </table> <p>TEXTURE:</p> <table> <tr> <td>Sand</td><td>100</td><td>—</td><td>50</td><td>20</td><td>—</td><td>5</td></tr> <tr> <td>Silt</td><td>—</td><td>30</td><td>30</td><td>55</td><td>85</td><td>75</td></tr> <tr> <td>Clay</td><td>Tr</td><td>70</td><td>20</td><td>25</td><td>15</td><td>20</td></tr> </table> <p>COMPOSITION:</p> <table> <tr> <td>Quartz</td><td>15</td><td>2</td><td>35</td><td>15</td><td>2</td><td>5</td></tr> <tr> <td>Feldspar</td><td>10</td><td>2</td><td>20</td><td>10</td><td>2</td><td>10</td></tr> <tr> <td>Rock fragments</td><td>5</td><td>1</td><td>20</td><td>10</td><td>1</td><td>—</td></tr> <tr> <td>Mica</td><td>—</td><td>—</td><td>Tr</td><td>—</td><td>—</td><td>—</td></tr> <tr> <td>Clay</td><td>—</td><td>—</td><td>—</td><td>15</td><td>8</td><td>—</td></tr> <tr> <td>Volcanic glass</td><td>—</td><td>—</td><td>—</td><td>—</td><td>—</td><td>Tr</td></tr> <tr> <td>Calcite/dolomite</td><td>1</td><td>70</td><td>—</td><td>5</td><td>2</td><td>55</td></tr> </table> <p>Accessory minerals</p> <table> <tr> <td>Pyrite</td><td>—</td><td>5</td><td>10</td><td>10</td><td>—</td><td>5</td></tr> <tr> <td>Phosphate</td><td>40</td><td>—</td><td>5</td><td>15</td><td>—</td><td>Tr</td></tr> <tr> <td>Hornblende</td><td>4</td><td>—</td><td>1</td><td>—</td><td>—</td><td>—</td></tr> <tr> <td>Foraminifers</td><td>—</td><td>—</td><td>4</td><td>—</td><td>—</td><td>Tr</td></tr> <tr> <td>Nannofossils</td><td>—</td><td>—</td><td>—</td><td>—</td><td>Tr</td><td>—</td></tr> <tr> <td>Diatoms</td><td>—</td><td>20</td><td>5</td><td>20</td><td>85</td><td>25</td></tr> <tr> <td>Fish remains</td><td>25</td><td>—</td><td>—</td><td>—</td><td>—</td><td>Tr</td></tr> </table> <p>5, 36 D</p> <p>6, 52 M</p> <p>TEXTURE:</p> <table> <tr> <td>Sand</td><td>5</td><td>20</td></tr> <tr> <td>Silt</td><td>60</td><td>50</td></tr> <tr> <td>Clay</td><td>35</td><td>30</td></tr> </table> <p>COMPOSITION:</p> <table> <tr> <td>Quartz</td><td>20</td><td>15</td></tr> <tr> <td>Feldspar</td><td>15</td><td>10</td></tr> <tr> <td>Rock fragments</td><td>15</td><td>5</td></tr> <tr> <td>Mica</td><td>Tr</td><td>—</td></tr> <tr> <td>Calcite/dolomite</td><td>35</td><td>43</td></tr> </table> <p>Accessory minerals</p> <table> <tr> <td>Pyrite</td><td>5</td><td>5</td></tr> <tr> <td>Glaucconite</td><td>—</td><td>2</td></tr> <tr> <td>Diatoms</td><td>10</td><td>20</td></tr> <tr> <td>Sponge spicules</td><td>—</td><td>Tr</td></tr> </table>	1, 32 D	1, 37 M	2, 57 D	2, 97 D	3, 6 M	3, 114 D	Sand	100	—	50	20	—	5	Silt	—	30	30	55	85	75	Clay	Tr	70	20	25	15	20	Quartz	15	2	35	15	2	5	Feldspar	10	2	20	10	2	10	Rock fragments	5	1	20	10	1	—	Mica	—	—	Tr	—	—	—	Clay	—	—	—	15	8	—	Volcanic glass	—	—	—	—	—	Tr	Calcite/dolomite	1	70	—	5	2	55	Pyrite	—	5	10	10	—	5	Phosphate	40	—	5	15	—	Tr	Hornblende	4	—	1	—	—	—	Foraminifers	—	—	4	—	—	Tr	Nannofossils	—	—	—	—	Tr	—	Diatoms	—	20	5	20	85	25	Fish remains	25	—	—	—	—	Tr	Sand	5	20	Silt	60	50	Clay	35	30	Quartz	20	15	Feldspar	15	10	Rock fragments	15	5	Mica	Tr	—	Calcite/dolomite	35	43	Pyrite	5	5	Glaucconite	—	2	Diatoms	10	20	Sponge spicules	—	Tr
1, 32 D	1, 37 M	2, 57 D	2, 97 D	3, 6 M	3, 114 D																																																																																																																																																																						
Sand	100	—	50	20	—	5																																																																																																																																																																					
Silt	—	30	30	55	85	75																																																																																																																																																																					
Clay	Tr	70	20	25	15	20																																																																																																																																																																					
Quartz	15	2	35	15	2	5																																																																																																																																																																					
Feldspar	10	2	20	10	2	10																																																																																																																																																																					
Rock fragments	5	1	20	10	1	—																																																																																																																																																																					
Mica	—	—	Tr	—	—	—																																																																																																																																																																					
Clay	—	—	—	15	8	—																																																																																																																																																																					
Volcanic glass	—	—	—	—	—	Tr																																																																																																																																																																					
Calcite/dolomite	1	70	—	5	2	55																																																																																																																																																																					
Pyrite	—	5	10	10	—	5																																																																																																																																																																					
Phosphate	40	—	5	15	—	Tr																																																																																																																																																																					
Hornblende	4	—	1	—	—	—																																																																																																																																																																					
Foraminifers	—	—	4	—	—	Tr																																																																																																																																																																					
Nannofossils	—	—	—	—	Tr	—																																																																																																																																																																					
Diatoms	—	20	5	20	85	25																																																																																																																																																																					
Fish remains	25	—	—	—	—	Tr																																																																																																																																																																					
Sand	5	20																																																																																																																																																																									
Silt	60	50																																																																																																																																																																									
Clay	35	30																																																																																																																																																																									
Quartz	20	15																																																																																																																																																																									
Feldspar	15	10																																																																																																																																																																									
Rock fragments	15	5																																																																																																																																																																									
Mica	Tr	—																																																																																																																																																																									
Calcite/dolomite	35	43																																																																																																																																																																									
Pyrite	5	5																																																																																																																																																																									
Glaucconite	—	2																																																																																																																																																																									
Diatoms	10	20																																																																																																																																																																									
Sponge spicules	—	Tr																																																																																																																																																																									



SITE 687

SITE 687 HOLE A CORE 7X CORED INTERVAL 361.8-371.3 mbsl; 55.0-64.5 mbsf

TIME-ROCK UNIT	BIOSTRAT. ZONE/ FOSSIL CHARACTER				PALEOMAGNETICS	PHYS. PROPERTIES	CHEMISTRY	SECTION	METERS	GRAPHIC LITHOLOGY	DRILLING DISTURB.	SED. STRUCTURES	SAMPLES	LITHOLOGIC DESCRIPTION																																																																																																																																																										
	FORAMINIFERS	NANNOFOSSILS	RADIOLARIANS	DIATOMS																																																																																																																																																																				
QUATERNARY	B*				Matuyama	Y-1.42 N-77.16		1	0.5				*	DIATOM-FORAMINIFER-BEARING MUD, DOLOMICRITE, SANDY MUD, and DOLOMITIC DIATOMACEOUS MUD Section 1, 0-150 cm: diatom-foraminifer-bearing mud and dolomitic, dark olive gray (5Y 3/2) to olive (5Y 4/4), bioturbated or laminated (96-113 cm). Section 2, 0-51 cm: sandy mud, black (5Y 2.5/2) to very dark olive gray (5Y 3/20), bioturbated above 30 cm, laminated below. Black (5Y 2.5/1) to very dark gray sand with phosphate nodules interbedded (22-29 cm). CC, 0-25 cm: dolomitic diatomaceous mud, dark olive gray (5Y 3/2) to black (5Y 2.5/2), laminated. Quartz-feldspar-lithic sand at 17-25 cm, graded. SMEAR SLIDE SUMMARY (%): <table><tr><td></td><td>1, 1</td><td>1, 87</td><td>1, 120</td><td>2, 17</td><td>2, 27</td><td>CC, 20</td></tr><tr><td></td><td>M</td><td>M</td><td>D</td><td>D</td><td>M</td><td>D</td></tr></table> TEXTURE: <table><tr><td>Sand</td><td>5</td><td>—</td><td>15</td><td>25</td><td>5</td><td>70</td></tr><tr><td>Silt</td><td>80</td><td>10</td><td>55</td><td>45</td><td>5</td><td>30</td></tr><tr><td>Clay</td><td>15</td><td>90</td><td>30</td><td>30</td><td>90</td><td>—</td></tr></table> COMPOSITION: <table><tr><td>Quartz</td><td>20</td><td>5</td><td>10</td><td>10</td><td>5</td><td>30</td></tr><tr><td>Feldspar</td><td>35</td><td>3</td><td>10</td><td>10</td><td>3</td><td>25</td></tr><tr><td>Rock fragments</td><td>15</td><td>2</td><td>5</td><td>5</td><td>Tr</td><td>35</td></tr><tr><td>Mica</td><td>Tr</td><td>—</td><td>—</td><td>—</td><td>—</td><td>—</td></tr><tr><td>Clay</td><td>—</td><td>—</td><td>25</td><td>25</td><td>—</td><td>—</td></tr><tr><td>Volcanic glass</td><td>Tr</td><td>—</td><td>—</td><td>—</td><td>—</td><td>Tr</td></tr><tr><td>Calcite/dolomite</td><td>30</td><td>85</td><td>20</td><td>15</td><td>5</td><td>2</td></tr></table> Accessory minerals <table><tr><td>Pyrite</td><td>—</td><td>—</td><td>3</td><td>5</td><td>—</td><td>2</td></tr><tr><td>Phosphate peloids</td><td>—</td><td>—</td><td>10</td><td>—</td><td>—</td><td>—</td></tr><tr><td>Phosphate</td><td>Tr</td><td>—</td><td>Tr</td><td>10</td><td>2</td><td>—</td></tr><tr><td>Apatite</td><td>—</td><td>—</td><td>—</td><td>—</td><td>85</td><td>—</td></tr><tr><td>Hornblende</td><td>—</td><td>Tr</td><td>Tr</td><td>2</td><td>—</td><td>5</td></tr><tr><td>Pyroxene</td><td>—</td><td>Tr</td><td>—</td><td>—</td><td>—</td><td>1</td></tr></table> Foraminifers <table><tr><td>Foraminifers</td><td>Tr</td><td>—</td><td>10</td><td>10</td><td>—</td><td>—</td></tr><tr><td>Nannofossils</td><td>—</td><td>Tr</td><td>—</td><td>—</td><td>—</td><td>—</td></tr><tr><td>Diatoms</td><td>—</td><td>5</td><td>7</td><td>8</td><td>—</td><td>—</td></tr><tr><td>Sponge spicules</td><td>—</td><td>—</td><td>—</td><td>Tr</td><td>—</td><td>—</td></tr></table>		1, 1	1, 87	1, 120	2, 17	2, 27	CC, 20		M	M	D	D	M	D	Sand	5	—	15	25	5	70	Silt	80	10	55	45	5	30	Clay	15	90	30	30	90	—	Quartz	20	5	10	10	5	30	Feldspar	35	3	10	10	3	25	Rock fragments	15	2	5	5	Tr	35	Mica	Tr	—	—	—	—	—	Clay	—	—	25	25	—	—	Volcanic glass	Tr	—	—	—	—	Tr	Calcite/dolomite	30	85	20	15	5	2	Pyrite	—	—	3	5	—	2	Phosphate peloids	—	—	10	—	—	—	Phosphate	Tr	—	Tr	10	2	—	Apatite	—	—	—	—	85	—	Hornblende	—	Tr	Tr	2	—	5	Pyroxene	—	Tr	—	—	—	1	Foraminifers	Tr	—	10	10	—	—	Nannofossils	—	Tr	—	—	—	—	Diatoms	—	5	7	8	—	—	Sponge spicules	—	—	—	Tr	—	—
	1, 1	1, 87	1, 120	2, 17	2, 27	CC, 20																																																																																																																																																																		
	M	M	D	D	M	D																																																																																																																																																																		
Sand	5	—	15	25	5	70																																																																																																																																																																		
Silt	80	10	55	45	5	30																																																																																																																																																																		
Clay	15	90	30	30	90	—																																																																																																																																																																		
Quartz	20	5	10	10	5	30																																																																																																																																																																		
Feldspar	35	3	10	10	3	25																																																																																																																																																																		
Rock fragments	15	2	5	5	Tr	35																																																																																																																																																																		
Mica	Tr	—	—	—	—	—																																																																																																																																																																		
Clay	—	—	25	25	—	—																																																																																																																																																																		
Volcanic glass	Tr	—	—	—	—	Tr																																																																																																																																																																		
Calcite/dolomite	30	85	20	15	5	2																																																																																																																																																																		
Pyrite	—	—	3	5	—	2																																																																																																																																																																		
Phosphate peloids	—	—	10	—	—	—																																																																																																																																																																		
Phosphate	Tr	—	Tr	10	2	—																																																																																																																																																																		
Apatite	—	—	—	—	85	—																																																																																																																																																																		
Hornblende	—	Tr	Tr	2	—	5																																																																																																																																																																		
Pyroxene	—	Tr	—	—	—	1																																																																																																																																																																		
Foraminifers	Tr	—	10	10	—	—																																																																																																																																																																		
Nannofossils	—	Tr	—	—	—	—																																																																																																																																																																		
Diatoms	—	5	7	8	—	—																																																																																																																																																																		
Sponge spicules	—	—	—	Tr	—	—																																																																																																																																																																		
								2	1.0				*																																																																																																																																																											
								CC					*																																																																																																																																																											



SITE 687 HOLE A CORE 8X CORED INTERVAL 371.3-380.8 mbsl; 64.5-74.0 mbsf

TIME-ROCK UNIT	BIOSTRAT. ZONE/ FOSSIL CHARACTER				PALEOMAGNETICS	PHYS. PROPERTIES	CHEMISTRY	SECTION	METERS	GRAPHIC LITHOLOGY	DRILLING DISTURB. SED. STRUCTURES	SAMPLES	LITHOLOGIC DESCRIPTION
	FORAMINIFERS	NANNOFOSSILS	RADIOLARIANS	DIATOMS									
QUATERNARY	B *		B *	B *				CC				*	<p>DIATOMACEOUS MUD and LITHIC SAND</p> <p>Major lithology: CC, 0-24 cm: diatomaceous mud (at 0-3 cm), olive gray (5Y 4/2), and dark gray (5Y 4/1) lithic sand, with shell fragments at 16 cm.</p> <p>SMEAR SLIDE SUMMARY (%):</p> <p>CC, 10 D</p> <p>TEXTURE:</p> <p>Sand 80 Silt 20</p> <p>COMPOSITION:</p> <p>Quartz 30 Feldspar 18 Rock fragments 30 Volcanic glass 2 Accessory minerals Pyrite 5 Micrite 10 Hornblende 5 Pyroxene Tr</p>

SITE 687 HOLE A CORE 9X CORED INTERVAL 380.8-3990.3 mbsl; 74.0-83.5 mbsf

TIME-ROCK UNIT	BIOSTRAT. ZONE/ FOSSIL CHARACTER				PALEOMAGNETICS	PHYS. PROPERTIES	CHEMISTRY	SECTION	METERS	GRAPHIC LITHOLOGY	DRILLING DISTURB. SED. STRUCTURES	SAMPLES	LITHOLOGIC DESCRIPTION				
	FORAMINIFERS	NANNOFOSSILS	RADIOLARIANS	DIATOMS													
QUATERNARY	non diagnostic *			P. <i>doliolus</i> Zone *									ROCK FRAGMENTS				
													Major lithology: four rock fragments: black, hard phosphate nodule, fine-grained sandstone, dolomitic siltstone, and cemented silty sand, in CC.				
													SMEAR SLIDE SUMMARY (%):				
													CC, 0 D	CC, 0 D	CC, 0 D	CC, 0 D	
													TEXTURE:				
													Sand	20	—	30	15
													Silt	10	50	50	85
													Clay	70	50	20	—
													COMPOSITION:				
													Quartz	10	20	30	35
													Feldspar	10	15	20	25
													Rock fragments	5	10	20	20
													Mica	—	—	2	—
													Calcite/dolomite	75	50	5	—
													Accessory minerals	—	—	5	—
													Pyrite	—	5	—	—
													Foraminifers	—	—	5	10
													Diatoms	—	—	5	5
													Sponge spicules	—	—	3	5
													Fish remains	—	—	5	—

687A-8X

CC

5
10
15
20
25
30
35
40
45
50
55
60
65
70
75
80
85
90
95
100
105
110
115
120
125
130
135
140
145
150



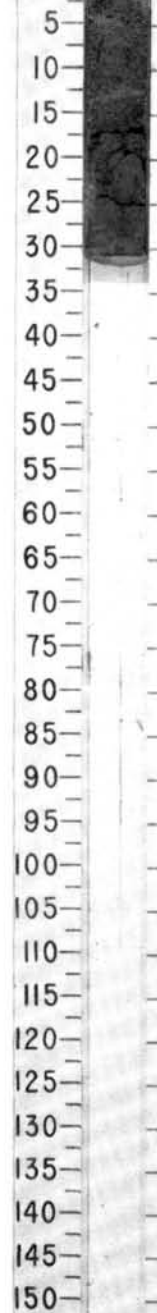
SITE 687 HOLE A CORE 10X CORED INTERVAL 390.3-399.8 mbsl; 83.5-93.0 mbsf

TIME-ROCK UNIT	BIOSTRAT. ZONE/ FOSSIL CHARACTER				PALEOMAGNETICS	PHYS. PROPERTIES	CHEMISTRY	SECTION	METERS	GRAPHIC LITHOLOGY	DRILLING DISTURB. SED. STRUCTURES	SAMPLES	LITHOLOGIC DESCRIPTION
	FORAMINIFERS	NANNOFOSILS	RADIOLARIANS	DIATOMS									
QUATERNARY	non diagnostic *			<i>P. dolioles</i> Zone *				CC				*	LITHIC SILTY SAND Major lithology: lithic silty sand, gray (5Y 4/1), CC, 0-32 cm. SMEAR SLIDE SUMMARY (%): 1, 14 D TEXTURE: Sand 60 Silt 40 COMPOSITION: Quartz 40 Feldspar 18 Rock fragments 20 Mica Tr Volcanic glass 2 Accessory minerals Pyrite 5 Glauconite Tr Micrite 10 Hornblende 5 Rutile Tr Olivine Tr Foraminifers Tr

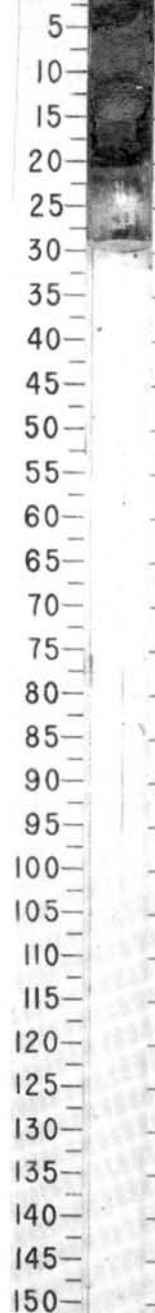
SITE 687 HOLE A CORE 11X CORED INTERVAL 399.8-409.3 mbsl; 93.0-102.5 mbsf

TIME-ROCK UNIT	BIOSTRAT. ZONE/ FOSSIL CHARACTER				PALEOMAGNETICS	PHYS. PROPERTIES	CHEMISTRY	SECTION	METERS	GRAPHIC LITHOLOGY	DRILLING DISTURB.	SED. STRUCTURES	SAMPLES	LITHOLOGIC DESCRIPTION
	FORAMINIFERS	NANNOFOSSILS	RADIOLARIANS	DIATOMS										
?	non diagnostic *			B *				CC						DOLOMITIC, PHOSPHATIC, LITHIC SILTY SAND
														Major lithology: dolomitic, phosphatic, lithic silty sand, gray (5Y 4/1, 5/1, 6/1), CC, 0-19 cm.
														SMEAR SLIDE SUMMARY (%):
														CC, 8 CC, 14 D M
														TEXTURE:
														Sand 80 25
														Silt 10 40
														Clay 10 35
														COMPOSITION:
														Quartz 25 20
														Feldspar 15 15
														Rock fragments 15 15
														Mica — 3
														Calcite/dolomite 10 30
														Accessory minerals
														Pyrite — 5
														Phosphate peloids 30 —
														Hornblende 5 2
														Diatoms — 5
														Sponge spicules — 5

687A-10X CC

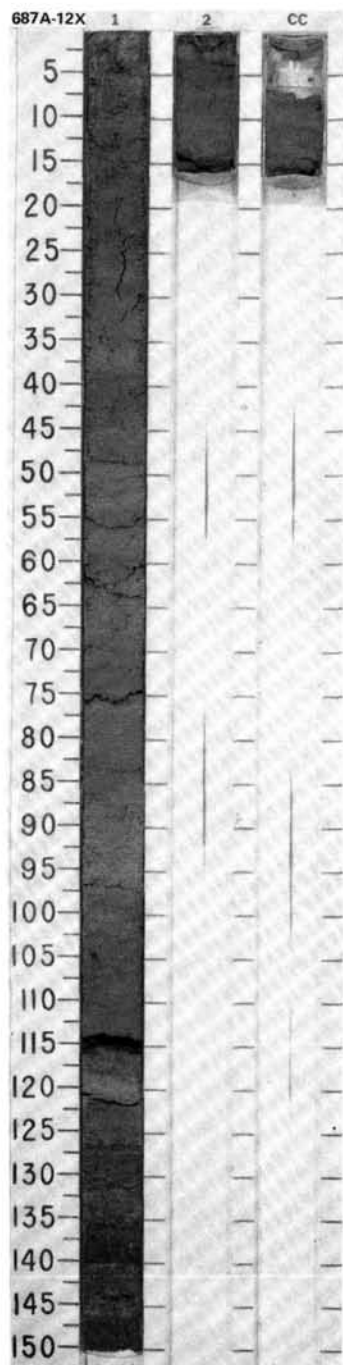


687A-11X CC



SITE 687 HOLE A CORE 12X CORED INTERVAL 409.3-418.8 mbsl; 102.5-112.0 mbsf

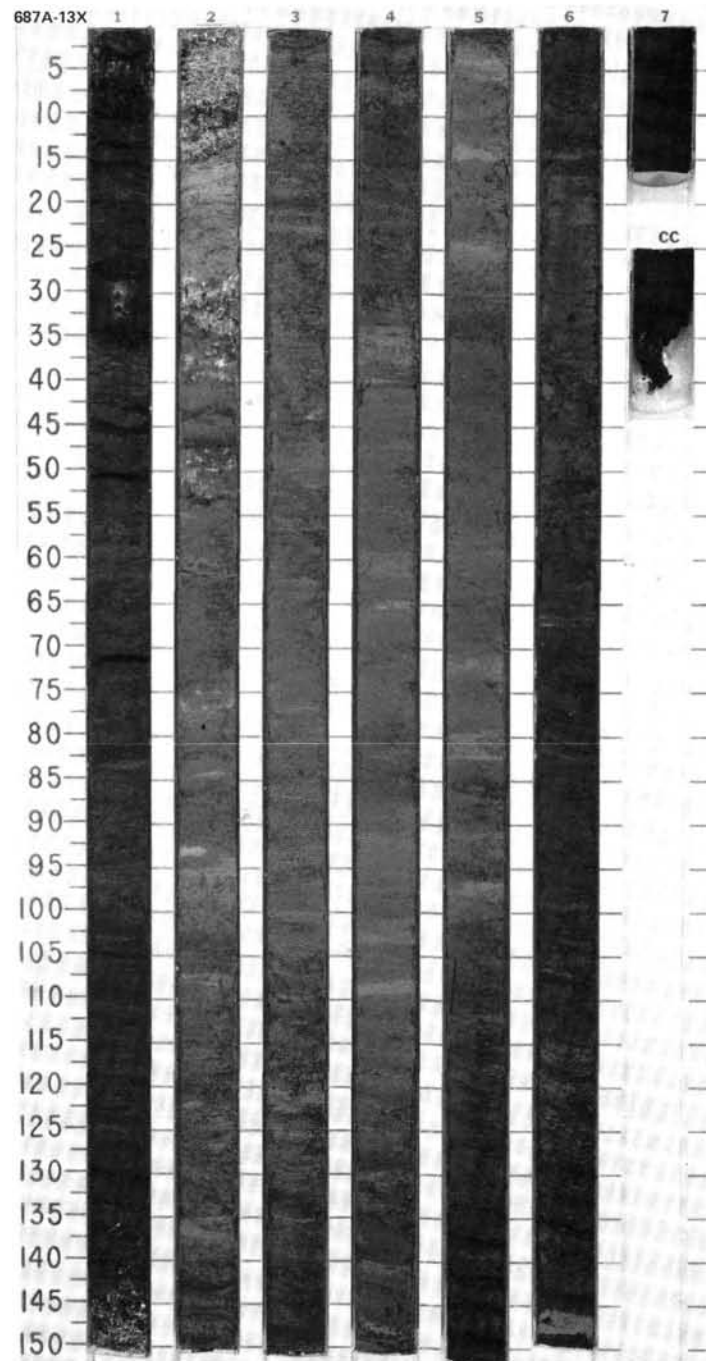
TIME-ROCK UNIT	BIOSTRAT. ZONE/ FOSSIL CHARACTER				PALEOMAGNETICS	PHYS. PROPERTIES	CHEMISTRY	SECTION	METERS	GRAPHIC LITHOLOGY	DRILLING DISTURB. SED. STRUCTURES	SAMPLES	LITHOLOGIC DESCRIPTION
	FORAMINIFERS	NANNOFOSSILS	RADIOLARIANS	DIATOMS									
QUATERNARY	non diagnostic*			<i>P. dolioles</i> [<i>R. matuyamai</i>] Zone*		✓ 1.90 ● 0.58, 0.4		1	0.5		***	*	MICRITIC SILT and LITHIC SILTY SAND Major lithology: Section 1, 0-150 cm: micritic silt, gray (5Y 5/1), coarsely bedded with bioturbation. Graded beds at 48, 70, and 140 cm. Shell layers at 87, 104, and 143.5 cm. Section 2, 0-16 cm: lithic silty sand, gray (5Y 5/1) with gastropod shells at 16 cm. Graded bed at 13 cm. CC, 6-16 cm: lithic silty sand, gray (5Y 5/1). SMEAR SLIDE SUMMARY (%): 1, 68 D 1, 120 M TEXTURE: Sand 30 30 Silt 60 20 Clay 10 50 COMPOSITION: Quartz 30 10 Feldspar 25 10 Rock fragments 15 5 Mica — Tr Clay — 10 Volcanic glass 5 45 Accessory minerals Hornblende 4 — Amphibole — Tr Micrite 20 — Foraminifers Tr — Diatoms — 15 Sponge spicules 1 5
								2	1.0				



SITE 687

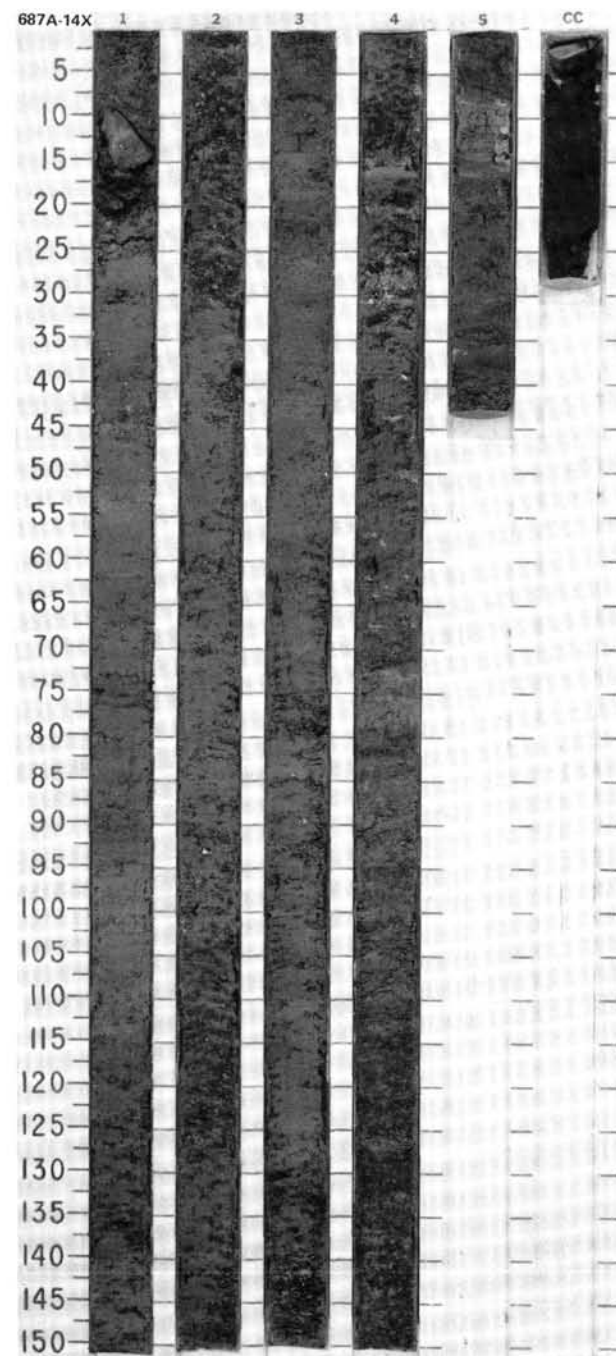
SITE 687 HOLE A CORE 13X CORED INTERVAL 418.8-428.3 mbsl; 112.0-121.5 mbsf

TIME-ROCK UNIT	BIOSTRAT. ZONE/ FOSSIL CHARACTER				PALEOMAGNETICS	PHYS. PROPERTIES	CHEMISTRY	SECTION	METERS	GRAPHIC LITHOLOGY	DRILLING DISTURB.	SED. STRUCTURES	SAMPLES	LITHOLOGIC DESCRIPTION																																																								
	FORAMINIFERS	NANNOFOSSILS	RADIOLARIANS	DIATOMS																																																																		
QUATERNARY	* non diagnostic																																																																					
	* <i>P. dololus</i> (<i>Mesocena quadrangula</i>) Zone																																																																					
SILTY MUD, MUD, and DIATOMACEOUS MUD																																																																						
Major lithology: Section 1, 0–150 cm: silty mud, olive gray (5Y 4/2), massive to bioturbated. Shell hash at 144–150 cm. Section 2, 0–150 cm: mud, olive gray (5Y 4/20), bioturbated. Shelly hash to 54 cm. Greenish gray (5GY 4/1) silty beds at 38–46, 95–102, and 135–140 cm. Section 3, 0–150 cm: silty mud, olive gray (5Y 5/2), laminated and bioturbated. Section 4, 0–150 cm: silty mud, olive gray (5Y 4/2), massive to bioturbated with greenish gray (5GY 5/1) graded silt layer. Section 5, 0–150 cm: mud, olive gray (5Y 5/2), bioturbated, interbedded with greenish gray (5GY 5/1) graded silt and sand (base at 34, 82, 93, and 102 cm). Section 6, 0–150 cm, and Section 7, 0–16 cm: diatomaceous mud, dark olive gray (5Y 3/2) with olive (5Y 4/3) diatom-rich layers. Graded sand bed at 146–149 cm. CC, 0–16 cm: diatomaceous mud, dark olive gray (5Y 3/2), massive with collapsed sponges at 9 cm.																																																																						
SMEAR SLIDE SUMMARY (%):																																																																						
<table><tr><td></td><td>1, 22</td><td>2, 47</td><td>3, 23</td></tr><tr><td></td><td>D</td><td>M</td><td>D</td></tr></table>																1, 22	2, 47	3, 23		D	M	D																																																
	1, 22	2, 47	3, 23																																																																			
	D	M	D																																																																			
TEXTURE:																																																																						
<table><tr><td>Sand</td><td>5</td><td>90</td><td>25</td></tr><tr><td>Silt</td><td>50</td><td>10</td><td>45</td></tr><tr><td>Clay</td><td>45</td><td>—</td><td>30</td></tr></table>															Sand	5	90	25	Silt	50	10	45	Clay	45	—	30																																												
Sand	5	90	25																																																																			
Silt	50	10	45																																																																			
Clay	45	—	30																																																																			
COMPOSITION:																																																																						
<table><tr><td>Quartz</td><td>5</td><td>15</td><td>8</td></tr><tr><td>Feldspar</td><td>5</td><td>15</td><td>6</td></tr><tr><td>Rock fragments</td><td>5</td><td>15</td><td>6</td></tr><tr><td>Clay</td><td>35</td><td>—</td><td>20</td></tr><tr><td>Calcite/dolomite</td><td>Tr</td><td>Tr</td><td>2</td></tr><tr><td>Accessory minerals</td><td></td><td></td><td></td></tr><tr><td> Pyrite</td><td>5</td><td>—</td><td>6</td></tr><tr><td> Phosphate peloids</td><td>—</td><td>35</td><td>—</td></tr><tr><td> Amphibole</td><td>—</td><td>Tr</td><td>—</td></tr><tr><td>Foraminifers</td><td>—</td><td>20</td><td>25</td></tr><tr><td>Diatoms</td><td>45</td><td>—</td><td>25</td></tr><tr><td>Radiolarians</td><td>Tr</td><td>—</td><td>—</td></tr><tr><td>Sponge spicules</td><td>—</td><td>—</td><td>2</td></tr><tr><td>Silicoflagellates</td><td>Tr</td><td>—</td><td>—</td></tr></table>															Quartz	5	15	8	Feldspar	5	15	6	Rock fragments	5	15	6	Clay	35	—	20	Calcite/dolomite	Tr	Tr	2	Accessory minerals				Pyrite	5	—	6	Phosphate peloids	—	35	—	Amphibole	—	Tr	—	Foraminifers	—	20	25	Diatoms	45	—	25	Radiolarians	Tr	—	—	Sponge spicules	—	—	2	Silicoflagellates	Tr	—	—
Quartz	5	15	8																																																																			
Feldspar	5	15	6																																																																			
Rock fragments	5	15	6																																																																			
Clay	35	—	20																																																																			
Calcite/dolomite	Tr	Tr	2																																																																			
Accessory minerals																																																																						
Pyrite	5	—	6																																																																			
Phosphate peloids	—	35	—																																																																			
Amphibole	—	Tr	—																																																																			
Foraminifers	—	20	25																																																																			
Diatoms	45	—	25																																																																			
Radiolarians	Tr	—	—																																																																			
Sponge spicules	—	—	2																																																																			
Silicoflagellates	Tr	—	—																																																																			



SITE 687 HOLE A CORE 14X CORED INTERVAL 428.3-437.8 mbsl; 121.5-131.0 mbsf

TIME-ROCK UNIT	BIOSTRAT. ZONE/ FOSSIL CHARACTER				PALEOMAGNETICS	PHYS. PROPERTIES	CHEMISTRY	SECTION	METERS	GRAPHIC LITHOLOGY	DRILLING DISTURB.	SED. STRUCTURES	SAMPLES	LITHOLOGIC DESCRIPTION
	FORAMINIFERS	NANOFOSSILS	RADIOLARIANS	DIATOMS										
QUATERNARY	*B *insignificant *non diagnostic *P. dololus Zone													
					γ=1.58 δ=71.65									
					γ=1.38 δ=63.47									



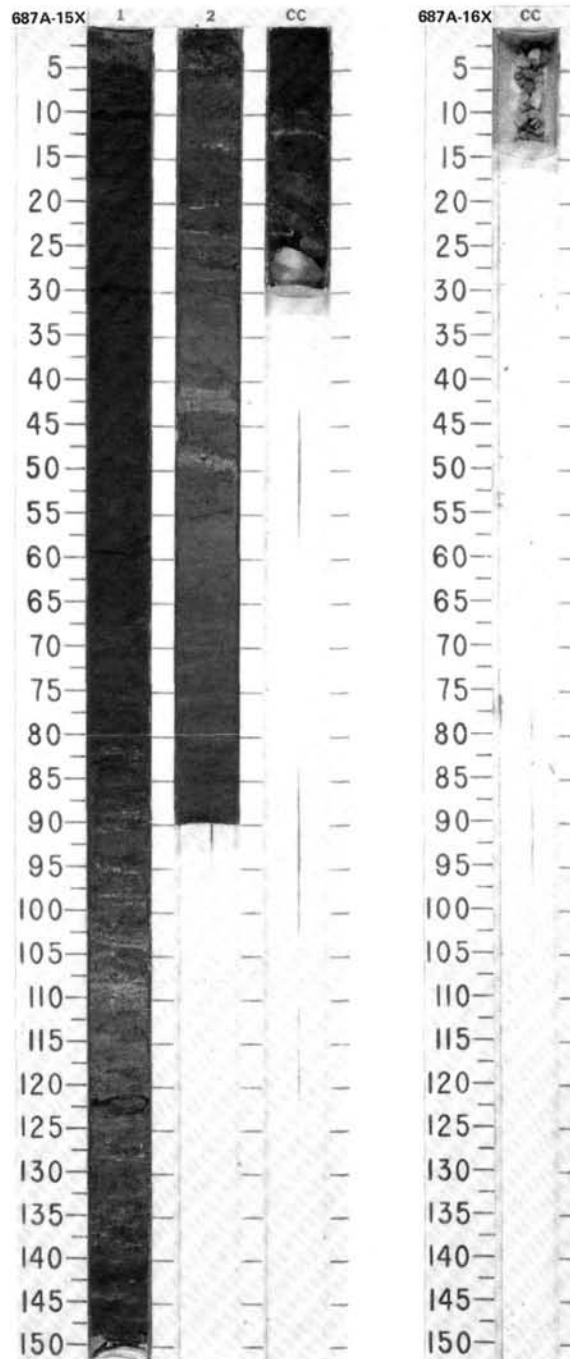
SITE 687

SITE 687 HOLE A CORE 15X CORED INTERVAL 437.8-447.3 mbsl; 131.0-140.5 mbsf

TIME-ROCK UNIT	BIOSTRAT. ZONE/ FOSSIL CHARACTER			PALEOMAGNETICS	PHYS. PROPERTIES	CHEMISTRY	SECTION	METERS	GRAPHIC LITHOLOGY	DRILLING DISTURB.	SED. STRUCTURES	SAMPLES	LITHOLOGIC DESCRIPTION
	FORAMINIFERS	NANNOFOSSILS	RADIOLARIANS										
	DIATOMS												
PLIOCENE ?	* B												
	* B												
	* <i>N. reinholdii</i> (N. fossilis) Zone												

SITE 687 HOLE A CORE 16X CORED INTERVAL 447.3-456.8 mbsl; 140.5-150.0 mbsf

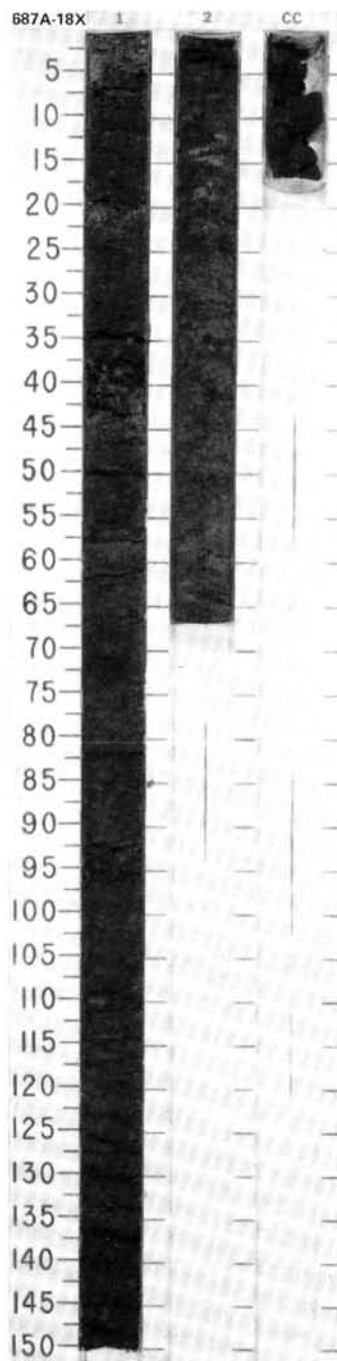
TIME-ROCK UNIT	BIOSTRAT. ZONE/ FOSSIL CHARACTER			PALEOMAGNETICS	PHYS. PROPERTIES	CHEMISTRY	SECTION	METERS	GRAPHIC LITHOLOGY	DRILLING DISTURB.	SED. STRUCTURES	SAMPLES	LITHOLOGIC DESCRIPTION
	FORAMINIFERS	NANNOFOSSILS	RADIOLARIANS										
	DIATOMS												
PLIOCENE	N. fossilis Zone*						CC					*	CEMENTED SANDSTONE Major lithology: cemented sandstone, angular gravel-sized fragments of gray (5Y 4/1) and olive (5Y 5/4) dolomitic limestone in CC, 0-13 cm. SMEAR SLIDE SUMMARY (%): CC M TEXTURE: Silt 20 Clay 80 COMPOSITION: Calcite/dolomite 100 Pollen Tr

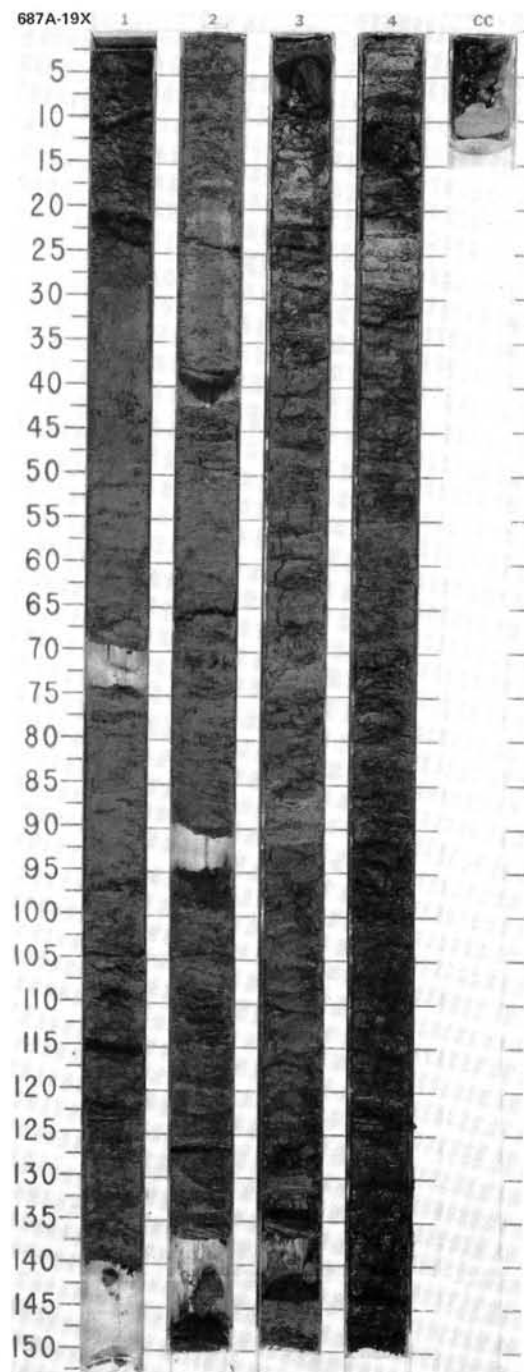


[illegible]


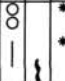
SITE 687 HOLE A CORE 18X CORED INTERVAL 466.3-475.8 mbsl; 159.5-169.0 mbsf

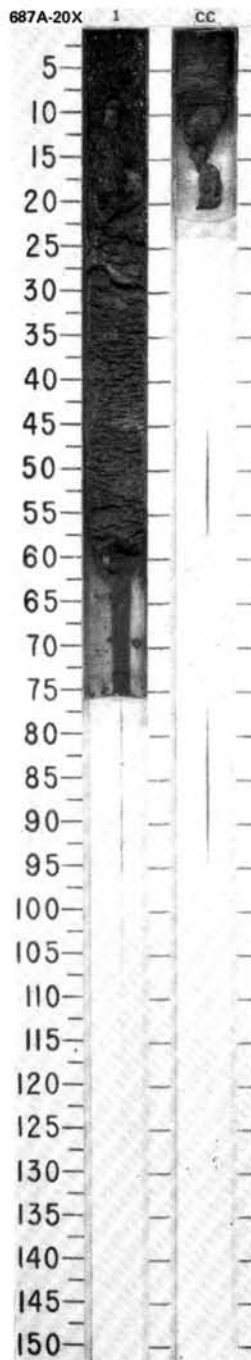
TIME-ROCK UNIT	BIOSTRAT. ZONE/ FOSSIL CHARACTER				PALEOMAGNETICS	PHYS. PROPERTIES	CHEMISTRY	SECTION	METERS	GRAPHIC LITHOLOGY	DRILLING DISTURB.	SED. STRUCTURES	SAMPLES	LITHOLOGIC DESCRIPTION																																																
	FORAMINIFERS	NANNOFOSSILS	RADIOLARIANS	DIATOMS																																																										
PLIOCENE ?	B *		non diagnostic *	undifferentiated W. fossil Zone *		Y=1.40 D=78.03		1	0.5 1.0					DIATOM-FORAMINIFER-MUD Major lithology: Section 1, 0-150 cm: diatom-foraminifer-mud, olive gray (5Y 4/2), bioturbated, with dolomite layers at 20-21 and 36-42 cm and some diatom-rich layers. Section 2, 0-66 cm: diatom-foraminifer mud, olive gray (5Y 4/20) with olive (5Y 4/3) layers (diatom-rich). CC, 0-17 cm: diatom-foraminifer mud, olive gray (5Y 4/2). SMEAR SLIDE SUMMARY (%): <table><tr><td></td><td>1. 72</td><td>2. 33</td></tr><tr><td>D</td><td></td><td>M</td></tr></table> TEXTURE: <table><tr><td>Sand</td><td>20</td><td>5</td></tr><tr><td>Silt</td><td>35</td><td>30</td></tr><tr><td>Clay</td><td>45</td><td>65</td></tr></table> COMPOSITION: <table><tr><td>Quartz</td><td>10</td><td>Tr</td></tr><tr><td>Feldspar</td><td>5</td><td>Tr</td></tr><tr><td>Rock fragments</td><td>5</td><td>1</td></tr><tr><td>Clay</td><td>35</td><td>10</td></tr><tr><td>Volcanic glass</td><td>—</td><td>2</td></tr><tr><td>Accessory minerals</td><td></td><td></td></tr><tr><td>Pyrite</td><td>5</td><td>5</td></tr><tr><td>Micrite</td><td>—</td><td>2</td></tr><tr><td>Foraminifers</td><td>15</td><td>Tr</td></tr><tr><td>Nannofossils</td><td>—</td><td>3</td></tr><tr><td>Diatoms</td><td>25</td><td>77</td></tr></table>		1. 72	2. 33	D		M	Sand	20	5	Silt	35	30	Clay	45	65	Quartz	10	Tr	Feldspar	5	Tr	Rock fragments	5	1	Clay	35	10	Volcanic glass	—	2	Accessory minerals			Pyrite	5	5	Micrite	—	2	Foraminifers	15	Tr	Nannofossils	—	3	Diatoms	25	77
	1. 72	2. 33																																																												
D		M																																																												
Sand	20	5																																																												
Silt	35	30																																																												
Clay	45	65																																																												
Quartz	10	Tr																																																												
Feldspar	5	Tr																																																												
Rock fragments	5	1																																																												
Clay	35	10																																																												
Volcanic glass	—	2																																																												
Accessory minerals																																																														
Pyrite	5	5																																																												
Micrite	—	2																																																												
Foraminifers	15	Tr																																																												
Nannofossils	—	3																																																												
Diatoms	25	77																																																												
								2																																																						



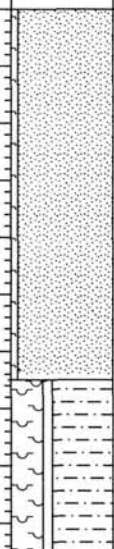
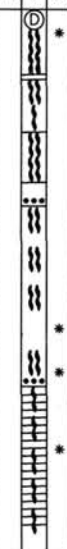
SITE 687

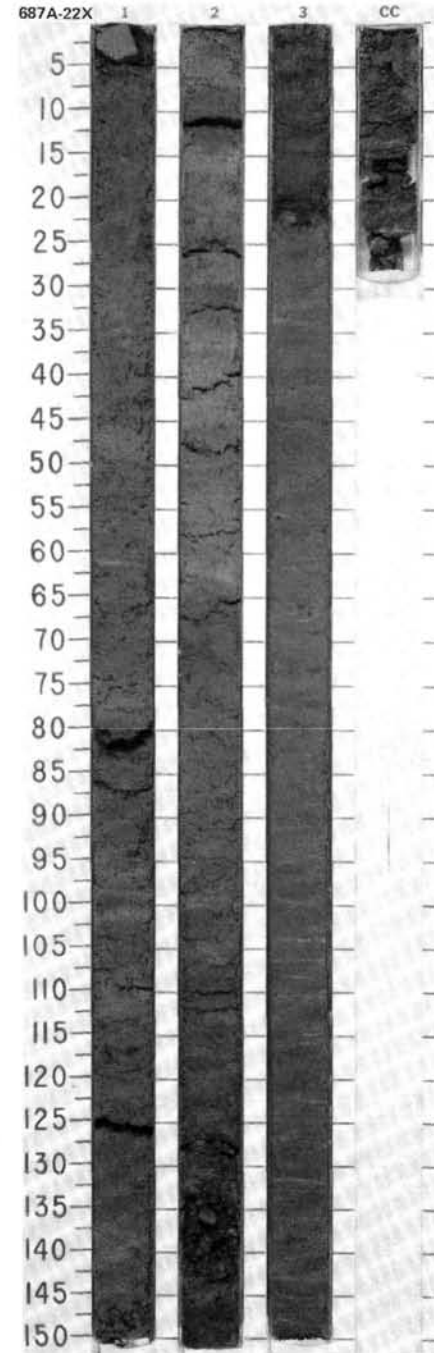
SITE 687 HOLE A CORE 20X CORED INTERVAL 485.3-494.8 mbsl; 178.5-188.0 mbsf

TIME-ROCK UNIT	BIOSTRAT. ZONE/ FOSSIL CHARACTER				PALEOMAGNETICS	PHYS. PROPERTIES	CHEMISTRY	SECTION	METERS	GRAPHIC LITHOLOGY	DRILLING DISTURB.	SED. STRUCTURES	SAMPLES	LITHOLOGIC DESCRIPTION																																																						
	FORAMINIFERS	NANNOFOSSILS	RADIOLARIANS	DIATOMS																																																																
?	B *		B *	undifferentiated *				1	0.5			*	*	<p>MUD and SILT</p> <p>Major lithology: Section 1, 0-60 cm: mud and silt, olive gray (5Y 4/20) with shell and dolomite fragments. CC, 0-12 cm: silt, dark gray (5Y 4/1) with shell fragments.</p> <p>SMEAR SLIDE SUMMARY (%):</p> <table><tr><td></td><td>1, 8</td><td>1, 34</td></tr><tr><td>D</td><td>D</td><td>D</td></tr></table> <p>TEXTURE:</p> <table><tr><td>Sand</td><td>20</td><td>85</td></tr><tr><td>Silt</td><td>45</td><td>15</td></tr><tr><td>Clay</td><td>35</td><td>—</td></tr></table> <p>COMPOSITION:</p> <table><tr><td>Quartz</td><td>15</td><td>40</td></tr><tr><td>Feldspar</td><td>5</td><td>30</td></tr><tr><td>Rock fragments</td><td>5</td><td>10</td></tr><tr><td>Mica</td><td>—</td><td>5</td></tr><tr><td>Clay</td><td>20</td><td>—</td></tr><tr><td>Calcite/dolomite</td><td>3</td><td>—</td></tr><tr><td>Accessory minerals</td><td></td><td></td></tr><tr><td>Pyrite</td><td>10</td><td>5</td></tr><tr><td>Amphibole</td><td>2</td><td>Tr</td></tr><tr><td>Phosphate peloids</td><td>—</td><td>10</td></tr><tr><td>Glauconite</td><td>—</td><td>Tr</td></tr><tr><td>Foraminifers</td><td>10</td><td>—</td></tr><tr><td>Diatoms</td><td>30</td><td>—</td></tr></table>		1, 8	1, 34	D	D	D	Sand	20	85	Silt	45	15	Clay	35	—	Quartz	15	40	Feldspar	5	30	Rock fragments	5	10	Mica	—	5	Clay	20	—	Calcite/dolomite	3	—	Accessory minerals			Pyrite	10	5	Amphibole	2	Tr	Phosphate peloids	—	10	Glauconite	—	Tr	Foraminifers	10	—	Diatoms	30	—
	1, 8	1, 34																																																																		
D	D	D																																																																		
Sand	20	85																																																																		
Silt	45	15																																																																		
Clay	35	—																																																																		
Quartz	15	40																																																																		
Feldspar	5	30																																																																		
Rock fragments	5	10																																																																		
Mica	—	5																																																																		
Clay	20	—																																																																		
Calcite/dolomite	3	—																																																																		
Accessory minerals																																																																				
Pyrite	10	5																																																																		
Amphibole	2	Tr																																																																		
Phosphate peloids	—	10																																																																		
Glauconite	—	Tr																																																																		
Foraminifers	10	—																																																																		
Diatoms	30	—																																																																		



SITE 687 HOLE A CORE 22X CORED INTERVAL 504.3-513.8 mbsf; 197.5-207.0 mbsf

TIME-ROCK UNIT	BIOSTRAT. ZONE/ FOSSIL CHARACTER	PALEOMAGNETICS	PHYS. PROPERTIES	CHEMISTRY	SECTION	METERS	GRAPHIC LITHOLOGY	DRILLING DISTURB. SED. STRUCTURES	SAMPLES	LITHOLOGIC DESCRIPTION																																																																																										
PLIOCENE ?	*B * insignificant *B * undifferentiated [<i>Cosmiodiscus insignis</i>]		γ ₁ 2.04 γ ₂ 1.54 ● 0.49, 0.87 ● 0.75, 7.5		1 2 3 CC	0.5 1.0			* * * *	QUARTZO-FELDSPATHIC-LITHIC SAND, and SANDY DIATOMACEOUS MUD Major lithology: Section 1, 0–150 cm: quartz-feldspathic-lithic sand, dark gray, bioturbated. Dolomite piece at Section 1, 0–3 cm. Section 2, 0–150 cm: quartz-feldspar-lithic sand, gray (5Y 5/1), bioturbated. Olive gray (5Y 5/20 sandy dolomite. Gray (5Y 5/1) cemented dolomitic sandstone. Section 3, 0–150 cm: quartz-feldspathic-lithic sand, dark gray (5Y 4/1), bioturbated, with lighter colored laminae. Graded bed with phosphatic grains at 22 cm. CC, 0–28 cm: sandy diatomaceous mud, olive gray (5Y 4/2), laminated, bioturbated. SMEAR SLIDE SUMMARY (%): <table><tr><td></td><td>1, 23</td><td>2, 130</td><td>3, 19</td><td>3, 84</td></tr><tr><td>D</td><td></td><td>M</td><td>D</td><td>D</td></tr></table> TEXTURE: <table><tr><td>Sand</td><td>90</td><td>20</td><td>80</td><td>25</td></tr><tr><td>Silt</td><td>10</td><td>5</td><td>20</td><td>35</td></tr><tr><td>Clay</td><td>—</td><td>75</td><td>—</td><td>40</td></tr></table> COMPOSITION: <table><tr><td>Quartz</td><td>25</td><td>10</td><td>25</td><td>15</td></tr><tr><td>Feldspar</td><td>25</td><td>5</td><td>25</td><td>10</td></tr><tr><td>Rock fragments</td><td>20</td><td>Tr</td><td>15</td><td>5</td></tr><tr><td>Clay</td><td>—</td><td>Tr</td><td>—</td><td>30</td></tr><tr><td>Calcite/dolomite</td><td>—</td><td>75</td><td>—</td><td>—</td></tr><tr><td>Accessory minerals</td><td></td><td></td><td></td><td></td></tr><tr><td>Pyrite</td><td>10</td><td>—</td><td>5</td><td>5</td></tr><tr><td>Amphibole</td><td>8</td><td>—</td><td>5</td><td>—</td></tr><tr><td>Phosphate peloids</td><td>5</td><td>10</td><td>20</td><td>—</td></tr><tr><td>Foraminifers</td><td>—</td><td>—</td><td>—</td><td>5</td></tr><tr><td>Diatoms</td><td>5</td><td>Tr</td><td>—</td><td>30</td></tr><tr><td>Sponge spicules</td><td>2</td><td>—</td><td>—</td><td>Tr</td></tr><tr><td>Fish remains</td><td>—</td><td>—</td><td>5</td><td>—</td></tr></table>		1, 23	2, 130	3, 19	3, 84	D		M	D	D	Sand	90	20	80	25	Silt	10	5	20	35	Clay	—	75	—	40	Quartz	25	10	25	15	Feldspar	25	5	25	10	Rock fragments	20	Tr	15	5	Clay	—	Tr	—	30	Calcite/dolomite	—	75	—	—	Accessory minerals					Pyrite	10	—	5	5	Amphibole	8	—	5	—	Phosphate peloids	5	10	20	—	Foraminifers	—	—	—	5	Diatoms	5	Tr	—	30	Sponge spicules	2	—	—	Tr	Fish remains	—	—	5	—
	1, 23	2, 130	3, 19	3, 84																																																																																																
D		M	D	D																																																																																																
Sand	90	20	80	25																																																																																																
Silt	10	5	20	35																																																																																																
Clay	—	75	—	40																																																																																																
Quartz	25	10	25	15																																																																																																
Feldspar	25	5	25	10																																																																																																
Rock fragments	20	Tr	15	5																																																																																																
Clay	—	Tr	—	30																																																																																																
Calcite/dolomite	—	75	—	—																																																																																																
Accessory minerals																																																																																																				
Pyrite	10	—	5	5																																																																																																
Amphibole	8	—	5	—																																																																																																
Phosphate peloids	5	10	20	—																																																																																																
Foraminifers	—	—	—	5																																																																																																
Diatoms	5	Tr	—	30																																																																																																
Sponge spicules	2	—	—	Tr																																																																																																
Fish remains	—	—	5	—																																																																																																

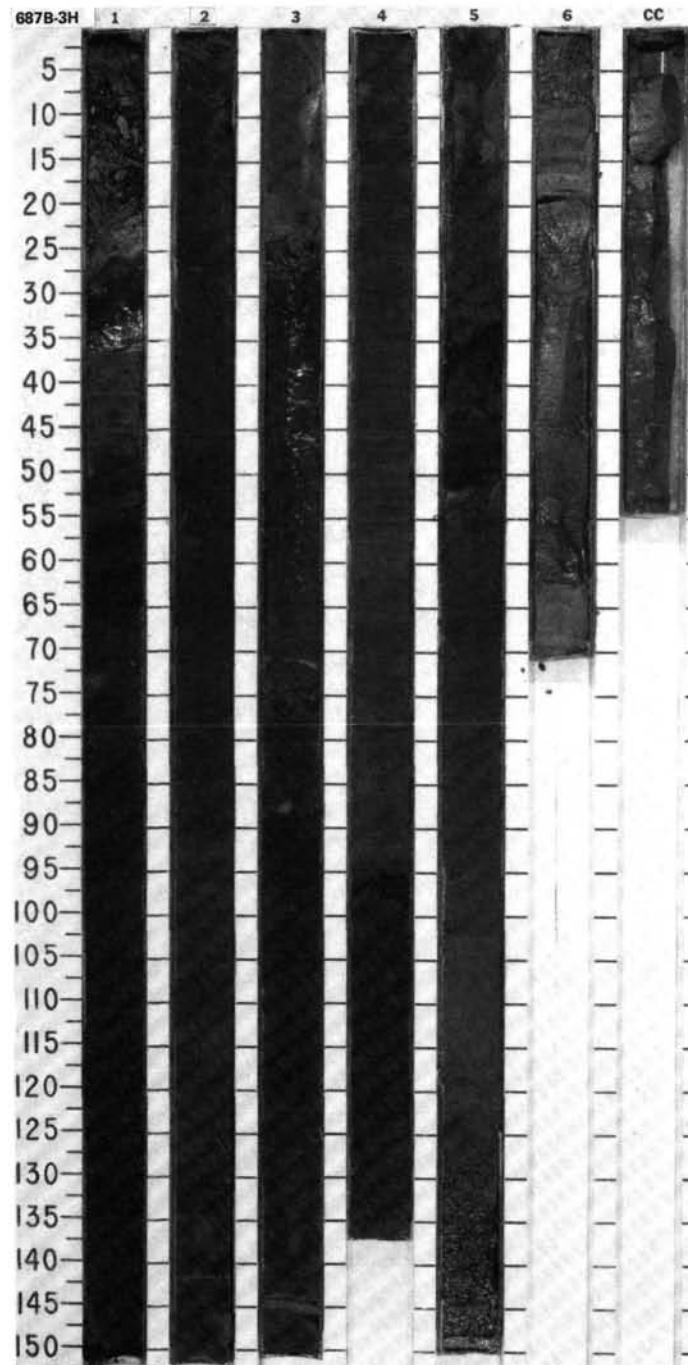


CORE 112-687B-2H NO RECOVERY



SITE 687 HOLE B CORE 3H CORED INTERVAL 321.5-331.0 mbsl; 14.7-24.2 mbsf

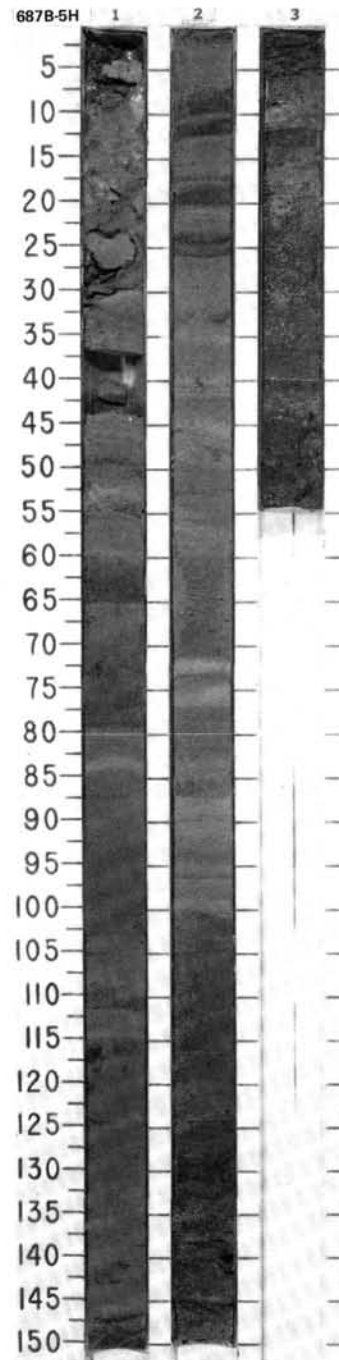
TIME-ROCK UNIT	BIOSTRAT. ZONE/ FOSSIL CHARACTER				PALEOMAGNETICS	PHYS. PROPERTIES	CHEMISTRY	SECTION	METERS	GRAPHIC LITHOLOGY	DRILLING DISTURB.	SED. STRUCTURES	SAMPLES	LITHOLOGIC DESCRIPTION
	FORAMINIFERS	NANNOFOSSILS	RADIOLARIANS	DIATOMS										
QUATERNARY	*B								0.5 1.0	1				CONGLOMERATE, SAND, MUD, DIATOMACEOUS SAND AND MUD, and SILT Major lithology: Section 1, 0-21 cm: conglomerate with sandstone cemented by dolomite pebbles and phosphate nodules in a muddy matrix, dark olive gray (5Y 3/2); 21-35 cm: sand, gray (N 6/1); 35-54 cm: mud, dark olive gray (5Y 3/2) with fish debris; 54-78 cm: mud, black (5Y 2.5/1) to dark olive gray (5Y 3/2); 78-79 cm: sandy bed, olive (5Y 4/4), coarse grained; 79-85 cm: very finely laminated mud; 85-110 cm: diatomaceous mud, black (5Y 2.5/1), mottled, slumps; and 110-150 cm: diatomaceous mud, gray (5Y 5/1) to black (5Y 2.5/2); laminated, below 118 cm slumps. Section 2, 0-10 cm: phosphate nodules, black and olive (5Y 4/4) sandstone pebble in a muddy matrix; and 10-150 cm: mud, black (5Y 2.5/2), mainly massive, slumps at 29-32 and 84-100 cm, dewatering veins associated with minor normal faulting. Section 3, 0-24 and 70-150 cm: diatomaceous mud and sand, black (5Y 2.5/1) and dark olive gray (5Y 4/1), laminated (especially 129-143 cm), sandstone cemented by dolomite and phosphate pebbles at 20-25 cm, phosphate pebbles between 70 and 92 cm, gray (N 6/1) sand at 143-146 cm are associated with normal faults; and 24-70 cm: graded sand, dark gray (N 4/1). Section 4, 0-95 cm: diatomaceous silty mud, olive gray (5Y 4/2) and dark olive gray (5Y 3/2), laminated with olive laminations rich in diatoms, small fold nose at 40-43 cm, yellow brown (7.5YR 4/4) phosphatic debris at 78-79 cm; 95-100 cm: phosphorite nodules, black (5Y 2.5/1) in dark olive gray (5Y 3/2) phosphatic sand matrix, bioturbated erosional contact below; and 100-137 cm: diatomaceous mud, dark olive gray (5Y 3/2), faint laminated, bioturbated. Section 5, 0-32 and 51-102 cm: silty mud, dark olive gray (5Y 3/2), homogeneous to bioturbated; 32-42 cm: phosphorite nodules, black (5Y 2.5/1), moldic porosity; 42-51 cm: phosphatic sand and small nodules, dark olive gray (5Y 3/2) to black (5Y 2.5/1) at base, bioturbated, erosional contact with underlying mud; 102-124 cm: silty mud, olive gray (5Y 4/2), mottled, bioturbated; and 124-150 cm: interlaminated silty mud, olive gray (5Y 4/2), and fine sand, dark olive gray (5Y 3/1). Section 6, 0-9 cm: interlaminated silty mud, olive gray (5Y 4/2), and fine sand, dark olive gray (5Y 3/1) (same as Section 5, 124-150 cm); 9-19 cm: silty mud, gray (5Y 5/1) and olive gray (5Y 5/2), interbedded with sand at 15-16 cm; and 19-70 cm: laminated calcareous silty mud (olive gray to gray) and fine sand (dark gray) interbedded with dark gray fine sand (48-62 cm), olive gray silt (62-63 cm), and finely laminated silty mud and sand. CC, 5-54 cm: silt, dark gray (5Y 4/1).
QUATERNARY	*P. dolioolus Zone								0.5 1.0	2				
QUATERNARY	*B								0.5 1.0	3				
QUATERNARY	*B								0.5 1.0	4				
QUATERNARY	*B								0.5 1.0	5				
QUATERNARY	*B								0.5 1.0	6				
QUATERNARY	*B								0.5 1.0	CC				



SITE 687 HOLE B CORE 4H CORED INTERVAL 331.0-340.5 mbsl; 24.2-33.7 mbsf

TIME-ROCK UNIT	BIOSTRAT. ZONE/ FOSSIL CHARACTER				PALEOMAGNETICS	PHYS. PROPERTIES	CHEMISTRY	SECTION	METERS	GRAPHIC LITHOLOGY	DRILLING DISTURB.	SED. STRUCTURES	SAMPLES	LITHOLOGIC DESCRIPTION
	FORAMINIFERS	NANNOFOSSILS	RADIOLARIANS	DIATOMS										
QUATERNARY														

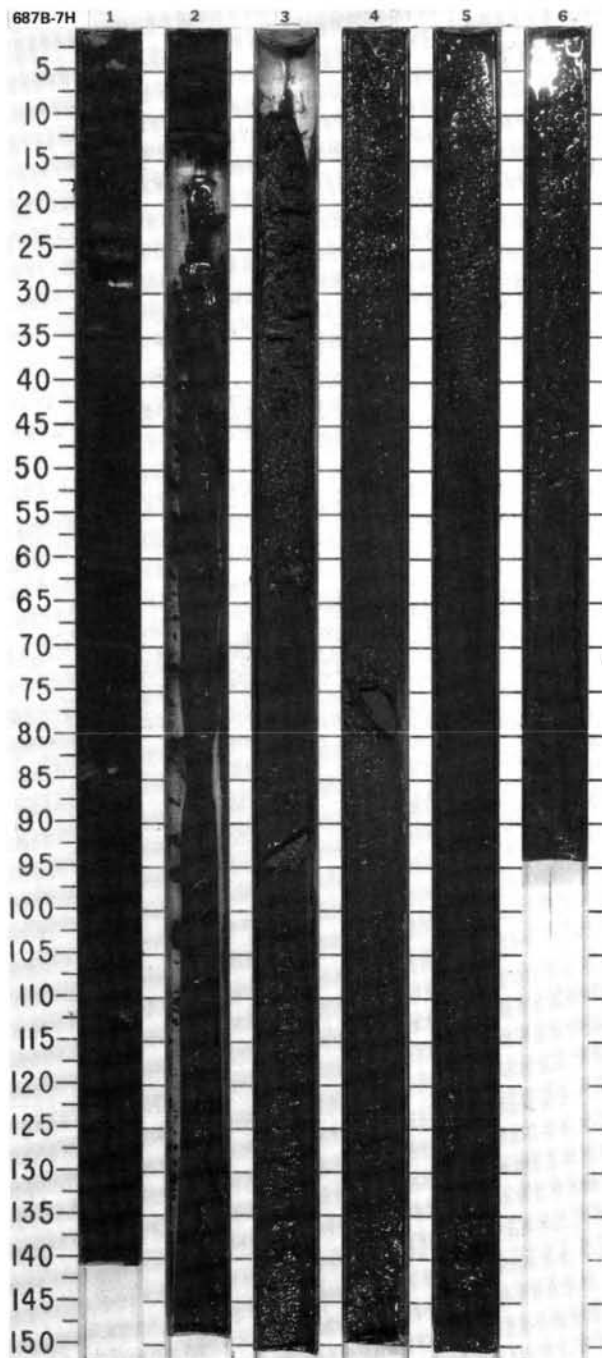
SITE	687	HOLE	B	CORE	5H	CORED INTERVAL	340.5-350.0 mbsl; 33.7-43.2 mbsf
------	-----	------	---	------	----	----------------	----------------------------------

[illegible]

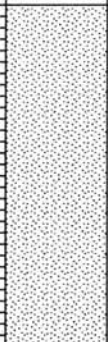
[illegible]

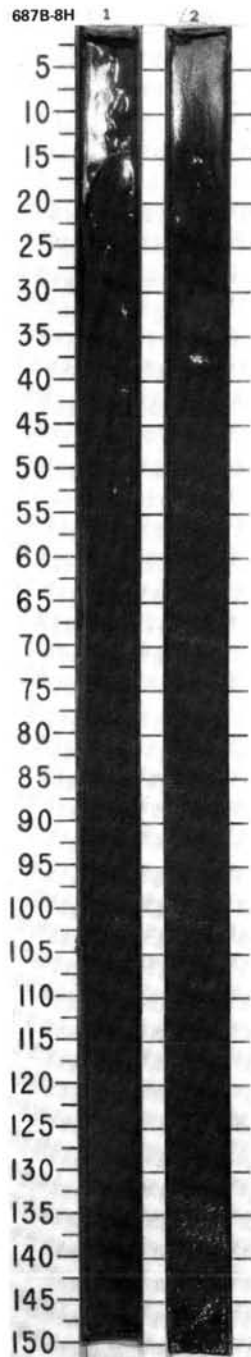
SITE 687 HOLE B CORE 7H CORED INTERVAL 359.5-369.0 mbsl; 52.7-62.2 mbsf

TIME-ROCK UNIT	BIOSTRAT. ZONE/ FOSSIL CHARACTER				PALEOMAGNETICS	PHYS. PROPERTIES	CHEMISTRY	SECTION	METERS	GRAPHIC LITHOLOGY	DRILLING DISTURB.	SED. STRUCTURES	SAMPLES	LITHOLOGIC DESCRIPTION
	FORAMINIFERS	NANNOFOSSILS	RADIOLARIANS	DIATOMS										
QUATERNARY	*B			* <i>P. dolioolus</i> Zone *		1.31 0.82-74 0.71 0.61-10		1	0.5 1.0					FORAMINIFER-BEARING DIATOMACEOUS MUD, DIATOMACEOUS MUD, SAND, and SILT Major lithology: Section 1, 0-140 cm: foraminifer-bearing diatomaceous mud, olive (5Y 5/4) to dark olive gray (5Y 3/2), laminations, and phosphates at 75, 86, 105, 113, and 121 cm; Section 2, 0-12 cm: diatomaceous mud, dark olive gray (5Y 3/20); Section 2, 12-150 cm: sand, dark gray (N 4/); Section 3, 0-150 cm: sand and silt, dark gray (N 4/), with dolomitic sandstone at 58-62 and 90-94 cm; Section 4, 0-150 cm: sand, dark gray (N 4/), with dolomitic sandstone at 74-79 cm; and Section 5, 0-150, and Section 6, 0-88 cm: sand, dark gray (N 4/).
								2				IW		SMEAR SLIDE SUMMARY (%): 1, 25 1, 93 3, 40 M D D TEXTURE: Sand — — 60 Silt 99 25 30 Clay 1 75 10 COMPOSITION: Quartz 3 2 30 Feldspar — 2 25 Rock fragments — 1 10 Mica — 2 1 Clay — 63 3 Volcanic glass — — 2 Calcite/dolomite 66 10 5 Accessory minerals Pyrite 1 2 10 Collophane — 3 2 Hornblende — — 5 Micrite — 5 — Foraminifers — 3 2 Diatoms 30 7 5 Radiolarians — — Tr Sponge spicules — — Tr Silicoflagellates — Tr —
								3				*		
								4				***		
								5				***		
								6				***		



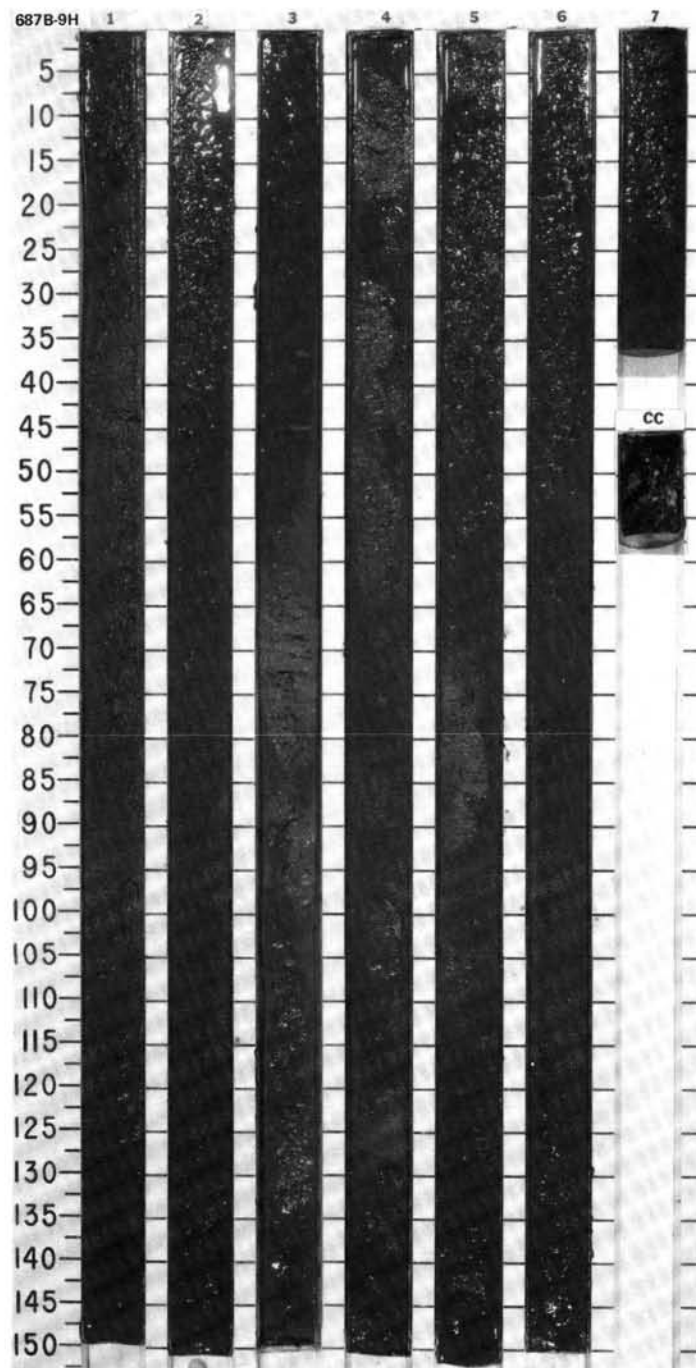
SITE 687 HOLE B CORE 8H CORED INTERVAL 369.0-378.5 mbsl; 62.2-71.7 mbsf

TIME-ROCK UNIT	BIOSTRAT. ZONE/ FOSSIL CHARACTER				SECTION	METERS	GRAPHIC LITHOLOGY	DRILLING DISTURB.	SED. STRUCTURES	SAMPLES	LITHOLOGIC DESCRIPTION
	FORAMINIFERS	NANNOFOSSILS	RADIOLARIANS	DIATOMS							
PALEOMAGNETICS				PHYS. PROPERTIES				CHEMISTRY			
?	* non diagnostic			* non diagnostic		1					SAND Major lithology: Section 1, 0-150 cm, and Section 2, 0-150 cm: sand, dark gray (N 4/). SMEAR SLIDE SUMMARY (%): <div>2. 135 D</div> TEXTURE: <div>Sand 70 Silt 30</div> COMPOSITION: <div>Quartz 25 Feldspar 35 Mica 2 Calcite/dolomite 15 Accessory minerals 3 Hornblende 5 Glaucinite 1 Opauques 10 Diatoms 3 Sponge spicules 1</div>
						2					



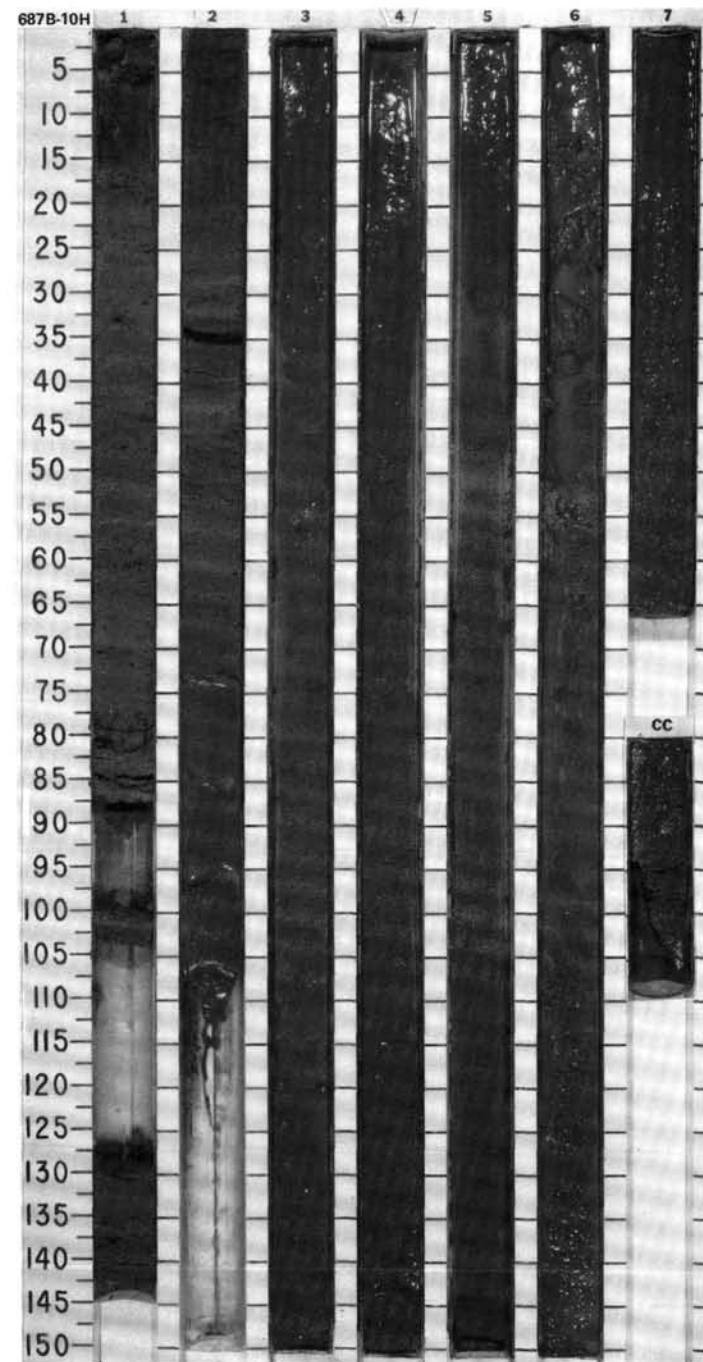
SITE 687 HOLE B CORE 9H CORED INTERVAL 378.5-388.5 mbsl; 71.7-81.2 mbsf

TIME-ROCK UNIT	BIOSTRAT. ZONE/ FOSSIL CHARACTER				PALEOMAGNETICS	PHYS. PROPERTIES	CHEMISTRY	SECTION	METERS	GRAPHIC LITHOLOGY	DRILLING DISTURB.	SED. STRUCTURES	SAMPLES	LITHOLOGIC DESCRIPTION																																																			
	FORAMINIFERS	NANNOFOSSILS	RADOLARIANS	DIAZONIS																																																													
QUATERNARY	*non diagnostic								0.5					<p>SAND, SILT, FINE-GRAINED SAND, and SILTY CALCAREOUS MUD</p> <p>Major lithology: Section 1, 0–150, and Section 2, 0–150 cm: sand, gray (N 5); Section 3, 0–150 cm: sand and silt, gray (N 5) to greenish gray (SY 5/1); Section 4, 0–150 cm: sand, gray (N 4), and gray (SY 5/1) silty mud, with shell debris at 30–38 cm; Section 5, 0–150 cm: fine-grained sand, dark gray (N 4), with gray (SY 5/1) calcareous mud at 20–30 and 73–92 cm; Section 6, 0–150 cm: fine-grained sand, dark gray (N 4); Section 7, 0–7 cm: silty calcareous mud, gray (SY 5/1); and Section 7, 7–36 cm, and CC, 0–11 cm: fine-grained sand, dark gray (N 4).</p> <p>SMEAR SLIDE SUMMARY (%):</p> <table><tr><td></td><td>1, 4</td><td>2, 135</td></tr><tr><td></td><td>M</td><td>D</td></tr></table> <p>TEXTURE:</p> <table><tr><td>Sand</td><td>85</td><td>70</td></tr><tr><td>Silt</td><td>15</td><td>30</td></tr></table> <p>COMPOSITION:</p> <table><tr><td>Quartz</td><td>20</td><td>25</td></tr><tr><td>Feldspar</td><td>30</td><td>35</td></tr><tr><td>Rock fragments</td><td>8</td><td>—</td></tr><tr><td>Mica</td><td>10</td><td>2</td></tr><tr><td>Calcite/dolomite</td><td>7</td><td>15</td></tr><tr><td>Accessory minerals</td><td>5</td><td>3</td></tr><tr><td>Opales</td><td>10</td><td>10</td></tr><tr><td>Glauconite</td><td>2</td><td>1</td></tr><tr><td>Hornblende</td><td>3</td><td>5</td></tr><tr><td>Foraminifers</td><td>Tr</td><td>—</td></tr><tr><td>Nannofossils</td><td>Tr</td><td>—</td></tr><tr><td>Diatoms</td><td>5</td><td>3</td></tr><tr><td>Sponge spicules</td><td>Tr</td><td>1</td></tr></table>		1, 4	2, 135		M	D	Sand	85	70	Silt	15	30	Quartz	20	25	Feldspar	30	35	Rock fragments	8	—	Mica	10	2	Calcite/dolomite	7	15	Accessory minerals	5	3	Opales	10	10	Glauconite	2	1	Hornblende	3	5	Foraminifers	Tr	—	Nannofossils	Tr	—	Diatoms	5	3	Sponge spicules	Tr	1
		1, 4	2, 135																																																														
		M	D																																																														
	Sand	85	70																																																														
	Silt	15	30																																																														
	Quartz	20	25																																																														
	Feldspar	30	35																																																														
Rock fragments	8	—																																																															
Mica	10	2																																																															
Calcite/dolomite	7	15																																																															
Accessory minerals	5	3																																																															
Opales	10	10																																																															
Glauconite	2	1																																																															
Hornblende	3	5																																																															
Foraminifers	Tr	—																																																															
Nannofossils	Tr	—																																																															
Diatoms	5	3																																																															
Sponge spicules	Tr	1																																																															
	*NN19a							1	1.0																																																								
	*non diagnostic							2																																																									
								3					*																																																				
								4			X	X																																																					
											X	X																																																					
								5			X	X																																																					
								6																																																									
								7																																																									

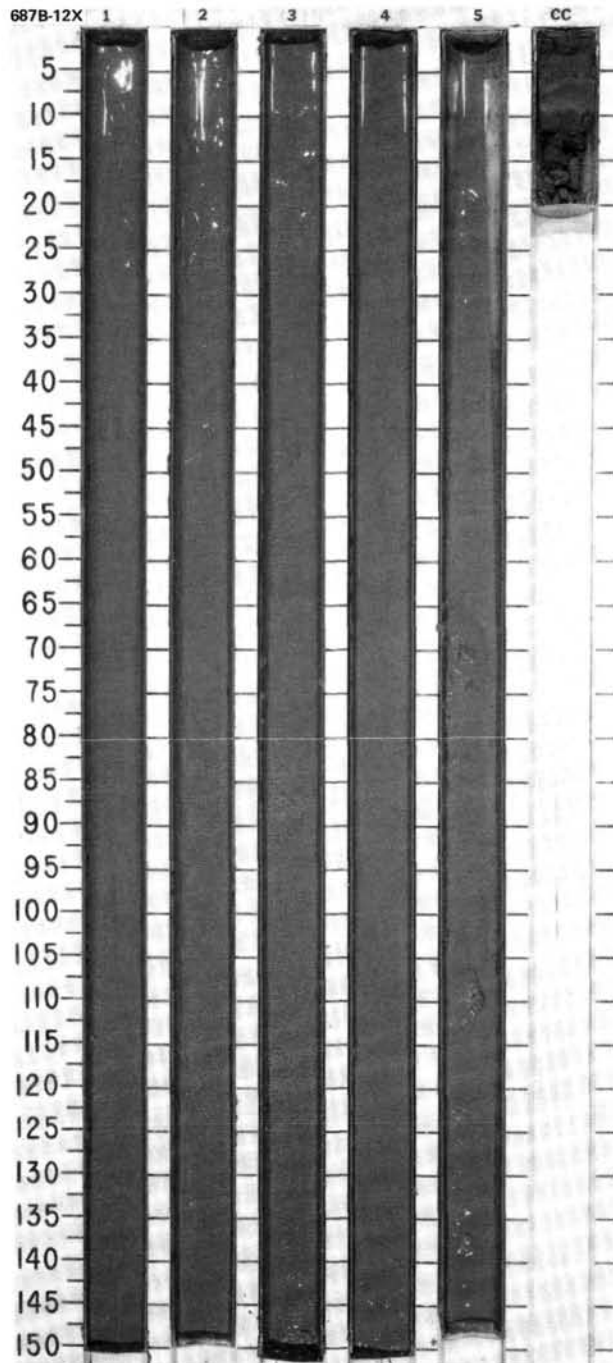


TIME-ROCK UNIT	BIOSTRAT. ZONE/ FOSSIL CHARACTER				SECTION	METERS	GRAPHIC LITHOLOGY	DRILLING DISTURB. SED. STRUCTURES	SAMPLES	LITHOLOGIC DESCRIPTION																																																																				
	FORAMINIFERS	NANNOFOSSILS	RADIOLARIANS	DIATOMS																																																																										
?	*non diagnostic									SILTY MUD, SILTY DIATOMACEOUS MUD, FINE QUARTZ-FELDSPAR SAND, and FINE SAND Major lithology: Section 1, 0-150 cm: silty mud, coarse bands of gray (5Y 5/1) and dark gray (N 4/1) silt or silty sand, bioturbated, mottled contacts, graded bed at 56 cm, with dolomitic sandstone, gray (5Y 5/1), at 0-2 cm; Section 2, 0-73 cm: silty diatomaceous mud, interbedded gray (5Y 5/1) and dark gray (5Y 4/1) silt or silty sand, mottled and bioturbated, with fine fragments of white shell debris in silty matrix; Section 2, 73-110 cm: fine quartz-feldspar sand, dark gray (5Y 4/1); Sections 3 through 5: fine sand, dark gray (5Y 4/1); Section 6, 0-150 cm: fine sand, dark gray (5Y 4/1), with gray (5Y 5/1) muddy interval at 50-65 cm; and Section 7, 0-66 cm, and CC, 0-19 cm: sand, fine-grained, dark gray (5Y 4/1). SMEAR SLIDE SUMMARY (%): <table><tr><td></td><td>2, 28</td><td>2, 62</td><td>2, 84</td></tr><tr><td>D</td><td></td><td>D</td><td>D</td></tr></table> TEXTURE: <table><tr><td>Sand</td><td>—</td><td>20</td><td>70</td></tr><tr><td>Silt</td><td>45</td><td>55</td><td>30</td></tr><tr><td>Clay</td><td>55</td><td>25</td><td>—</td></tr></table> COMPOSITION: <table><tr><td>Quartz</td><td>2</td><td>33</td><td>50</td></tr><tr><td>Feldspar</td><td>1</td><td>9</td><td>15</td></tr><tr><td>Rock fragments</td><td>1</td><td>5</td><td>14</td></tr><tr><td>Mica</td><td>1</td><td>7</td><td>10</td></tr><tr><td>Clay</td><td>50</td><td>20</td><td>—</td></tr><tr><td>Volcanic glass</td><td>—</td><td>2</td><td>1</td></tr><tr><td>Accessory minerals</td><td></td><td></td><td></td></tr><tr><td>Pyrite</td><td>5</td><td>4</td><td>2</td></tr><tr><td>Glaucanite</td><td>—</td><td>2</td><td>—</td></tr><tr><td>Hornblende</td><td>—</td><td>3</td><td>3</td></tr><tr><td>Micrite</td><td>10</td><td>10</td><td>5</td></tr><tr><td>Diatoms</td><td>30</td><td>5</td><td>Tr</td></tr></table>		2, 28	2, 62	2, 84	D		D	D	Sand	—	20	70	Silt	45	55	30	Clay	55	25	—	Quartz	2	33	50	Feldspar	1	9	15	Rock fragments	1	5	14	Mica	1	7	10	Clay	50	20	—	Volcanic glass	—	2	1	Accessory minerals				Pyrite	5	4	2	Glaucanite	—	2	—	Hornblende	—	3	3	Micrite	10	10	5	Diatoms	30	5	Tr
			2, 28	2, 62	2, 84																																																																									
		D		D	D																																																																									
		Sand	—	20	70																																																																									
		Silt	45	55	30																																																																									
		Clay	55	25	—																																																																									
		Quartz	2	33	50																																																																									
		Feldspar	1	9	15																																																																									
		Rock fragments	1	5	14																																																																									
		Mica	1	7	10																																																																									
Clay	50	20	—																																																																											
Volcanic glass	—	2	1																																																																											
Accessory minerals																																																																														
Pyrite	5	4	2																																																																											
Glaucanite	—	2	—																																																																											
Hornblende	—	3	3																																																																											
Micrite	10	10	5																																																																											
Diatoms	30	5	Tr																																																																											
					0.5																																																																									
					1.0	VOID																																																																								
						VOID																																																																								
					2																																																																									
						VOID																																																																								
					3																																																																									
					4																																																																									
					5																																																																									
					6																																																																									
					7																																																																									
					CC																																																																									

CORE 112-687B-11H NO RECOVERY

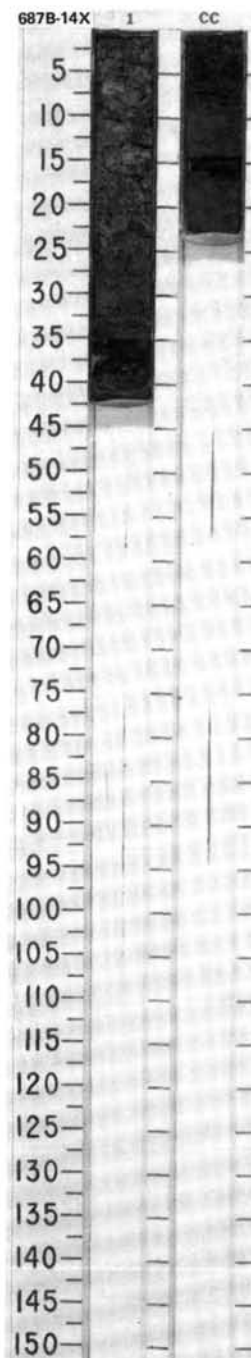
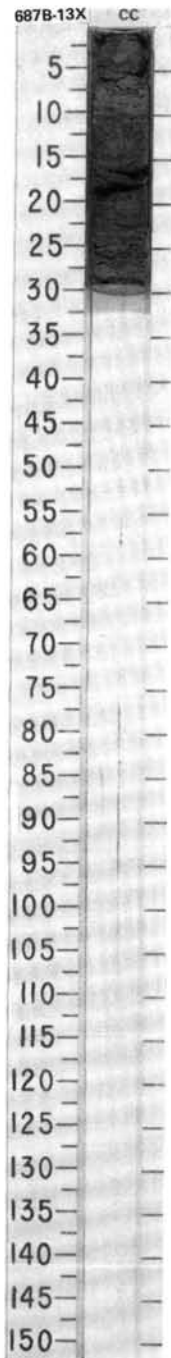


SITE 687 HOLE B CORE 12X CORED INTERVAL 397.6-407.1 mbsl; 90.8-100.3 mbsf

[illegible]

SITE 687 HOLE B CORE 13X CORED INTERVAL 407.1-416.6 mbsl; 100.3-109.8 mbsf

TIME-ROCK UNIT	BIOSTRAT. ZONE/ FOSSIL CHARACTER				PALEOMAGNETICS	PHYS. PROPERTIES	CHEMISTRY	SECTION	METERS	GRAPHIC LITHOLOGY	DRILLING DISTURB.	SED. STRUCTURES	SAMPLES	LITHOLOGIC DESCRIPTION
	FORAMINIFERS	NANNOFOSSILS	RADIOLARIANS	DIATOMS										
?	B*			non diagnostic*				CC					*	<p>SAND</p> <p>Major lithology: sand, dark gray (N 4), foraminifer-bearing, in CC, 0-29 cm.</p> <p>SMEAR SLIDE SUMMARY (%):</p> <p style="text-align: right;">CC, 20 D</p> <p>TEXTURE:</p> <p>Sand 25 Silt 73 Clay 2</p> <p>COMPOSITION:</p> <p>Quartz 30 Feldspar 10 Rock fragments 5 Mica 5 Clay 7 Calcite/dolomite 8 Accessory minerals 2 Hornblende 3 Opalines 20 Foraminifers 5 Diatoms 5 Sponge spicules Tr</p>

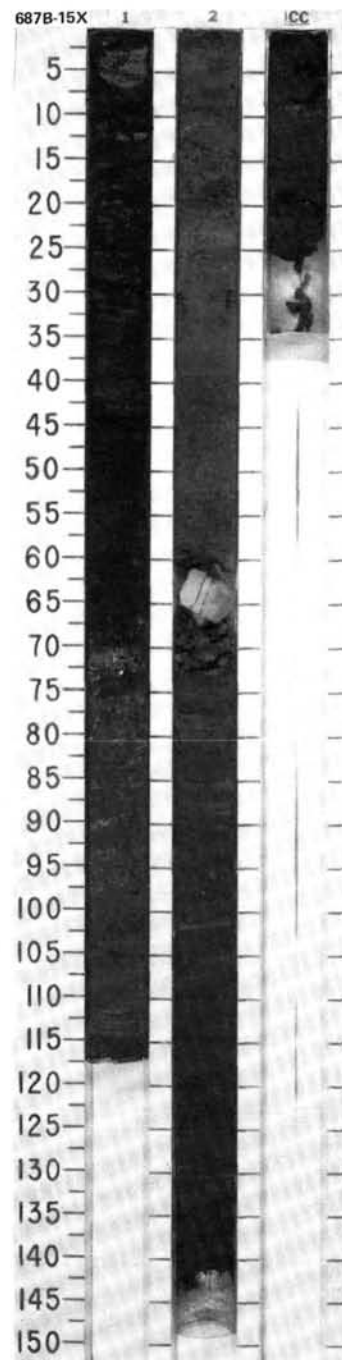


SITE 687 HOLE B CORE 14X CORED INTERVAL 416.6-426.1 mbsl; 109.8-119.3 mbsf

TIME-ROCK UNIT	BIOSTRAT. ZONE/ FOSSIL CHARACTER				PALEOMAGNETICS	PHYS. PROPERTIES	CHEMISTRY	SECTION	METERS	GRAPHIC LITHOLOGY	DRILLING DISTURB.	SED. STRUCTURES	SAMPLES	LITHOLOGIC DESCRIPTION
	FORAMINIFERS	NANNOFOSSILS	RADIOLARIANS	DIATOMS										
PLIOCENE ?	non diagnostic*			<i>N. fossilis</i> Zone*				1	0.5				*	<p>DIATOMACEOUS MUD</p> <p>Major lithology: Section 1, 0-42 cm: diatomaceous mud, olive (5Y 4/4), mottled. Fragments of shell from 1-25 cm. CC, 0-23 cm: diatomaceous mud, olive (5Y 4/4), mainly massive.</p> <p>SMEAR SLIDE SUMMARY (%):</p> <p style="text-align: right;">1, 31 D</p> <p>TEXTURE:</p> <p>Silt 65 Clay 35</p> <p>COMPOSITION:</p> <p>Quartz 10 Feldspar 5 Rock fragments 2 Mica 1 Clay 33 Calcite/dolomite 5 Accessory minerals 1 Pyrite 3 Foraminifers 2 Nannofossils Tr Diatoms 38 Sponge spicules Tr Silicoflagellates Tr</p>

SITE 687 HOLE B CORE 15X CORED INTERVAL 426.1-435.6 mbsl; 119.3-128.8 mbsf

TIME-ROCK UNIT	BIOSTRAT. ZONE/ FOSSIL CHARACTER				PALEOMAGNETICS	PHYS. PROPERTIES	CHEMISTRY	SECTION	METERS	GRAPHIC LITHOLOGY	DRILLING DISTURB.	SED. STRUCTURES	SAMPLES	LITHOLOGIC DESCRIPTION
	FORAMINIFERS	NANNOFOSSILS	RADIOLARIANS	DIATOMS										
PLIOCENE ? * Quaternary ? * <i>N. fossilis</i> Zone														DIATOMACEOUS MUD and CALCAREOUS MUD Major lithology: Section 1, 0-69 cm: diatomaceous mud, dark olive gray (5Y 3/2), homogenous; and 69-117 cm: calcareous mud, dark gray (5Y 4/1), with white shell fragments, concentrated near upper contact (erosional contact). Section 2, 0-142 cm: diatomaceous mud, gray (5Y 4/1) to olive gray (5Y 5/2), homogenous and with crude laminations (below 68 cm), with dark gray (N 4/) fine sand and silt (2-9 cm). Shell fragments at 29 cm (bioturbated basal contact). Gray (5Y 5/1) calcitic dolomite with shell fragments at base at 63-68 cm. CC, 0-25 cm: diatomaceous mud, olive gray (5Y 4/2), with thin foraminifer concentrations near 3 and 6 cm. Shell debris near 19 cm. SMEAR SLIDE SUMMARY (%): TEXTURE: Sand — 10 10 Silt 65 65 60 Clay 35 25 30 COMPOSITION: Quartz 15 20 10 Feldspar 10 15 15 Rock fragments 5 5 8 Mica 3 3 1 Clay 31 25 21 Calcite/dolomite 3 5 5 Accessory minerals 1 — — Glauconite 2 1 1 Hornblende 2 2 1 Pyrite 3 4 2 Micrite — 2 — Collophane 5 — 1 Pyroxene — Tr — Foraminifers — 3 5 Nannofossils — 1 — Diatoms 20 15 30 Sponge spicules — Tr Tr Silicoflagellates Tr Tr —



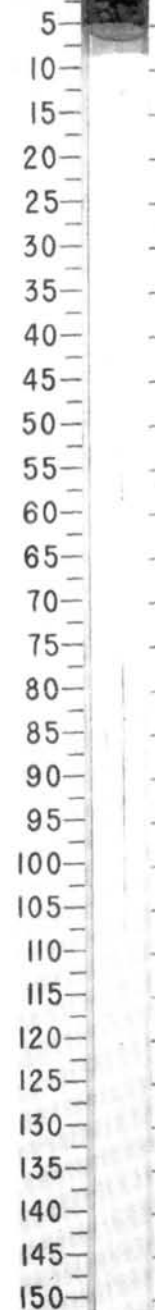
SITE 687 HOLE B CORE 18X CORED INTERVAL 454.6-464.1 mbsl; 147.8-157.3 mbsf

TIME-ROCK UNIT	BIOSTRAT. ZONE/ FOSSIL CHARACTER			PALEOMAGNETICS	PHYS. PROPERTIES	CHEMISTRY	SECTION	METERS	GRAPHIC LITHOLOGY	DRILLING DISTURB.	SED. STRUCTURES	SAMPLES	LITHOLOGIC DESCRIPTION
	FORAMINIFERS	NANNOFOSSILS	RADIOLARIANS										
?													DOLOMITIC SANDSTONE Major lithology: dolomitic sandstone, ten little pieces, gray to dark gray (N 4/-N 5/), in CC, 0-5 cm. SMEAR SLIDE SUMMARY (%): CC. 2 M TEXTURE: Sand 60 Silt 40 COMPOSITION: Quartz 35 Feldspar 12 Rock fragments 9 Mica 4 Calcite/dolomite 5 Cement 30 Accessory minerals 3 Opalines 2 Pyroxene Tr Glauconite Tr Diatoms Tr

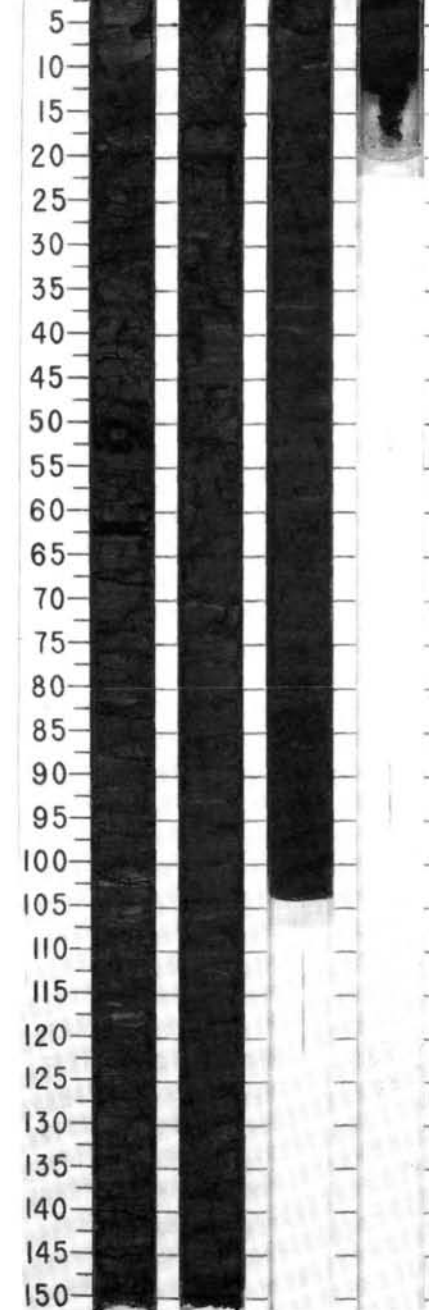
SITE 687 HOLE B CORE 19X CORED INTERVAL 464.1-473.6 mbsl; 157.3-166.8 mbsf

TIME-ROCK UNIT	BIOSTRAT. ZONE/ FOSSIL CHARACTER			PALEOMAGNETICS	PHYS. PROPERTIES	CHEMISTRY	SECTION	METERS	GRAPHIC LITHOLOGY	DRILLING DISTURB.	SED. STRUCTURES	SAMPLES	LITHOLOGIC DESCRIPTION
	FORAMINIFERS	NANNOFOSSILS	RADIOLARIANS										
PLIOCENE ?													DIATOMACEOUS MUD Major lithology: Section 1, 0-150 cm: diatomaceous mud, olive gray (5Y 4/2), with crude olive (5Y 5/4) laminae rich in diatoms, and olive (5Y 5/4) dolomite at 17-19 cm; Section 2, 0-150 cm: diatomaceous mud, olive gray (5Y 4/2), with crude olive (5Y 5/4) laminations rich in diatoms, and mud brittle with incipient fissility; and Section 3, 0-104 cm, and CC, 0-11 cm: diatomaceous mud, olive gray (5Y 4/2), with crude, bioturbated, olive (5Y 5/4) laminations rich in diatoms. SMEAR SLIDE SUMMARY (%): 1, 101 3, 61 M D TEXTURE: Sand 5 — Silt 70 90 Clay 25 10 COMPOSITION: Quartz 3 10 Feldspar 2 5 Mica Tr — Clay 5 20 Calcite/dolomite Tr 1 Accessory minerals 1 — Pyroxene — 1 Phosphate — Tr Glauconite — Tr Foraminifers — Tr Nannofossils Tr Tr Diatoms 89 63 Silicoflagellates Tr —

687B-18X CC



687B-19X 1 2 3 CC

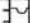
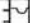


SITE 687 HOLE B CORE 20X CORED INTERVAL 473.6-483.1 mbsl; 166.8-176.3 mbsf

TIME-ROCK UNIT	BIOSTRAT. ZONE/ FOSSIL CHARACTER				PALEOMAGNETICS	PHYS. PROPERTIES	CHEMISTRY	SECTION	METERS	GRAPHIC LITHOLOGY	DRILLING DISTURB.	SED. STRUCTURES	SAMPLES	LITHOLOGIC DESCRIPTION	
	FORAMINIFERS	NANNOFOSSILS	RADIOLARIANS	DIATOMS											
7	* non diagnostic	* insignificant	* non diagnostic												

CORE 112-687B-21X NO RECOVERY

SITE 687 HOLE B CORE 22X CORED INTERVAL 492.6-502.1 mbsl; 185.8-195.3 mbsf

TIME-ROCK UNIT	BIOSTRAT. ZONE/ FOSSIL CHARACTER				PALEOMAGNETICS	PHYS. PROPERTIES	CHEMISTRY	SECTION	METERS	GRAPHIC LITHOLOGY	DRILLING DISTURB.	SED. STRUCTURES	SAMPLES	LITHOLOGIC DESCRIPTION																														
	FORAMINIFERS	NANNOFOSSILS	RADIOLARIANS	DIATOMS																																								
	FOSSIL CHARACTER																																											
?	B *	insignificant *		non diagnostic *				CC			O	***	*	DOLOMITE-CEMENTED SILTSTONE																														
<p>Major lithology: dolomite-cemented siltstone, gray (5Y 5/1), in CC, 19–25 cm.</p> <p>CC, 0–19 cm: drill slurry.</p> <p>SMEAR SLIDE SUMMARY (%):</p> <table><tr><td></td><td>CC, 9</td></tr><tr><td></td><td>D</td></tr></table> <p>TEXTURE:</p> <table><tr><td>Silt</td><td>70</td></tr><tr><td>Clay</td><td>30</td></tr></table> <p>COMPOSITION:</p> <table><tr><td>Quartz</td><td>10</td></tr><tr><td>Feldspar</td><td>10</td></tr><tr><td>Rock fragments</td><td>4</td></tr><tr><td>Mica</td><td>Tr</td></tr><tr><td>Clay</td><td>30</td></tr><tr><td>Calcite/dolomite</td><td>15</td></tr><tr><td>Accessory minerals</td><td></td></tr><tr><td> Glauconite</td><td>Tr</td></tr><tr><td> Pyroxene</td><td>6</td></tr><tr><td> Micrite</td><td>5</td></tr><tr><td> Diatoms</td><td>20</td></tr></table>																CC, 9		D	Silt	70	Clay	30	Quartz	10	Feldspar	10	Rock fragments	4	Mica	Tr	Clay	30	Calcite/dolomite	15	Accessory minerals		Glauconite	Tr	Pyroxene	6	Micrite	5	Diatoms	20
	CC, 9																																											
	D																																											
Silt	70																																											
Clay	30																																											
Quartz	10																																											
Feldspar	10																																											
Rock fragments	4																																											
Mica	Tr																																											
Clay	30																																											
Calcite/dolomite	15																																											
Accessory minerals																																												
Glauconite	Tr																																											
Pyroxene	6																																											
Micrite	5																																											
Diatoms	20																																											

